Detection of alpha-synuclein conformational variants from gastro-intestinal biopsy tissue as a potential biomarker for Parkinson's disease

Claudio Ruffmann

St Cross College
University of Oxford

A thesis submitted for the degree of
DOCTOR OF PHILOSOPHY IN CLINICAL NEUROSCIENCES

Nuffield Department of Clinical Neurosciences
Medical Sciences Division
University of Oxford

Michaelmas term, 2017

ABSTRACT

Detection of alpha-synuclein conformational variants from gastro-intestinal biopsy tissue as a potential biomarker for Parkinson's disease

A thesis submitted for the degree of Doctor of Philosophy in the University of Oxford, Claudio Ruffmann, St Cross College, Michaelmas Term, 2017

Gastrointestinal (GI) alpha-synuclein (ASN) detection may represent a clinically useful biomarker of Parkinson's disease (PD), but this has been challenged by conflicting results of recent studies employing different immunohistochemical (IHC) methods and reporting diverse morphological patterns with variable biological interpretation. To increase sensitivity and specificity, we applied three different techniques to detect different possible conformations of ASN in GI tissue derived from biopsies of the GI tract, which were obtained from a longitudinally followed, clinically well-characterized cohort of PD subjects and healthy controls (HC) (Oxford *Discovery* study). With IHC, we used antibodies reactive for total (T-ASN-Abs), phosphorylated (P-ASN-Abs) and oligomeric (O-ASN-Abs) ASN; with the ASN Proximity Ligation Assay (AS-PLA), we targeted oligomeric ASN species specifically; finally, with the Paraffin-Embedded Tissue Blot (PET-Blot) we aimed to detect fibrillary conformations of ASN specifically. Optimisation and validation of

the PET-Blot and PLA techniques was carried out with studies on brain tissue from subjects with ASN pathology, and these experiments were used to gain insight into morphology and distribution of different conformational variants of ASN in the brain of subjects with Lewy pathology.

We specified all the detected morphological staining patterns with each technique interpreting them as pathologic or non-specific. Correlation to clinical symptoms was assessed to investigate the potential predictive or diagnostic value of specific staining patterns as biomarkers.

A total of 163 GI tissue blocks were collected from 51 PD patients (113 blocks) and 21 healthy controls (50 blocks). In 31 PD patients, GI biopsies had been taken before PD diagnosis (Prodromal PD group); while in 20 PD patients biopsies were obtained after PD diagnosis (Manifest PD group). The majority of these tissues blocks were from large intestine (62%), followed by small intestine (21%), stomach (10%) and oesophagus (7%). With IHC, four ASN staining patterns were detected in GI tissue (Neuritic, Ganglionic, Epithelial, and Cellular), while two distinct staining patterns were detected with AS-PLA (*cellular* and *diffuse* signal) and with AS-PET-Blot (*ASN-localised* and *peri-crypt* signal). The level of agreement between different techniques was generally low, and no single technique or staining pattern was able to reliably distinguish PD patients (Prodromal or Manifest) from HC.

Overall, our study suggests that even specific detection of ASN conformational variants currently considered pathologic was not adequate for the prediction of PD. Future studies with these or other novel techniques focusing on the upper part of the GI tract could overcome current limitations in sensitivity and specificity.

DECLARATION STATEMENT

I, Claudio Ruffmann, declare that the results presented here are from original experimental work which has been carried out by me at the Nuffield Department of Clinical Neurosciences, University of Oxford, between Michaelmas 2013 and Michaelmas 2016. This work was supervised by Dr Laura Parkkinen and co-supervised by Prof Kevin Talbot. All the work described in this thesis is my own, unless otherwise specifically stated, and I clearly stated the contribution of others to my thesis in the acknowledgments section. No part of this work has been submitted for any other degrees or qualification at this or any other university.

ACKNOWLEDGEMENTS

I would like to thank my principal supervisor, Dr. Laura Parkkinen, for her continued guidance throughout the duration of this project. Through your example, I have learnt the importance of patience and attention for detail in research.

I would like to thank my co-supervisor, Prof. Kevin Talbot, for always being supportive and providing effective guidance on the many occasions when I have sought counsel.

I would also like to thank Prof Michele Hu for being the driving force behind the Oxford *Discovery* study, which provided the necessary context for my project and has been a unique learning experience for me.

Many thanks to Dr Nora Bengoa-Vergniory for her crucial input and advice in optimizing the PLA protocol for application to GI tissue and for quantification of fluorescent AS-PLA staining in the GI tract.

Many thanks to Dr Ilaria Poggiolini for her help in PET-Blot staining and for technical support and advice in the lab.

Many thanks to Dr Javier Alegre-Abarrategui for screening all gastrointestinal biopsy samples for quality/comorbid pathology and for his advice on the PLA technique.

Many thanks to all the Oxford *Discovery* study administrative staff, research nurses and research fellows for their invaluable help and support in obtaining archived gastrointestinal biopsy specimens.

I would also like to thank Carolyn Sloane, Connor Scott and Marie Hammard from the Neuropathology University Lab at the John Radcliffe Hospital for their continued assistance in the lab.

Thank you to all the other people who participated in this project and contributed to it.

DEDICATION

To my parents: thank you for being the guiding stars for my ship

To my wife: thank you for always giving me energy and stability, and for putting up with all the 'extra' time this work has required. I could not have done this without you

To my children: you never fail to remind me of all that is good in life

PUBLICATIONS AND PRESENTATIONS ARISING FROM THIS WORK

Publications in peer-reviewed scientific journals:

Claudio Ruffmann, Laura Parkkinen. **Colonic mucosal α-synuclein lacks specificity as a biomarker for Parkinson disease**. *Neurology* 2015 85(9):834-5.

Claudio Ruffmann, Laura Parkkinen. **Gut feelings about α-synuclein in gastro-intestinal biopsies: biomarker in the making?** *Mov Disord.* 2016 Feb;31(2):193-202.

Claudio Ruffmann, Nora Bengoa-Vergniory, Ilaria Poggiolini, Diane Ritchie, Michele T. Hu, Javier Alegre-Abarrategui, Laura Parkkinen. **Detection of alpha-synuclein conformational variants from gastro-intestinal biopsy tissue as a potential biomarker for Parkinson's disease.** *Neuropathol Appl Neurobiol.* 2018 Apr 19. doi: 10.1111/nan.12486.

Poster presentations:

Colonic α-synuclein: a potential diagnostic biomarker in Parkinson's disease
Ruffmann C, Hu M, Talbot K, Ansorge O, Parkkinen L.
International Symposium of the Movement Disorder Society: *Alpha-Synuclein: The Gateway to Parkinsonism.*11-13th February, 2015, Innsbruck, Austria.

Colonic α-synuclein: a potential diagnostic biomarker in Parkinson's disease
Claudio Ruffmann C, Poggiolini I, Hu M, Parkkinen L.
British Neuropathological Society Meeting, 2-4th March, 2016, London, UK.

Colonic α-synuclein: a potential diagnostic biomarker in Parkinson's disease
Ruffmann C, Poggiolini I, Bengoa-Vergniory N, Alegre-Abarrategui J, Hu M, Parkkinen L.
20th International Congress of Parkinson's disease and Movement Disorders, June 16-19th, 2016, Berlin, Germany.

LIST OF ABBREVIATIONS

ºC: Degrees Celsius

11C-DTBZ: 11C-dihydrotetrabenazine

123I-CIT: 123I-2β-carbomethoxy-3β-(4-iodophenyl)tropane

123I-MIBG: 123I-metaiodobenzylguanidine

AD: Alzheimer's Disease

ADLB: Alzheimer's Disease with Lewy bodies

ALS: Amyotrophic Lateral Sclerosis

AS-PET-blot: Alpha-synuclein paraffin embedded tissue blot

AS-PLA: Alpha-synuclein proximity ligation assay

ASN: Alpha-synuclein

ASN-Abs: Alpha-synuclein antibodies

ASN-IRS: Alpha-synuclein Immunoreactive Staining

CJD: Creutzfeldt-Jakob Disease

CNS: Central Nervous System

CSF: Cerebrospinal fluid

DaTScan: Dopamine Transporter Scan

DIF: Double Immunofluorescence

DLB: Dementia with Lewy Bodies

DMV: Dorsal motor nucleus of the vagus nerve

DTI: Diffusion tensor imaging

EDS: Excessive Daytime Sleepiness

ELISA: Enzyme Linked Immunosorbent Assay

ENS: Enteric Nervous System

ER: Endoplasmic Reticulum

HC: Healthy Controls

GI: Gastrointestinal

IHC: Immunohistochemistry

ILBD: Incidental Lewy Body Disease

LB: Lewy body

LC: Locus Coeruleus

LN: Lewy neurite
MCI: Mild Cognitive Impairment
MDS: Movement Disorder Society
MLPA: Multiplex ligation-dependent probe amplification
MMSE: Mini Mental State Examination
MOCA: Montreal Cognitive Assessment Score
NAC: Non-Amyloid Component
NBIA: Neurodegeneration with Brain Iron Accumulation
NCM: Nitrocellulose Membrane
O-ASN-Abs: Oligomeric ASN-reactive Antibodies
OPTIMA: Oxford Project to Investigate Memory and Ageing
P-ASN-Abs: Phosphorylated ASN-reactive Antibodies
PAF: Protein Aggregate Filtration
PCR: Polymerase Chain Reaction
PD: Parkinson's Disease
PET: Positron Emission Tomography
PET-Blot: Paraffin Embedded Tissue Blot
PK: Proteinase K
PLA: Proximity Ligation Assay
PNS: Peripheral Nervous System
RBD: Rapid eye movement (REM) sleep Behaviour Disorder
RCA: Rolling Circle Amplification
SN: Substantia Nigra
SNARE: Soluble NSF Attachment Protein Receptor
SPECT: Single Photon Emission Computed Tomography
T-ASN-Abs: Total ASN-reactive Antibodies
TBS-T: Tris Buffered Saline + 0.05% Tween
UPDRS: Unified Parkinson's Disease Rating Scale
UPSIT: University of Pennsylvania's smell identification test

TABLE OF CONTENTS

LIST OF FIGURES

LIST OF TABLES

1. CHAPTER ONE

INTRODUCTION

Parkinson's disease (PD) is the second most prevalent neurodegenerative disease after Alzheimer's disease (AD) and a major cause of disability and socio-economic burden (1, 2). There is currently no cure for PD, and treatment is purely symptomatic, however in recent years research has intensified to find appropriate molecular targets for the development of curative or preventative treatment (3).

Currently, the diagnosis of PD rests on clinical criteria and can only be confirmed with a post-mortem examination of the brain, which reveals intraneuronal inclusions of misfolded alpha-synuclein (ASN) protein known as Lewy pathology, coupled with neuronal loss in the substantia nigra (SN) (4).

In recent years, several studies have shown that ASN aggregation can also be detected *in vivo* outside of the central nervous system (CNS) (5, 6), particularly in the enteric nervous system (ENS) of the gastro-intestinal (GI) tract of PD patients (7-13). ASN accumulation has also been seen in colonic biopsies taken years prior to the development of motor symptoms (11, 14, 15) suggesting that ASN pathology may start and be detectable in the ENS long before it affects the brain. If confirmed, these findings could meet the current urgent need for a biomarker in PD, which could complement or perhaps even be superior to directly imaging changes in the nigrostriatal system in predicting or confirming a diagnosis of PD, in tracking its progression and in phenotypically stratifying PD patients (16).

1.1. Parkinson's Disease

PD is a neurodegenerative condition characterized by neuronal loss in specific grey matter regions of the CNS. While traditionally considered a disorder of movement characterized by bradykinesia, rigidity and tremor (17), improved treatment of the core symptoms has modified the natural history of the disease, leading to recognition of a plethora of non-motor symptoms, such as psychological and cognitive disturbances (18). An increased appreciation of the existence of a pre-motor, prodromal phase of PD has brought to light further non-motor, often dysautonomic symptoms heralding the onset of the classical symptoms of bradykinesia, rigidity and tremor by many years (19). Constipation often precedes motor onset by many years, and further dysautonomic symptoms such as urinary urgency, erectile dysfunction, and orthostatic hypotension can become manifest during the course of the disease. Thus, PD is now recognized clinically as a multisystem disorder, and the underlying pathological changes are extensive and involve several different brain regions and also the peripheral nervous system (PNS)(6).

1.1.2. Epidemiology

The incidence of PD rises steeply with age, from 17.4 in 100,000 person years between 50 and 59 years of age to 93.1 in 100,000 person years between 70 and 79 years of age, with a lifetime risk of developing the disease of 1.5% (20, 21) (22).

Age is the greatest risk factor for the development of PD. The prevalence and incidence of PD increase nearly exponentially with age and peak after 80 years of

age (23). This trend has important public health implications; with an aging population and rising life expectancy worldwide, the number of people with PD is expected to increase by more than 50% by 2030 (1).

1.1.3. Clinical characteristics

PD is traditionally considered to be a movement disorder and is characterized by bradykinesia coupled with rigidity and/or tremor, often followed by postural instability. In recent decades however, it has increasingly been recognized that PD involves a multitude of symptoms above and beyond the traditional triad of bradykinesia, rigidity and tremor. There is a host of non-motor symptoms that covers cognitive, psychiatric, and autonomic spheres. As such, PD can be clinically considered a multisystem disease.

PD is typically characterized by a subtle, asymmetric onset of motor symptoms, which are often preceded by non-motor symptoms including loss of sense of smell (hyposmia), constipation, urinary urgency, and sleep disturbances such as REM Behaviour Disorder (RBD). The motor symptoms gradually spread and involve the contralateral limbs, while cognitive impairment of a dysexecutive nature usually manifests several years after the onset of motor symptoms.

There is substantial variability in how the motor and non-motor features manifest in individual cases of PD, and attempts to classify subtypes of PD have traditionally indicated the existence of two major subgroups: tremor-dominant PD, where tremor is the main feature and there is relatively less rigidity and bradykinesia; and akinetic-rigid PD, where tremor is absent and rigidity and bradykinesia dominate the clinical picture (24). An additional subgroup of patients with PD has a mixed or indeterminate phenotype. Tremor-dominant PD is often

associated with a slower rate of progression and less functional disability than non-tremor-dominant PD (25). Furthermore, data from well-characterized cohorts has in recent years confirmed the significant heterogeneity in the constellation of symptoms and in the rate of disease progression between different individuals with PD (26). Our group recently published findings from the *Discovery* cohort delineating at least five clinical subgroups of PD patients (18).

Amongst demographic characteristics, older age has been associated with more aggressive forms of PD, with faster progression to end-stage disease, with loss of independence and need for nursing home placement (2).

Non-motor features include olfactory dysfunction, cognitive impairment, psychiatric symptoms, sleep disorders, autonomic dysfunction, pain, and fatigue. These symptoms are present throughout the course of PD and can drive reduced health-related quality of life even in early PD (27). Non-motor features are also frequently present in PD before the onset of the classical motor symptoms (28). Indeed, the presence of a pre-symptomatic, prodromal phase which can precede the onset of motor symptoms and clinical diagnosis of PD by decades is now increasingly well characterized **(figure 1)**.

Figure 1.1: Clinical symptoms and time course of PD progression

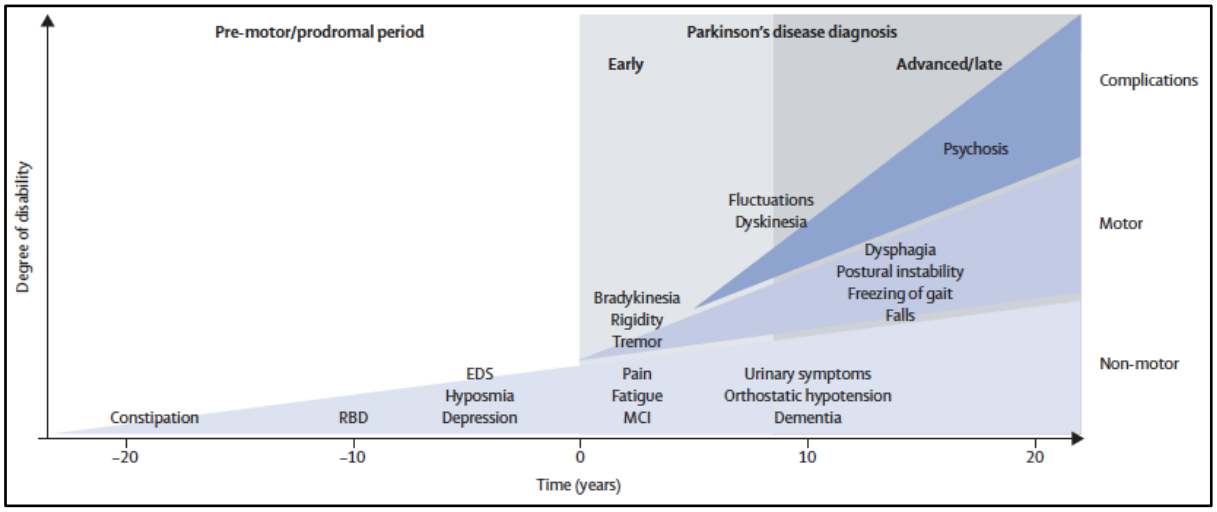

This figure gives an overview of the evolution of PD, from the early, pre-motor phase which can precede diagnosis by decades, to the development of symptoms characteristic of advanced PD, including severe postural instability and dementia. Diagnosis of PD occurs with the onset of motor symptoms (time 0 years).
EDS=excessive daytime sleepiness. MCI=mild cognitive impairment. RBD=REM sleep behaviour disorder (24).

1.1.4 Pathogenesis

The pathogenesis of PD is probably multifactorial and based on a complex and variable interaction between environmental toxins/insults and genetic predisposition. This interplay converges on key molecular pathways such as those involved in cellular trafficking and protein clearance, and may determine structural changes underlying synaptic and mitochondrial dysfunction (29, 30).

1.1.5 Pathology

The presence of characteristic intraneuronal inclusions constituted of misfolded ASN known as Lewy bodies and Lewy neurites (LB and LN, respectively), coupled with neuronal depletion in the pars compacta of the SN represent the fundamental pathologic hallmarks of PD (4) **(Figure1.2)**.

Figure 1.2: Lewy bodies and neurites in the SN of a PD subject

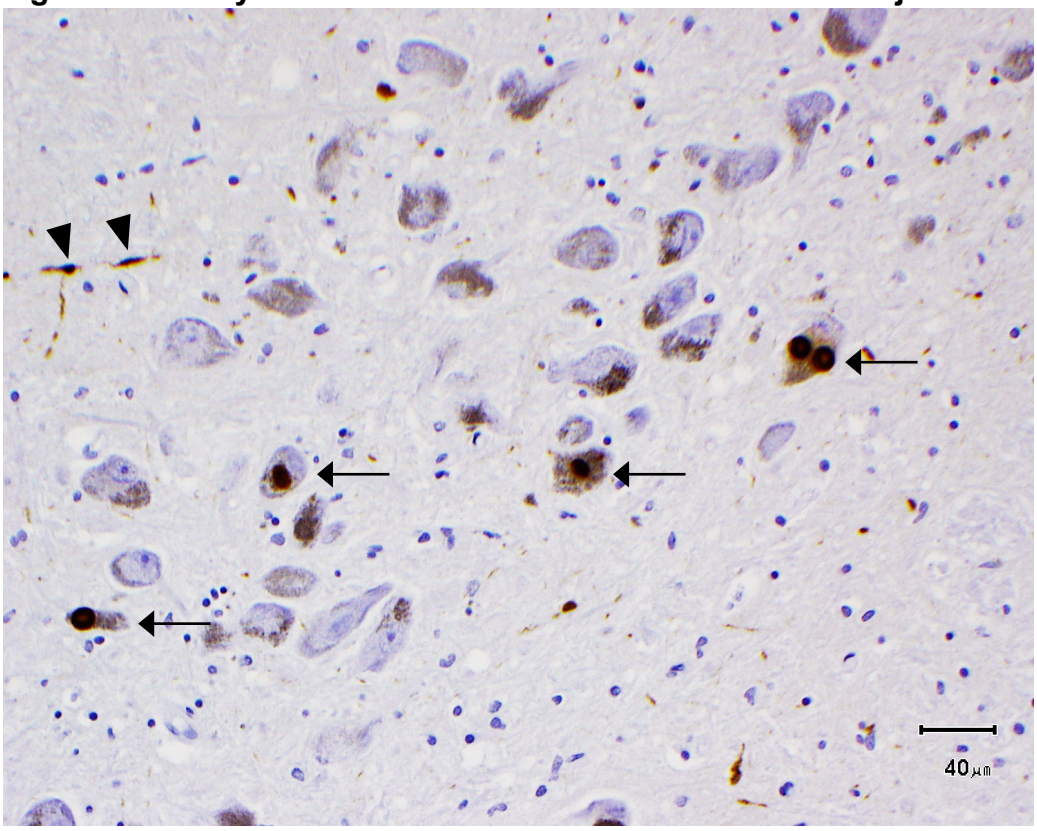

This image demonstrates round, intracytoplasmic inclusions in melanin containing neurons of the SN of a PD brain (arrows); dystrophic LNs are indicated by the arrowheads. LBs and LNs reflect ASN accumulation in the perikaryon in axonal processes, respectively.

The extent of pathological changes goes well beyond the SN, and it involves other neurotransmitter systems beyond the dopaminergic neurons, including cholinergic and serotonergic systems. Indeed, neuronal loss in PD occurs in several brain regions, including the locus coeruleus (LC), nucleus basalis of Meynert, pedunculopontine nucleus, raphe nucleus, dorsal motor nucleus of the vagus nerve (DMV), amygdala, hypothalamus, and neocortex.

Lewy pathology is not restricted to the brain but can also be found in the spinal cord and in the PNS, including the vagus nerve, sympathetic ganglia, cardiac plexus, ENS, salivary glands, adrenal medulla, cutaneous nerves, and sciatic nerve (5, 6).

Specific neuronal subpopulations seem to be specifically targeted by the pathological process underlying PD, a concept known as selective vulnerability. For example, even in brains of end-stage PD subjects, areas adjacent to primarily involved regions such as the DMV or the LC are entirely spared and devoid of Lewy pathology. Braak et al established that neurons with long, unmyelinated axons are more likely to be targeted by ASN accumulation in PD compared to neurons with short, myelinated axons (31). Also, degenerating neurons in PD all seem to have a role in pacemaker activity and at least some have an intense energetic consumption which may lead to oxidative stress (32).

1.1.6 Diagnosis

Currently, the definite diagnosis of PD depends on the post-mortem brain examination, which reveals neuronal loss in the SN and presence of LBs (4). However, the pathogenic and diagnostic role of LBs has come under scrutiny in recent years, particularly following reports of extensive incidental LB pathology found in healthy controls (33).

A diagnosis of probable PD usually rests on the clinical evidence of typical symptoms, their dependable response to dopaminergic medications, and possible confirmation of dopaminergic cell loss with a DaTSCAN (34).

1.2 *In vivo* Biomarker for PD: an unmet need

In its early stages, PD resembles other neurodegenerative disorders leading to misdiagnosis in up to 20% of subjects, even when seen by movement disorder specialists (35). Thus, the post-mortem detection of aggregation of ASN in the

brain coupled with neuronal loss in the SN remains the gold standard for the definite diagnosis of PD (4, 34). However, the progressive pathological changes start several years prior to clinical onset of symptoms and by the time of diagnosis, the disease is likely to be too advanced for any neuroprotective therapies to have full impact. Indeed, it is estimated that motor symptoms in PD do not manifest until there is >50% loss of nigral neurons (36) together with 50-90% reduction in their striatal dopaminergic innervation, which progresses to a complete loss by 4 years of post-diagnosis (37).

In vivo diagnostic biomarkers of PD are currently lacking and could help to identify individuals at a preclinical stage, possibly preceding significant neuronal loss in the SN. PD diagnostic biomarkers would potentially allow us to identify subjects at risk, monitor disease progression, optimize patient inclusion into clinical trials and help us to assess the efficacy of future therapies (38).

A number of potential PD biomarkers are currently under evaluation **(Figure 1.3)**. These can be subdivided into clinical, imaging, pathological, biochemical, and genetic. It is likely that combinations of biomarkers will increase reliability of diagnosis of PD.

Figure 1.3: Potential biomarkers for the diagnosis of PD

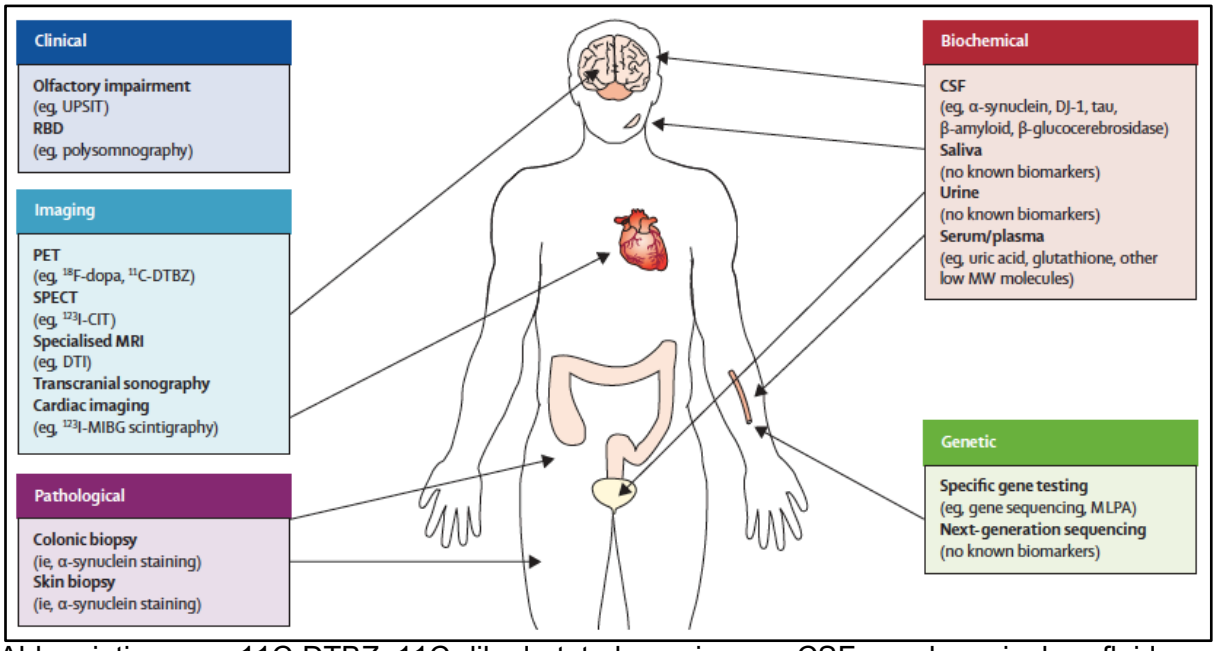

Abbreviations: 11C-DTBZ=11C-dihydrotetrabenazine. CSF=cerebrospinal fluid. DTI=diffusion tensor imaging. 123I-CIT=123I-2β-carbomethoxy-3β-(4-iodophenyl)tropane. 123I-MIBG=123I-metaiodobenzylguanidine. MLPA=multiplex ligation-dependent probe amplification. MW=molecular weight. PET=positron emission tomography. RBD=REM sleep behaviour disorder. SPECT=single photon emission computed tomography. UPSIT=University of Pennsylvania's smell identification test. (24)

1.2.1. Models of progression of pathology in PD

In 2003, Braak and Braak proposed a model of progressive spread of misfolded ASN in the brain of PD subjects, which elegantly reflected clinical evolution of symptoms and included the pre-symptomatic phase of disease (39) **(Figure 1.4)**.

Figure 1.4: Braak model depicting six stages of PD pathology

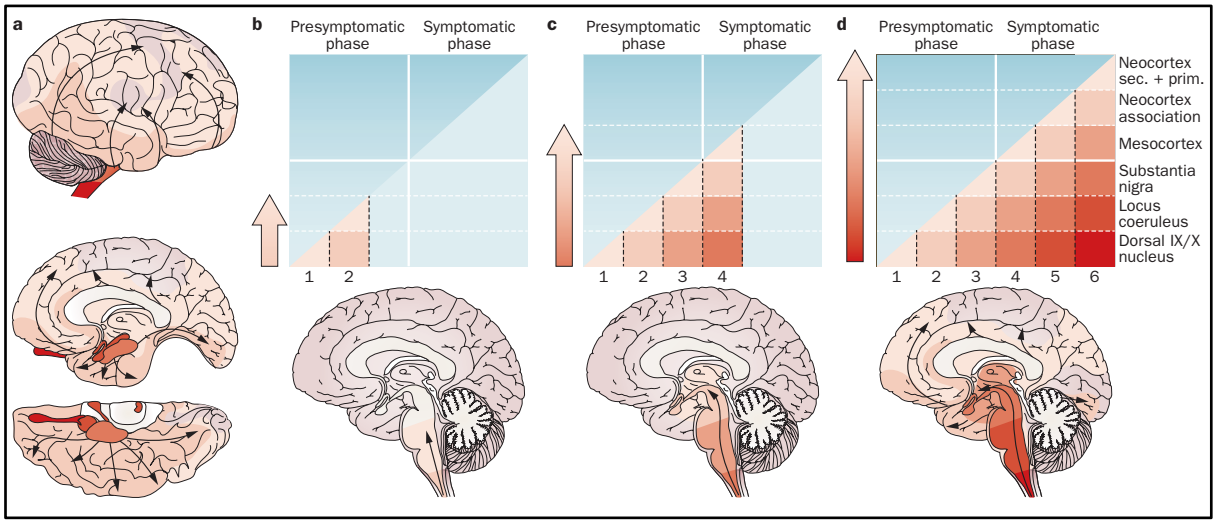

Progression between groups involves additional brain areas and worsening of pathology in previously affected brain regions; (**a)** Caudo-rostral progression of the pathological process (arrows). (**b)** Stage 1: lesions occur in the olfactory bulb and anterior olfactory nucleus, and in the dorsal motor nuclei of the vagal and glossopharyngeal nerves in the brainstem. Stage 2: lesions are observed in the pontine tegmentum (LC, magnocellular nucleus of the reticular formation, and lower raphe nuclei). (**c)** Stages 3 and 4: lesions reach the pedunculopontine nucleus, the cholinergic magnocellular nuclei of the basal forebrain, the pars compacta of the SN (stage 3), the hypothalamus, portions of the thalamus and the anteromedial temporal mesocortex (stage 4). (**d)** Stages 5 and 6: lesions reach neocortical high-order association areas (stage 5), followed by first-order association areas and primary fields (stage 6) (40).

This model agreed with the hypothesis of prion-like propagation of ASN as the underlying pathogenic mechanism of neurodegeneration in PD. According to this hypothesis, after an initial stochastic event of protein misfolding, nearby physiological proteins misfold using the initial pathologically conformed protein as a template, in a mechanism defined as ‘permissive templating’, which is the proven pathogenic mechanism of transmissible spongiform encephalopathies such as Creutzfeldt-Jakob Disease (CJD) (41, 42). Evidence from therapeutic trials using foetal mesencephalic transplants in PD subjects supports trans-synaptic spread of ASN pathology (43). A further evolution in PD pathogenic modelling was represented by the dual-hit hypothesis, which postulated that a putative pathogen capable of passing the mucosal lining of the GI tract might

induce ASN misfolding in the terminal axons of postganglionic enteric neurons, followed by retrograde transport and transynaptic propagation to the preganglionic neurons of the DMV (44). This theory has been supported by *in vivo* evidence showing the progression of pathology from the PNS to the CNS following intramuscular (45) and gastric (46) injection of ASN fibrils in animal models of PD. Furthermore, epidemiological studies in humans have shown vagotomy to be associated with a decreased risk of PD (47).

1.2.2. Why is the ENS a suitable target tissue?

The ENS is a network of neurons and astrocyte-like support cells embedded in the wall of the GI tract. It is organized in a meshwork of interconnected ganglia that form two plexuses, the myenteric plexus and the submucosal plexus **(Figure 1.5)**. The myenteric plexus, also known as Auerbach's plexus, is located between the inner circular and outer longitudinal muscle layers of the whole GI tract. The submucosal plexus, also known as Meissner's plexus, is found exclusively in the small and large intestine, while only scattered ganglia are found in the submucosal layer of the esophagus and stomach. The ganglia and related interconnecting strands are generally smaller than their myenteric counterparts (48). The individual ganglia generally contain few neurons but are so numerous as to account for millions of neurons scattered throughout the GI tract (48, 49).

Figure 1.5: ENS plexuses and their localization

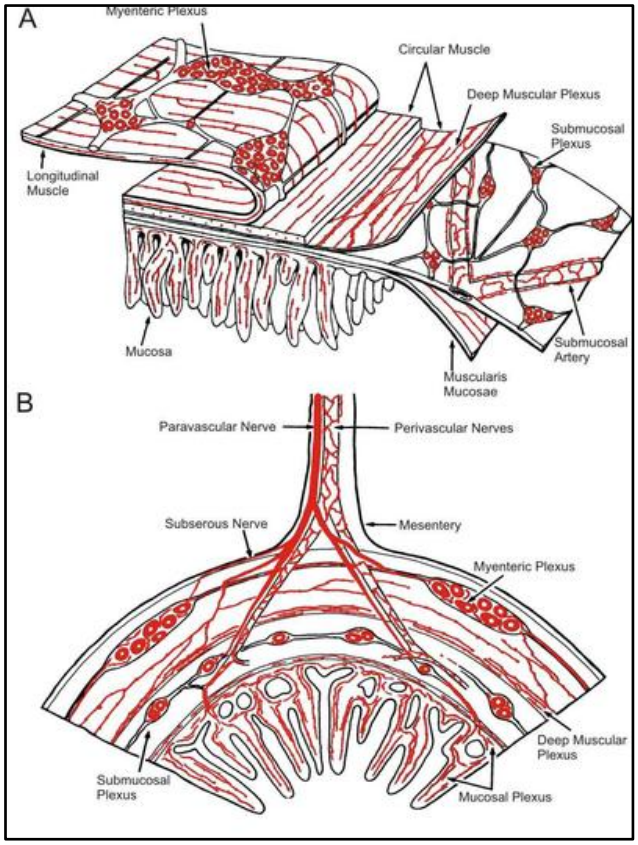

Accumulation of ASN is not limited to the CNS and we have recently reviewed a growing body of literature showing that ASN aggregation can be detected particularly in the ENS in *post mortem* but also in readily and safely accessible *in vivo* biopsies of the GI tract and associated digestive glands (50). Some studies suggest that ASN pathology may start and be detectable in the GI tract in the prodromal phase of PD perhaps before affecting the brain (11, 14, 15, 51), suggesting that GI ASN detection could be used as a predictive biomarker.

While the upper GI tract, including oesophagus, stomach and small bowel definitely receives vagal nerve fibres, there is still debate as to the extent of vagal innervation of the more distal GI tract, i.e. the large bowel and rectum. Several anatomical descriptions consider vagal innervation of the large bowel and rectum partial at best and report that 50% of ENS ganglia receive vagal input at the level of the ascending colon, whereas there is no vagal input in the descending colon or rectum, which receive parasympathetic innervation from the sacral plexus and pelvic nerves (52, 53).

This naturally poses the question of how ASN pathology is transmitted from the more distal regions of the ENS (which are the focus of most studies in the literature and of this study) to the medulla, which is postulated to occur according to the dual hit hypothesis (44) **(Figure 1.6)**.

Figure 1.6: Previous studies and GI parasympathetic innervation

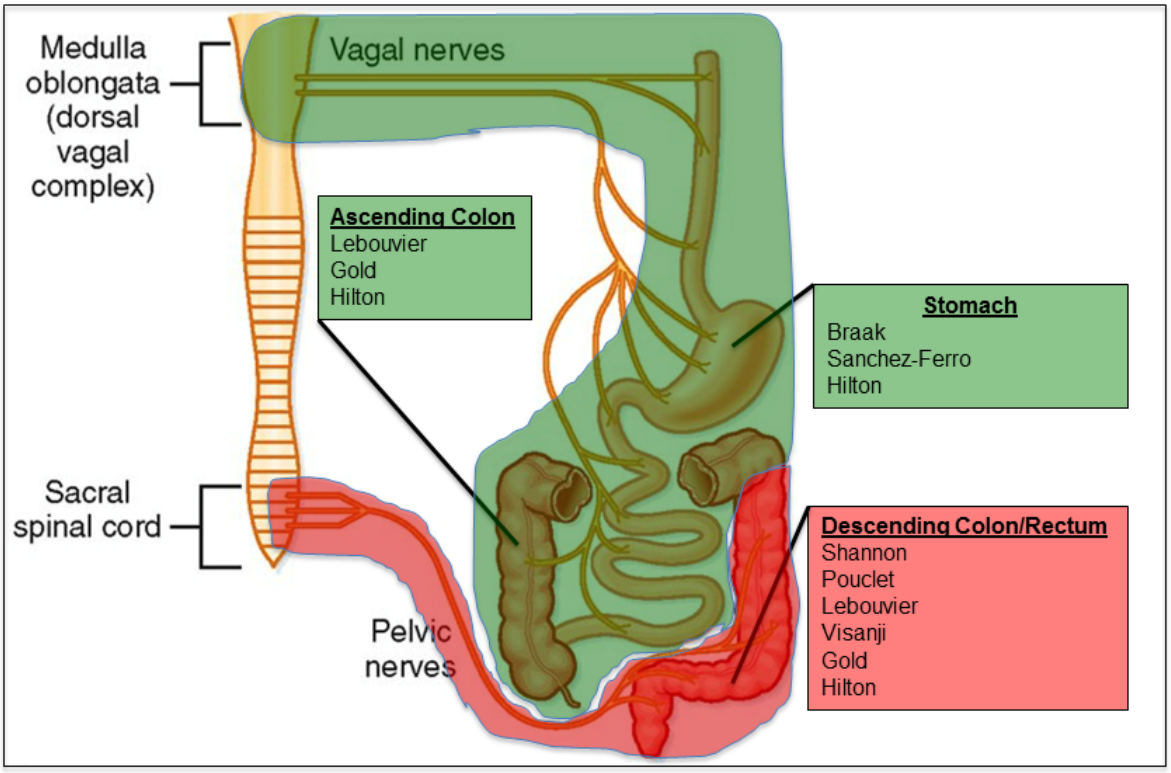

Parasympathetic innervation of the GI regions shaded in green originates in the brainstem nuclei of the vagus nerve, while parasympathetic innervation of the GI tract shaded in red is provided by nerve fibres originating in the sacral plexus. Modified with kind permission from BM Koeppen (54).

Propagation of misfolded ASN from the distal colon and rectum would potentially require an extra passage in the rostral direction, possibly through enteric interneurons to reach the vagal nerve endings. Alternatively, misfolded ASN in the distal colon and rectum could travel retrogradely to the pre-ganglionic parasympathetic neurons in the sacral plexus. However, according to anatomical studies by Braak and colleagues (55), this region is not involved by PD pathology until later stages and would thus not seem to be linked to early pathology in the distal GI tract. Furthermore, the neurons that do receive vagal fibres are almost exclusively found in the myenteric plexus (52), while reported staining in PD is most often confined to mucosal nerve fibres or to the submucosal ganglionic cells where the fibres originate. Thus, one would need to account for this further step in

the PNS-CNS pathway linking the mucosal nerve fibres emanating from submucosal neurons to the myenteric plexus (49).

Removal and preservation of tissue from the GI tract are a relatively frequent occurrence by way of biopsies and provide a source of PNS tissue that can be assessed with specific protein detection techniques easily and with no additional discomfort for the patient. It is thus a practically convenient target for biomarker research.

1.2.3. Why is ASN a suitable target protein?

ASN is a 14kDa neuronal protein from a family of structurally related proteins that are highly expressed in the brain (56).

Before its purification and sequencing from the human brain (57), the existence of alpha-synuclein was deduced from biochemical studies of Alzheimer's disease brains, where it was initially identified as a 'non-amyloid component' of pathological plaques (56).

Under physiological conditions, ASN is enriched at presynaptic terminals, where it promotes the assembly of the Soluble NSF Attachment Protein Receptor (SNARE) machinery and is proposed to play a role in neurotransmitter release, as well as protection of nerve terminals against injury (58-60).

The relevance of ASN in the pathogenesis of PD was initially highlighted by the discovery that LBs, the pathological hallmark of PD, are mainly constituted by misfolded ASN (61). In parallel, studies on genetic forms of PD highlighted the

role of ASN gene mutations in PD pathogenesis (62, 63). Since then, research has increasingly focused on how conformational changes in this protein relate to the pathogenesis of PD (58).

According to most studies, ASN is physiologically a soluble monomer, whereas LBs are formed by insoluble aggregates of fibrillary forms of ASN. Attention has thus shifted to understanding the biochemical nature of the early, pathological "species" of ASN. Post-translational modifications of ASN such as phosphorylation have been suggested to define its transformation into a pathogenic molecule, because the majority of aggregated ASN within LBs is phosphorylated at serine residue 129 (i.e. ~90% ASN phosphorylated in LBs versus ~4% ASN phosphorylated in the total brain) (64). Beyond phosphorylation, many other post-translational changes have been found in ASN extracted from LBs, including oxidation, nitration, and ubiquitination, all of which may also affect the propensity of ASN to form pathologic aggregates (65).

Cellular machinery dedicated to metabolism of proteins, including recycling or elimination of specific protein species can also affect the likelihood of ASN aggregation. This includes the chaperone networks that regulate protein folding (66), as well as the ubiquitin–proteasomal system (UPS) and the autophagy–lysosomal pathway (ALP), which regulate clearance of toxic proteins (67, 68).

ASN oligomers represent an intermediate conformation of ASN between physiological monomers and end-stage fibrillary aggregates **(Figure 1.7)**. They result from aggregation of two or more monomers and are also known as protofibrils (69). In bacterial models, oligomeric forms of ASN have been shown to inhibit protein refolding by the Heat Shock Protein 70 (HSP70) chaperone system,

which was not inhibited by monomers or other types of protein aggregates (70), and ASN oligomers have also been shown to inhibit protease activity of the proteasome *in vitro* (71). Furthermore, biochemical examination of postmortem brainstem specimens of PD patients revealed accumulation of ASN oligomers within the endoplasmic reticulum (ER) compartment, suggesting that toxic ASN oligomers in the intracellular space may mediate neurodegeneration by causing chronic ER stress (58) (72).

Figure 1.7: Conformational variants of ASN and aggregation pathway

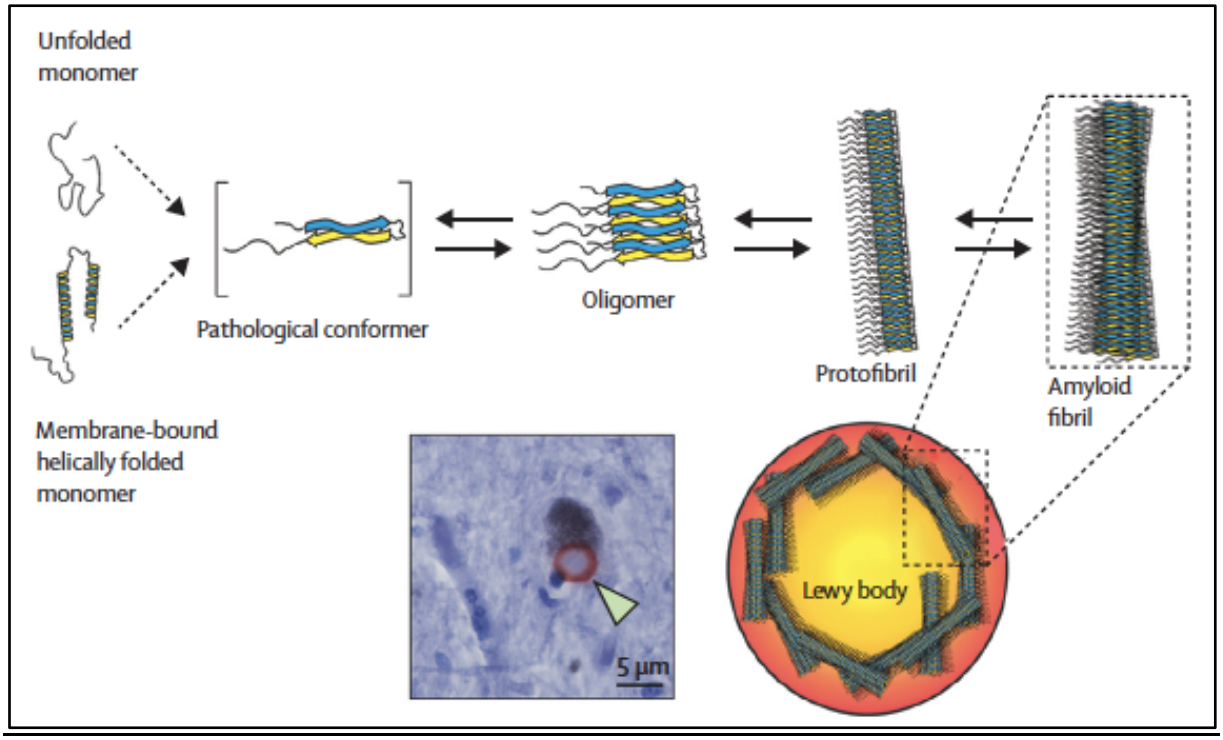

ASN has at least two structural isoforms: a natively unfolded monomer and a helix-rich membrane-bound form. Both isoforms can undergo substantial structural changes, resulting in the formation of β-sheet-rich assemblies. The monomer can aggregate first into several types of small oligomeric species that can be stabilised by β-sheet interactions, and then into higher-molecular-weight insoluble protofibrils, which can polymerise into amyloidogenic fibrils such as those identified in LBs. The photomicrograph shows one ASN-positive mesencephalic Lewy body (in red) in a neuromelanin-positive neuron from a patient with PD, indicated by the green arrowhead (73).

1.3. ASN Detection Techniques used in this study

1.3.1. Immunohistochemistry (IHC)

The typical pathological hallmark of PD is represented by intraneuronal inclusions that were first described by Frederick Lewy and were named after him (65). It has long been established that LBs can be histologically detected beyond the CNS, in various parts of the PNS, in subjects with PD (5, 6) and the first reports of Lewy pathology in the ENS of PD subjects date back to the 1980s (74, 75). It was however the IHC detection of ASN as the principal constituent of Lewy bodies that revolutionized pathological studies of PD (61), by shifting the focus of research from the histopathologic level (detection of Lewy bodies with H&E) to the molecular level. In 2006, Braak et al reported detection of ASN-reactive dystrophic neurites in the gastric ENS of subjects with a neuropathologically confirmed diagnosis of PD (76). This was the first IHC evidence of pathological conformations of ASN coexisting in the ENS and in the CNS of PD subjects. Shortly thereafter, Lebouvier and coworkers used IHC to demonstrate ASN staining *in vivo* in patients with a clinical diagnosis of PD (7). Subsequently, in 2012 for the first time IHC detection of enteric ASN was reported in PD subjects whose colonic biopsies had been taken before the diagnosis of PD, which suggested IHC GI ASN detection could potentially be used as a predictive marker of PD (14).

1.3.1.1. Limitations of previous studies based on IHC GI ASN detection

It has become increasingly apparent that the high sensitivity and specificity of GI ASN detection to identify PD patients reported in the earlier studies (7, 8, 10, 12, 76) has not been sustained in subsequent studies, which repeatedly detected ASN accumulation in the GI tract of neurologically healthy individuals (13, 77-79). This was also confirmed by a recent multi-center study, which showed limited diagnostic value for detecting ASN deposition in GI biopsies by IHC (80). Sensitivity as low as 10% was reported in one of the largest cohorts to date, in which ASN was detected in biopsies from various levels of the GI tract (11). However, case selection was potentially insufficiently rigorous in this study, as it relied entirely on retrospective review of medical records, and analyzed tissue was derived from biopsies done for reasons unrelated to PD. On the other hand, studies examining “ad hoc” fresh biopsies from patients included after clinical examination by a neurologist collectively have obtained a sensitivity as high as 86% (7, 8, 10, 12, 13).

Noticeably, heterogeneity of antibodies, antigen retrieval methods, and of sites of the GI tract assessed has produced significant variability of morphological patterns, which has confounded interpretation of what is pathological compared to non-specific (or possibly physiological) staining.

1.3.2 Paraffin-embedded tissue blot (PET-Blot)

The PET blot is a protein detection technique based on the incubation of paraffin-embedded tissue with proteinase K (PK), a 28.9 KDa serine protease with broad specificity. PK digests proteins through cleavage of peptide bonds preferentially after hydrophobic amino acids (81). Importantly, aggregates of misfolded, insoluble proteins resist digestion. Thus, prolonged PK treatment followed by antibody-mediated staining of tissue will reveal only aggregates of fibrillized proteins, thus increasing specificity for the pathological conformation of proteins that are present in cells (82). While brief (5-10 minutes) incubation with PK is a commonly used antigen retrieval technique in IHC, prolonged (hours) PK incubation at high temperatures is the distinguishing characteristic of the PET-blot technique. This treatment causes detachment of tissue from glass slides, thus tissue must be placed on nitrocellulose membranes (82).

The PET-blot was initially developed and applied in the field of prion disease, where it represented an improved method over three previously applied techniques (histoblot, western blot, and IHC) for detection of pathologic prion protein (82).

The main aims in the field of prion research were to have a sensitive and specific method of identifying pathological prion protein in available tissues, which for the most part were preserved in paraffin. While IHC guaranteed good anatomical resolution, it was hindered by a less than optimal sensitivity, because the harsh proteolytic treatments required to isolate the protease-resistant, pathologic conformations of prion protein resulted in unacceptable tissue damage. On the

other hand, the equally sensitive techniques of the histoblot and the western blot require unfixed tissue and could not provide *in situ* results (83). Blotting of paraffin-embedded tissue on nitrocellulose membranes such as those used for western blot was shown to provide significantly higher resistance to damage from proteolytic activity (82). Thus, one could apply high concentrations of PK for long durations and eliminate all soluble proteins without compromising tissue integrity, increasing both sensitivity and specificity for pathological prion protein detection. While not as good as that obtained with IHC, anatomical resolution with PET-Blot viewed under a dissecting microscope was acceptable.

More recently, the PET-blot method has been used for pathological characterization of other neurodegenerative conditions associated with pathological protein conformations, including AD (84), PD (85, 86), and Amyotrophic Lateral Sclerosis (ALS) (87). In one recent study, the PET-Blot technique was applied to the detection of pathological conformations of ASN in colonic tissue from individuals with PD (13).

1.3.3. Proximity Ligation Assay

The proximity ligation assay is a sensitive and specific technique for detection of proteins and, importantly, of interactions between proteins (88). It shares similarities with traditional protein detection techniques such as IHC, Enzyme Linked Immunosorbent Assay (ELISA) and immune-polymerase chain reaction (immune-PCR), in that a signal is generated in a multistep procedure, starting with interaction between a probe and a target protein (89). Compared to these methods however, the PLA has greater sensitivity detecting concentrations of target molecule in the zeptomolar range (10^{-21} mol). The PLA also ensures high

specificity, which is generated mainly by the critical prerequisite of *proximity* between two probes attached to complementary, short DNA sequences. Addition of a short, bridging oligonucleotide sequence then allows for the generation of a single, longer oligonucleotide sequence, which is then amplified with PCR or rolling circle amplification (RCA), thus providing an easily detectable signal (90). If the two probes, and their attached oligonucleotide sequences are not close enough, there will not be a ligation event, and no amplification will take place **(Figure 1.8)**.

Figure 1.8: Direct PLA

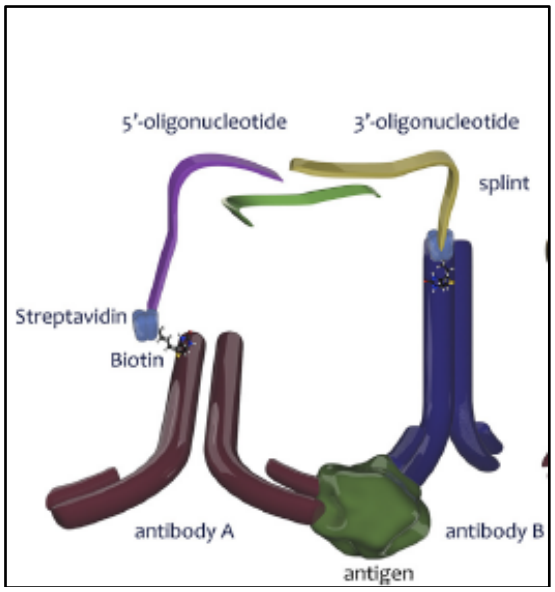

Biotinylated antibodies bind pairwise to adjacent epitopes on target proteins. This brings the two streptavidin-oligonucleotide tails (one coupled through its 5-end, the other through its 3-end) into close proximity. The connector oligonucleotide (splint, green strand) hybridises to both oligonucleotides. The resulting continuous DNA strand can be amplified and detected (90).

While initially DNA aptamers were used as probes, the availability of a plethora of target-specific mono- or polyclonal antibodies has led to their preferred use as probes. Further tailoring of the PLA has made possible its use in fixed tissue, allowing for *in situ* detection of proteins and protein interactions (88).

The PLA was originally developed for cancer research and later used in cardiology, immunology and microbiology (88, 91, 92). Since its first description by Fredriksson and colleagues, the PLA has been increasingly applied and adapted to suit diverse research and clinical needs (91). Indeed, there has been a fourfold increase in published studies using this technique from 41 to 156 between 2010 and 2014 (90).

The first PLA-based assay to detect ASN oligomers in human PD brain tissue (ASN-PLA) was recently introduced together with extensive data showing specificity of the assay for the oligomeric conformation of ASN by using *in vitro* ASN oligomerization systems (93). The main difference of this adaptation compared to previously applied PLA protocols is represented by use of only one type of primary antibody **(Figure 1.9)**. Generation of false positive signal due to interaction of two antibody molecules with the same ASN molecule was avoided by using ASN antibodies with blocking action.

Figure 1.9: ASN proximity ligation assay (AS-PLA)

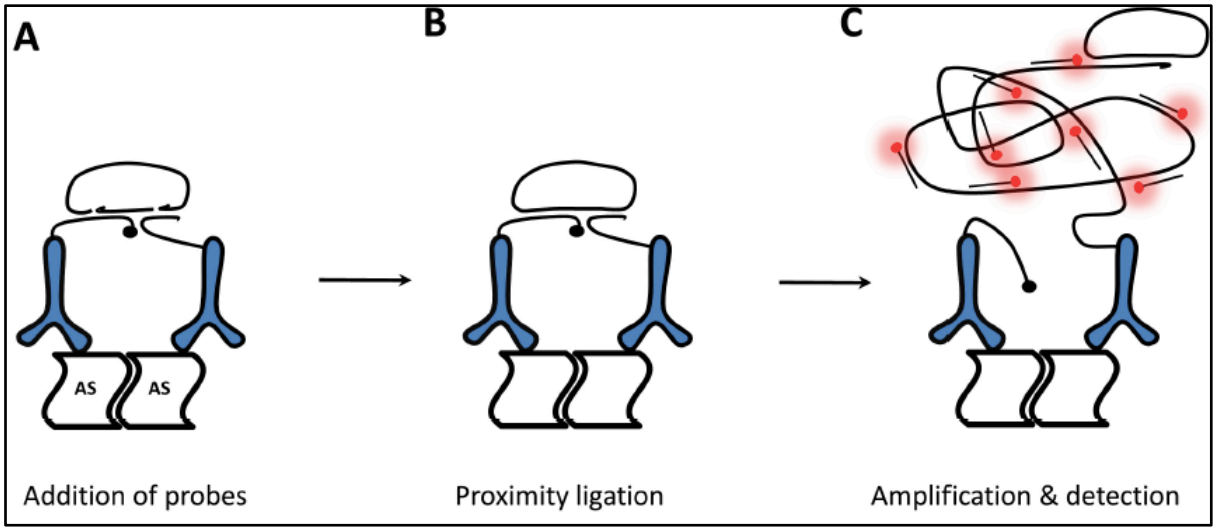

AS-PLA probes consist of an ASN antibody conjugated to one of two short oligonucleotides to form '+' and '-' probes. Proximity of a '+' and a '–' probe through binding of adjacent ASN molecules allows binding of complementary connector oligonucleotides **(A)**. The circular DNA structure produced by the connector oligonucleotides is ligated **(B)** and forms a valid substrate for rolling circle amplification (RCA). The DNA product of the amplification reaction is detected by fluorescently-labeled or horseradish peroxidase-tagged oligonucleotides **(C) (93)**.

If oligomeric ASN is indeed the pathogenic species of ASN, it is likely to be involved in early pathogenic events in PD, thus ASN-PLA could provide an excellent tool to detect the early ASN pathology in the GI tract of subjects in the pre-motor phase of PD.

1.4 Summary

This study was designed to tackle limitations and issues emerging from previous studies on GI ASN detection as a potential biomarker for PD. We detected ASN in paraffin-embedded GI biopsies from longitudinally followed PD patients and healthy controls participating in the Oxford *Discovery* study (94) using three different techniques: conventional IHC, the recently developed AS-PLA (93) and the AS-PET-blot (95). Each technique is specific for a particular variant or conformation of ASN. For IHC, we used T- and P-ASN-Abs as previously reported in the literature. We also used recently developed antibodies specific for the oligomeric forms of ASN (O-ASN-Abs) (96), as transformation of monomeric ASN to oligomeric conformations is increasingly recognized as the early, key pathological event in the fibrillization process of ASN (58).

1.5 Aims and hypotheses of the thesis

1. Examine whether the detection of ASN in the GI tract is pathologic and can be used as a biomarker in PD. We hypothesise that certain conformations of ASN may be more prevalent in nervous tissue from the GI tract of PD subjects

compared to HC. We also expect to find a degree of overlap in ASN-positive staining between and PD subjects and HC, i.e. non specific staining.

2. Optimize and adapt the PLA and PET-Blot techniques for ASN detection in (1) the brain and (2) GI tissue. Based on the hypothesis that the prevalence of conformations of ASN alternative to monomeric/soluble ASN is increased in PD subjects, we expect techniques that selectively detect oligomeric (PLA) or fibrillary (PET-Blot) conformations of ASN to facilitate separation of PD subjects from HC and to reduce confounding, non-specific staining, thus increasing both sensitivity and specificity.

3. Apply three different techniques for detection of pathological ASN species in the GI tract from a prospectively followed cohort of PD subjects and HC, describing the morphological staining patterns detected and whether they can be considered pathologic. We hypothesise that correlation between clinical and demographic characteristics and neuropathological staining results will allow improved characterisation of PD phenotypes. Furthermore, biopsy tissue from time points preceding clinical PD diagnosis in a subgroup of subjects will allow pre-symptomatic diagnosis of PD.

4. Compare results from the three detection techniques to one another, both in (1) brain and (2) GI tract. We expect a combination of techniques to potentially increase sensitivity and specificity of PD diagnosis in our sample.

If met, these aims could address both pragmatic and conceptual issues in the field of PD. From a pragmatic point of view, definition of a reliable *in vivo* biomarker would allow definitive diagnosis of PD with implications for clinical management

and for inclusion in clinical trials of new medications. Conceptually, characterization of conformational variants of ASN at different stages of disease and in different regions of the CNS and/or ENS would provide insight into pathogenic mechanisms and potentially facilitate development of targeted therapies. Furthermore, optimisation of the PLA and the PET-Blot for detection of ASN could lead to more widespread application of these protein detection techniques.

2. CHAPTER TWO

METHODS

2.1. Subjects

PD patients diagnosed within 3.5 years were recruited between September 2010 to September 2014, in the context of the Discovery study, an observational cohort study on early Parkinson's disease (http://opdc.medsci.ox.ac.uk) (94). Cases were eligible for inclusion if they met the UK PD Brain Bank criteria for diagnosis (97) irrespective of their age at PD onset, family history or cognitive status. Cases with more than one relative with a diagnosis of PD who otherwise fulfilled the criteria were still included. Patients who developed dementia within 12 months of the onset of their motor symptoms were excluded as having dementia with Lewy-bodies (DLB). Atypical parkinsonian features were screened using the National Institute of Neurological Disorders and Stroke Parkinson's tool. The neurologist rated the percentage likelihood of PD, with all cases excluded from analysis if they had a <90% probability of PD at their most recent clinic visit. All recruited PD subjects undergo regular, 18-month follow-up interviews and examinations.

The control population were recruited from spouses and friends of patients taking part in the study, and from the general public. The control population were clinically assessed to ensure they did not have PD and underwent a family history questionnaire to exclude the presence of first-degree relatives of patients with PD. Neurological status with reference to PD was monitored with a follow-up phone call questionnaire every 18 months after study entry.

Validated questionnaires were used to assess and quantify a range of clinical items in this cohort including: motor function (MDS UPDRS part III); cognitive impairment (MMSE and MOCA); constipation (Honolulu-Asia Ageing Study Constipation Questionnaire); hyposmia (the 16-stick Sniffin odor identification test); RBD (Epworth Sleepiness Scale and RBD Screening Questionnaire). Full details of the Discovery study protocol have been described previously (98).

2.2. Tissue retrieval

2.2.1. GI Biopsies

All participants were systematically screened for previous biopsies of the oesophagus, stomach or small/large bowel. For participants with previous biopsies, local pathology search engines were used to identify lab numbers of biopsy samples.

Tissue requests were sent from the Academic Unit of Neuropathology, John Radcliffe Hospital to the various Discovery site pathology departments. Informed consent was obtained prior to tissue request and retrieval.

Study specimens were excess to biopsies or surgical resections that had been removed from various regions of the alimentary canal, including large and small intestine, stomach and oesophagus. 5-μm thick tissue sections were obtained from each block and stained with routine haematoxylin and eosin for standard histopathological evaluation to confirm the anatomical localization and to assess the quality of the specimens. Any biopsies consisting entirely or predominantly of abnormal tissue (e.g. carcinoma) were excluded.

According to whether the biopsy had been performed before or after clinical diagnosis of PD, PD cases were classified as either ‘Prodromal PD’ or ‘Manifest PD’, respectively.

Tissue samples from appendix and colon were harvested in the course of an autopsy performed on a subject with neuropathologically confirmed PD (unrelated to the Discovery study), for which prior informed consent had been obtained. This tissue was used to investigate sensitivity and specificity of detection of ASN deposition in GI tissue of end-stage PD, in a case with post-mortem CNS pathological confirmation of disease.

2.2.2. Brain Tissue

Brain tissue samples were collected from the OPTIMA (Oxford Project to Investigate Memory and Ageing) cohort, based at the Oxford Brain Bank (99). The OPTIMA project (http://www.medsci.ox.ac.uk/optima) is a longitudinal study of elderly subjects with memory problems and of healthy controls in which a high proportion of enrolled subjects also agreed to donate their brain for research after their death.

Tissue sections were taken from the following brain regions: medulla, pons (including LC), midbrain (including SN), entorhinal cortex, amygdala, striatum, cingulate cortex, temporal cortex, frontal cortex.

2.3 Immunohistochemistry

2.3.1. ASN

In GI tissue, three different ASN-immunoreactive antibodies were applied with optimized antigen retrieval procedures **(Table 2.1)**: (1) KM51, reactive for all forms of alpha-synuclein [**T-ASN-Ab**; (Novocastra, 1:1000, antigen retrieval with autoclave in citrate buffer pH6.0 followed by 10 minute incubation in formic acid)]; (2) pSyn#64, reactive to ASN phosphorylated at serine 129 [**P-ASN-Ab**; (WAKO, 1:10.000, antigen retrieval with 5 minute incubation in proteinase K 20ug/ml)]; (3) O2, reactive to fibrillary and oligomeric ASN conformations [**O-ASN-Ab**; (kind gift from Dr El-Agnaf, 1:10.000, antigen retrieval with autoclave in citrate buffer pH6.0)].

Table 2.1: Antibodies used for IHC ASN detection in GI tract

Antibody	Source	Epitope	Dilution
KM51	Novocastra	Whole-length ASN	1:1000
pSER129	WAKO	Serine phosphorylated at position 129 of the ASN molecule	1:10000
O2	Kindly donated by O. El-Agnaf	Oligomeric and fibrillary ASN conformation	1:20000
Anti-Hu C/D	Kindly donated by P. McGill	Pan neuronal marker	1:1000
Anti-Calretinin (clone 5A5)	Leica Microsystems	Colonic neuronal marker	1:200

2.3.2. Neuronal Marker

To choose the optimal neuronal marker we screened several potential candidates. The S100 antibody was shown to stain glial cells rather than neurons. MAP2 decorated submucosal neurons but produced rather weak staining of the deeper myenteric plexus. NeuN did not stain enteric neurons, while synaptophysin showed a good definition of submucosal ganglia but also abundant non-specific staining. Antibodies reactive for the light chain of the neurofilament protein (NF-L) initially showed good staining of both submucosal and myenteric neuronal structures, although nerve fibres were better defined than neuronal somas. Finally, the best staining of colonic neurons was obtained with antibodies reactive for calretinin (clone 5A5). This antibody provided well-defined staining of both submucosal and mucosal colonic nerve cells and fibres (**Figure 2.1A-B**). Since calretinin antibodies are specific for neuronal tissue in the large bowel, they were used in combination with Anti-Hu C/D antibodies, which are established pan-neuronal markers and provided good staining of nervous tissue localized in non-colonic regions of the alimentary canal (**Figure 2.1C-D**), i.e. oesophagus, stomach, and small bowel.

Figure 2.1: Neuronal Markers

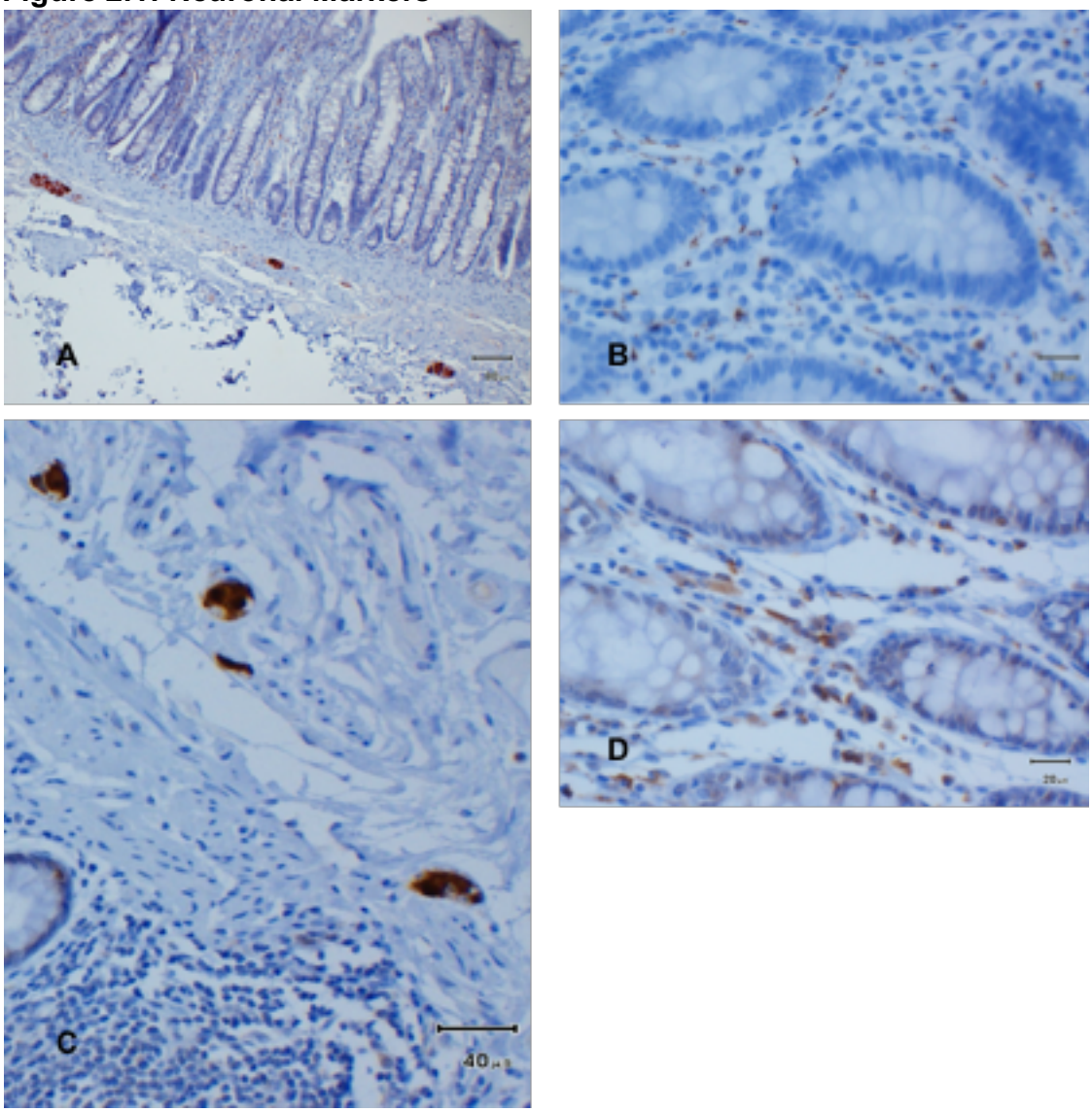

Calretinin (**A,B**) and Anti-Hu (**C,D**) staining of submucosal ganglia (**A,C**) and mucosal nerve fibres (**B,D**) in the GI tract.

For both selected neuronal antibodies, we used autoclave-based, heat-mediated antigen retrieval in citrate buffer (pH6.0). In each section, a semiquantitative assessment (0-3) of the intensity of staining with the neuronal marker was used as a measure of density of nervous tissue, including neurons and nerve cell processes (**Figure 2.2).**

In a subset of GI samples we also applied anti-phosphorylated tau protein antibodies (AT8; 1:500, no AR) and P62 antibodies (1:3000, with heat mediated AR using pH 6.0 citrate buffer in autoclave).

Immunohistochemical staining was developed with the Envision kit and DAB chromogen.

Figure 2.2: Neuronal marker semi-quantitative grading

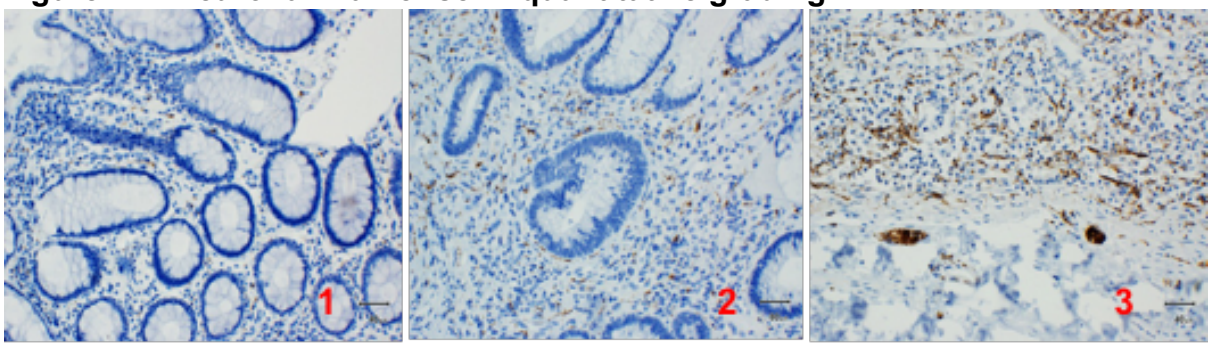

Semiquantitative Score:

0: no staining or non-specific staining

1: Low density of nerve fibres; no ganglionic cells

2: Low density of nerve fibres and ≥ 1 ganglionic cell, or moderate-high density of nerve fibres without ganglionic cells

3: Moderate-high density of nerve fibres and ≥ 1 ganglionic cell

2.4. Paraffin-Embedded Tissue Blot for ASN detection (AS-PET-blot)

2.4.1. Optimization

Optimization of the AS-PET-blot was carried out on brain sections from a case of Stage 6 Lewy body pathology according to the Braak staging scheme (39). Stained regions included the striatum and the cingulate cortex. These regions were of interest due to recent reports on ASN detection using the PET-Blot technique (95).

Table 2.2: PET-Blot Optimization

Variable	Range of Conditions	Optimal Results
Antibody	LB509 (Millipore) pSER129 (WAKO)	LB509
Antibody dilution	*LB509* – 1:5000, 1:10000, 1:20000 *pSER129* – 1:10000, 1:200000	1:10000
PK concentration (ug/ml)	0 (no PK) – 20 – 50 – 100 – 250	20 (Gut); 50 (Brain)
PK incubation time (hrs)	1 – 3 – 5 – 8 – 10	3
PK temperature (ºC)	20 (room temperature); 57	57
Brain region	Striatum, Cingulate Cortex, Medulla, Locus Coeruleus, Midbrain	Striatum
PD Braak stage	0 (negative control) – 1 – 3 – 5 – 6	6
+/- PK/Primary Antibody	PK+/Ab- PK-/Ab+ PK+/Ab+ PK-/Ab-	PK+/Ab+
Chromogen	DAB Alkaline Phosphatase	Alkaline Phosphatase
Visualization	Dissecting microscope Light microscope	Light microscope

2.4.1.1. Antibodies

For protocol optimization, we selected antibodies we had previously used successfully in association with PK digestion in IHC: LB509 and pSer129. For both antibodies, we used dilutions up to 1:20000 **(Table 2.2)**.

2.4.1.2. PK concentrations and Incubation time

A range of PK concentrations and incubation times were tested. Ultimately, the best staining was observed with a PK treatment consisting of incubation in 50ug/ml PK in digestion buffer in the oven at 57 degrees for 3 hours (**Table 2.2, Figure 2.3**).

Figure 2.3: PK incubation time and staining quality

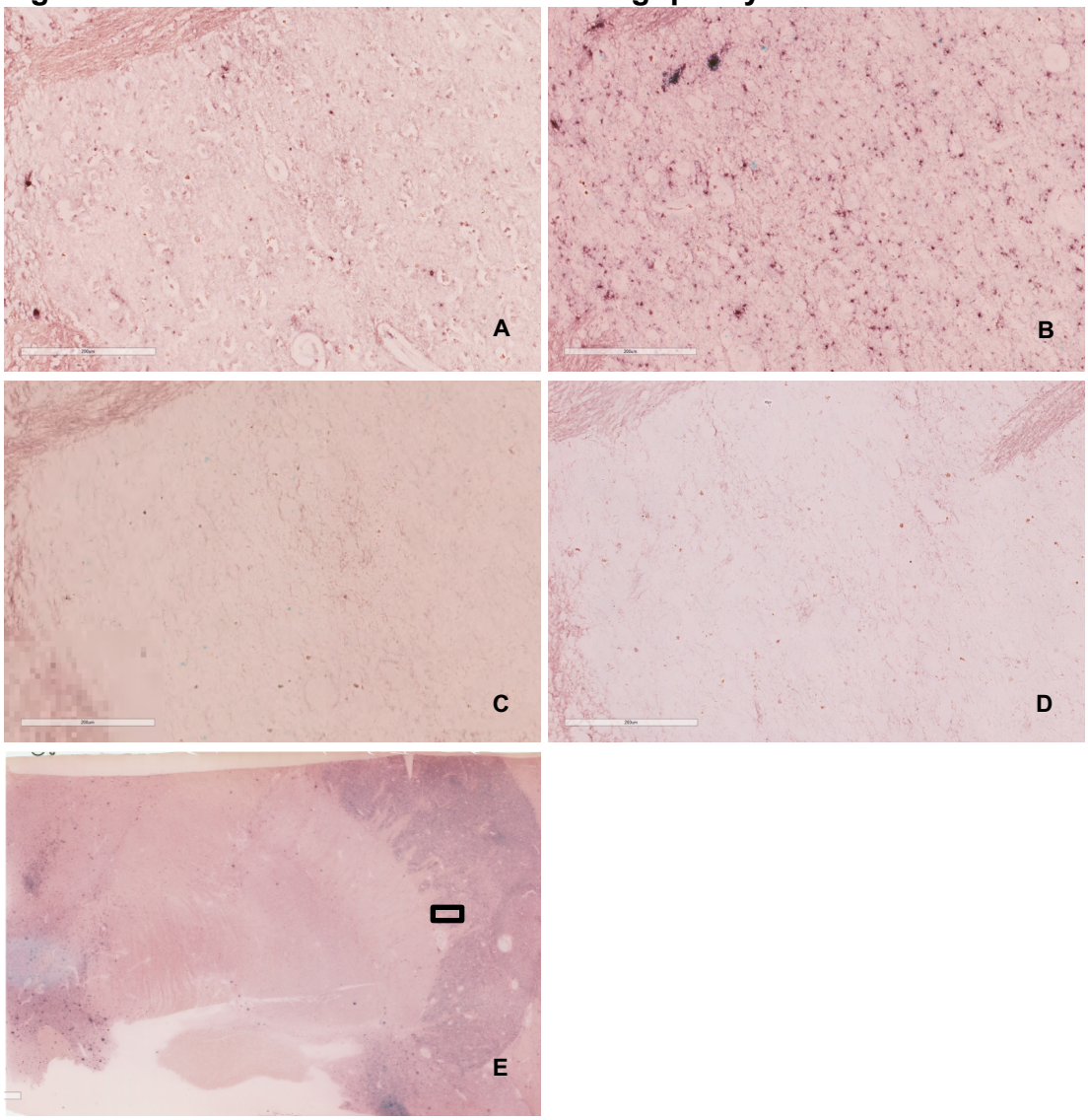

Staining was performed with constant PK concentration (50ug/ml) and variable incubation times. With 1 hour incubation there was good tissue preservation but not enough PK action, and only LBs were visible **(A)**; with 3 hour incubation, tissue preservation was still acceptable and optimal sensitivity reflecting 'neuropil' staining **(B)**; longer incubation times of 5 **(C)** and 8 **(D)** hours caused significant tissue damage. Images **A-D** were taken from the pallidal-putaminal border **(**boxed area in **E)**. Antibody: LB509 1:10000).

A PK concentration of 50 ug/ml was associated with diverse staining patterns, including (1) intraneuronal diffuse staining and (2) more dense and compact inclusions reminiscient of Lewy bodies **(Figure 2.4A)**. We also attempted staining with higher PK concentrations that had been reported in previous studies, i.e. 250

ug/ml, but these concentrations did not improve yield and caused significant tissue damage, even when applied for short times **(Figure 2.4B-C)**.

A shorter incubation time of 1 hour resulted in reliable staining of Lewy bodies and facilitated tissue preservation, but it was too short for the PK to exert its unmasking effect on finer neuropil staining. On the other hand, longer PK incubations of 5 or more hours generally caused significant tissue damage with no benefit to the staining signal **(Figure 2.3)**.

To test for the effect of PK treatment on staining, we withheld application of the primary antibody to PK treated sections, and confirmed absence of any staining, as opposed to that observed in the same, PK-treated sections in which the primary antibody was applied.

Figure 2.4: Effect of different PK concentrations on staining and tissue quality

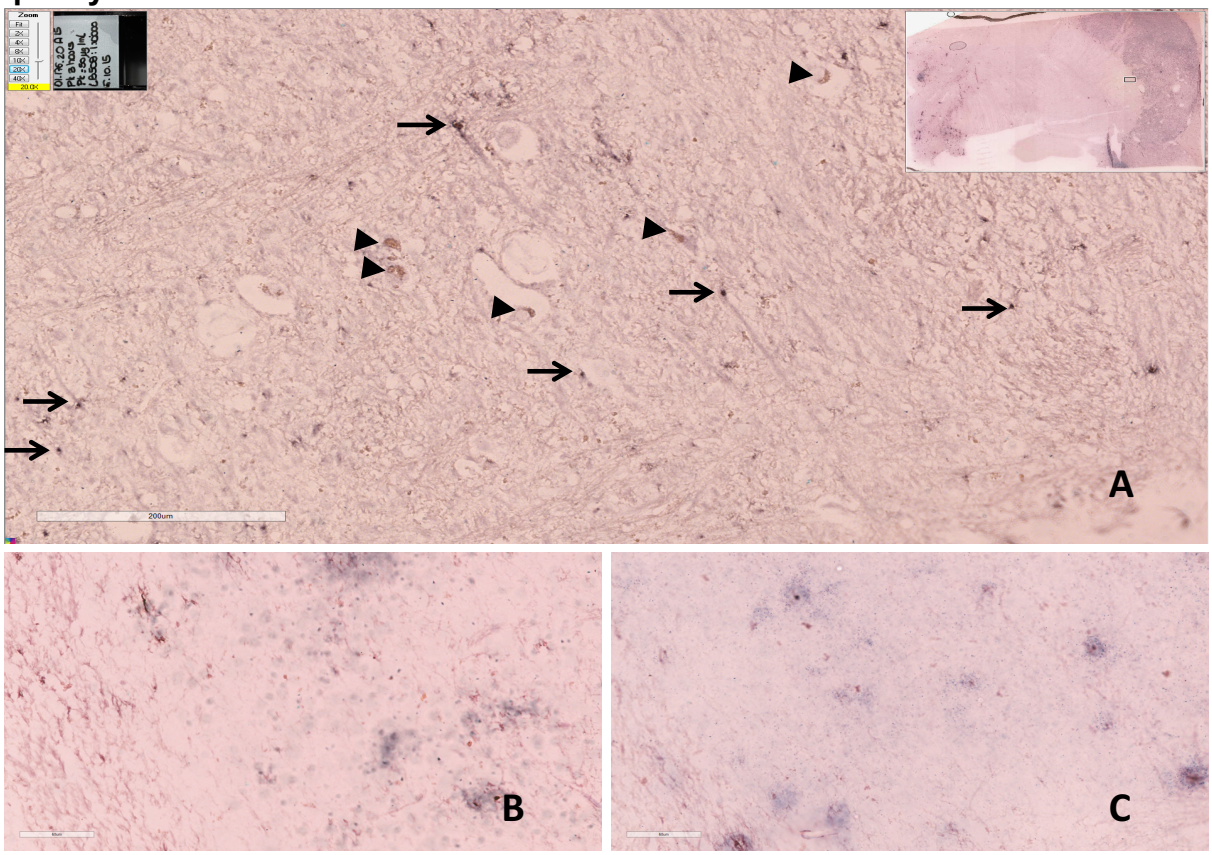

With a PK concentration of 50 ug/ml buffer, different types of staining are depicted: intraneuronal, granular, diffuse staining (**A**, arrowheads) and more dense, compact staining (**A**, arrows); higher concentrations of PK cause excessive tissue damage (**B**: 100 ug/ml; **C**: 250 ug/ml). Antibody: LB509 1:10000.

2.4.1.3. Visualisation

Preliminary images were taken with a dissecting microscope to compensate for the low transparency of the nitrocellulose membrane. With this visualization approach, we found diffuse granular staining in the putaminal region of PD cases, suggestive of localization in presynaptic areas, with the matter tracts being spared **(Figure 2.5)**. We also attempted visualization with a laser capture microdissection microscope, but this allowed only suboptimal definition of staining **(Figure 2.6)**. Visualization was significantly improved by inducing transparency through

immersion in xylene (see methods), which then allowed inspection with light microscopy **(Figure 3.1 and 3.2)**.

Figure 2.5: PET Blot ASN staining in striatum of PD stage 6 case, visualised with dissecting microscope

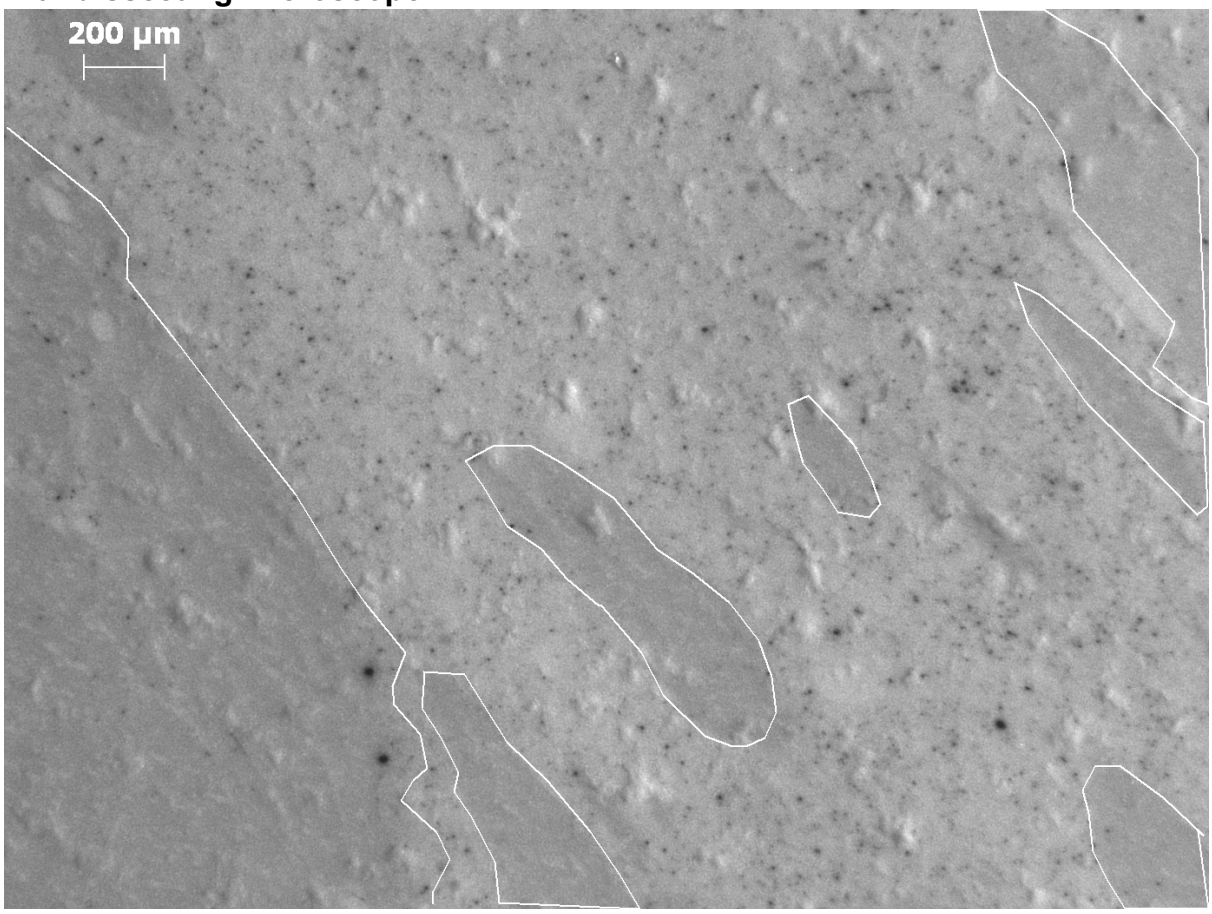

Stereoscopic imaging reveals dot-like staining in the grey matter areas of the striatum, sparing the adjacent white matter tracts, which are highlighted by white boundaries. Antibody: WAKO 1:10000.

Figure 2.6: PET-Blot ASN staining of PD stage 6 striatum, visualized with laser capture microdissection microscope

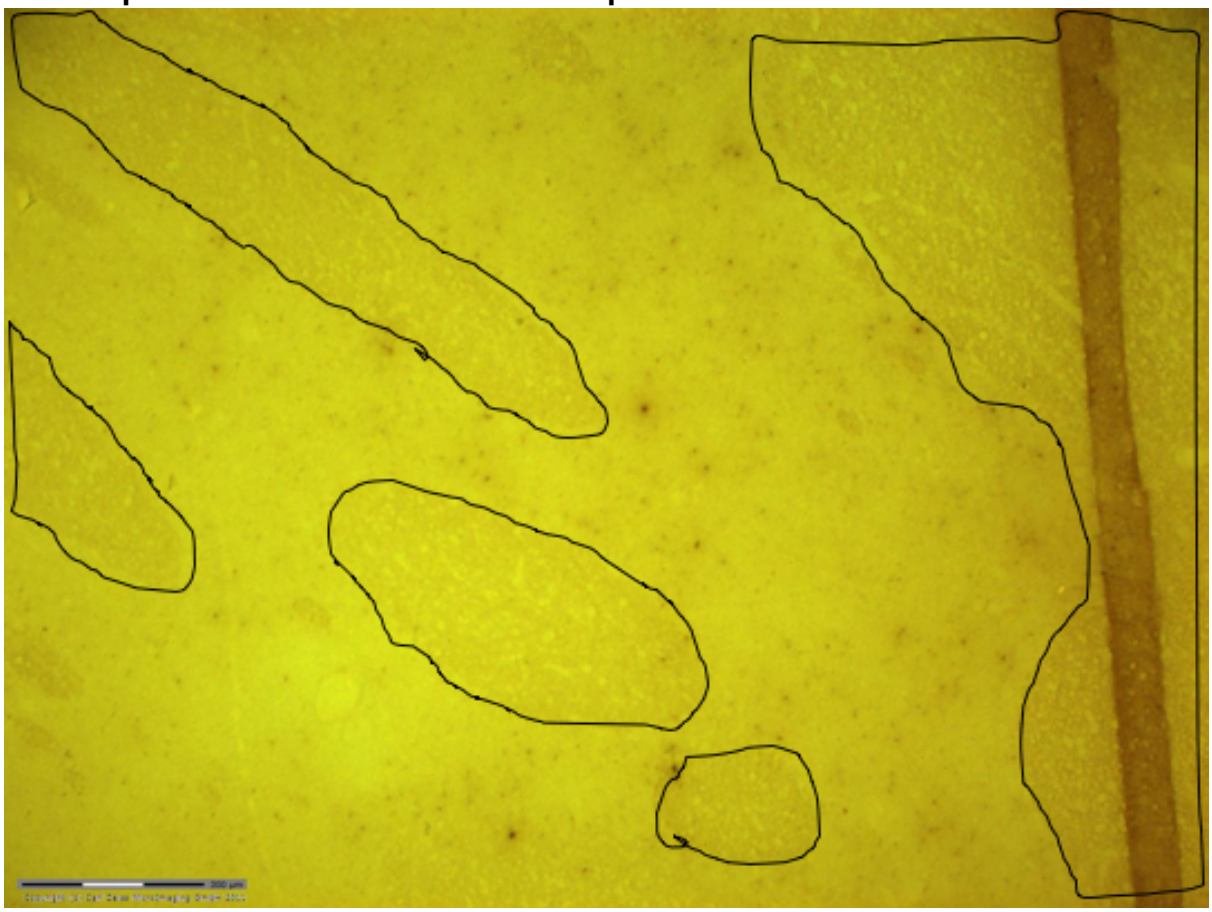

Suboptimal image quality due to reduced sample transparency reveals similar pattern of staining distribution in PD striatum sparing white matter tracts (enclosed in black boundaries). There is limited definition of dot-like staining. Antibody: LB509 1:1000.

2.4.2. AS-PET-Blot Protocol

Paraffin-embedded sections were cut at a thickness of 5 um and blotted onto nitrocellulose membranes (NCM) (0.45um, Biorad). These were then dried by oven heating at 55ºC for 24 hrs to improve adhesiveness of the tissue to the membrane.

NCMs were then re-hydrated in xylene followed by propanol progressively diluted in dH2O (100% - 95% - 85% - 70%). Sections were then dried for at least 4 hours. Excess membrane around the area with blotted tissue was cut and sections were placed in six-well plates. For rehydration, NCMs were placed on 1 glass slide

each for support and inserted in slide racks which were then placed in glass troughs containing initially xylene (x2) and then progressive dilutions of propanol.

In agreement with Moh et al (84), we noticed the tendency of tissue to detach from the NCM when the sections were brought directly from xylene to 100% propanol. A 5-minute drying step between xylene and 100% propanol solved this issue. For the same reason, we let the sections dry after 70% propanol, before immersion in Tris Buffered Saline + 0.05% Tween (TBS-T).

Metal paper clips were used to “fasten” each NCM to its glass slide (avoiding contact between the paper clips and the tissue), to prevent curling during immersion in propanol.

Sections were then dried overnight in open air, with 4 paperclips applied to each slide to prevent curling.

Sections were then incubated in TBS-T for 20 minutes. This was followed by incubation in PK (50ug/ml) at 57º C for 3 hrs.

After PK incubation, sections were washed in TBS-T (3 X 5 minutes) and then incubated in denaturing buffer containing 3M Guanidine Isothiocyanate for 10 minutes, which was followed by further washes with TBS-T (3 X 5 minutes) and then a blocking step with casein for 30 minutes.

Samples were then incubated overnight with primary (ASN-reactive) antibody (LB509 1:10000 – optimized protocol).

After washing with casein, sections were incubated with secondary anti-mouse biotinylated antibody (1:1000) for one hour, washed again with casein, and then incubated with avidin-biotin complex for 25 minutes. After further washes with casein, labelling was developed using alkaline phosphatase solution. Finally, sections were abundantly rinsed in dH2O.

All incubations were carried out on shaking table (except for PK incubation in oven) with 5ml aliquots/well.

After air-drying, sections were briefly dipped in xylene (which enabled visualization with a normal light microscope) and mounted using DPX mounting reagent.

Digital images of slides at ×20 magnification were obtained using Aperio Scanscope.

2.5. Proximity Ligation Assay for ASN (AS-PLA)

2.5.1. AS-PLA on brain tissue

Tissue samples were collected from 10 cases with progressive severity of ASN pathology according to the Braak PD staging scheme (39). All cases were screened for significant Alzheimer and/or vascular pathology, which was absent in all cases.

All brain regions stained with AS-PLA also underwent IHC staining with the O2 antibody, which is reactive for ASN pathology, including oligomeric conformations of ASN (96).

2.5.1.1. Optimization on Brain Tissue

Initial optimization of staining was carried out on entorhinal cortex sections from a neuropathologically confirmed PD case. Tonsil, cingulate cortex and cerebellum of a healthy subject were used as negative controls.

Probe dilutions of 1:100, 1:200 and 1:500 were assessed, using either microwave or autoclave for heat-mediated antigen retrieval in citrate buffer (pH 6.0). The optimal signal was obtained with a 1:200 concentration of each probe in the antibody solution, composed of TBS-T and 1:20 dilution of Duolink Assay Reagent (Sigma), after autoclave antigen retrieval.

In consideration of the significant cost of the Duolink reagents, initial volumes used for each section were kept as low as possible. However, for volumes below 180 ul per slide, staining appeared less uniform possibly due to partial drying. Reagent volumes were thus increased to 200 ul per section for overnight

incubation with the probes and 180 ul for the shorter incubations of the detection phase (ligation, amplification, and detection).

To optimize costs but avoid drying of sections, we switched from staining on flat trays to using 'sequencers', which allow for a reduction of volume to 120 ul per section. This approach, however, produced an artificial gradient in the intensity of staining across the tissue section and was thus abandoned.

2.5.1.2. AS-PLA Brain Protocol

Sections were briefly heated at 65ºC for initial de-waxing and then re-hydrated in xylene and a series of progressive ETOH dilutions (100 – 90 – 70 – 50) and finally washed in distilled water.

Antigen retrieval was performed with autoclave heating in citrate buffer (pH6.0).

Peroxidase quenching was performed with 10% Hydrogen Peroxide in distilled water (dh_20) for 20 minutes followed by rinse in dh_20.

Non-specific staining was blocked with 10% foetal calf serum in TBS-T.

Sections were incubated with PLA probe solution* (1:200 dilution), for 1hr at 37°C and then overnight at 4ºC.

Subsequently, samples were incubated with PLA ligation solution for 1hr at 37°C and then with PLA amplification solution for 2.5 hrs at 37°C. Samples were then incubated in PLA detection solution for 1hr on a shaking table. Next, samples were incubated in chromogen solution for 15-20 minutes on a shaking table and then counterstained with haematoxylin. This was followed by dehydration and mounting with DPX. Between each step, slides were rinsed 3 x 5 minutes in TBS-T solution, except following haematoxylin counterstaining, where samples were put under running tap water for 5 minutes.

*: Briefly, the conjugates were prepared using the Duolink Probemaker kit by incubating 20µl of mouse 211 anti-alpha-synuclein antibody (ab80627, Abcam) with the Probemaker activated oligonucleotide (+ or -) and conjugation buffer overnight at room temperature (RT). The conjugates were then incubated with Probemaker stop reagent for 30 min at RT and suspended in Probemaker storage buffer and stored at +4ºC.

2.5.2. Optimization on GI Tissue

Immunofluorescent AS-PLA was optimized in order to achieve a comparable signal to brightfield AS-PLA, followed by double immunolabelling with the neuronal marker calretinin **(Figure 2.7)**.

Figure 2.7: Optimization of PLA signal on GI Tissue

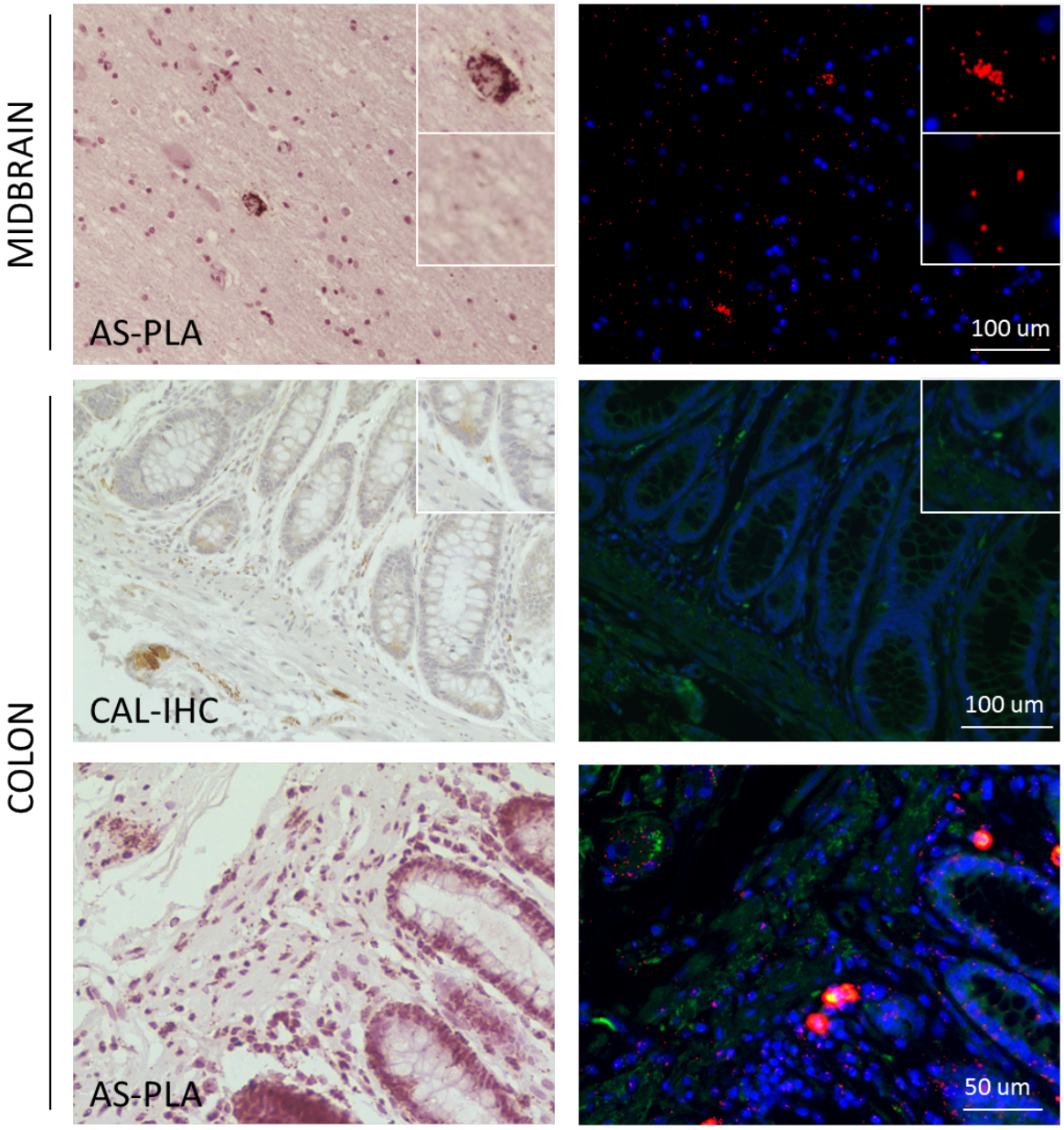

Under optimized antigen retrieval conditions and probe concentrations, we detected similar staining pattern for lesions and diffuse puncta in human PD midbrain for fluorescent and brightfield AS-PLA (top panel). Calretinin IHC and immunofluorescence also showed comparable staining patterns in colonic tissue (middle panel); finally we obtained fluorescent double-labelling of AS-PLA and calretinin (bottom panel).

2.5.2.1. AS-PLA Protocol on GI Tissue

AS-PLA was carried out using Duolink in situ detection kit (Sigma) according to the manufacturer's instructions. 5μm-thick paraffin-embedded sections were dewaxed in xylene and rehydrated in graded ethanol series. Antigen retrieval was carried out with autoclave in citrate buffer pH 6.0 followed by blocking endogenous peroxidases with hydrogen peroxide for 15 min at RT. For co-immunofluorescence, sections were blocked in 10% normal goat serum, 1 M glycine TBS-T and incubated for 1 hr in primary antibody; Calretinin (5A5, Novocastra, 1:100), washed with TBS-T and incubated for 1 hr in the dark with Alexa488 (Life Technologies). Sections were washed in TBS-T and incubated in Duolink block solution at 37°C for 1 h, followed by the conjugates diluted in PLA probe diluent (1:100) overnight at 4°C. After washing in TBS-T, sections were incubated with Duolink ligation solutions and ligase for 1 h at 37°C followed by Duolink amplification reagents and polymerase for 2.5 h at 37°C. For fluorescence, sections were washed in the dark and counterstained with DAPI 1:1000 and mounted with FluorSave (Millipore). For brightfield, sections were washed and incubated with Duolink detection solution for 1 hr at RT followed by Duolink substrate solution for 20 min at RT. Each step was followed by washes in TBS-T (3×5min). Sections were then counterstained with haematoxylin and dehydrated in graded ethanol series and xylene, before mounting with DPX mounting reagent.

All fluorescent images were acquired with an EVOS FL auto imaging system at ×20 magnification and automatically analyzed with Cell Profiler for nuclear DAPI

counting. ImageJ was used for the automatic quantification of AS-PLA-positive diffuse puncta. For each batch, global thresholding was performed using the *threshold* tool on imageJ. Samples of mouse brain over expressing human ASN served as calibrators between batches. All images for each batch were thresholded at the same intensity, then the *analyse particles* tool was used to select particles with a size of 3-25 pixel^2, generating a list of the number of positive puncta for each analysed slide.

Double-labelled AS-PLA and Calretinin-positive cells were counted manually, blinded to the clinical diagnosis. For each patient, four random images were taken and analyzed in order to provide a representative sampling of the tissue. When more than one biopsy was available per region, the means obtained from each biopsy were averaged for each patient.

2.6. Statistical Analysis

Univariate comparisons between two groups (PD vs HC) were made using the t-test for independent samples or Fisher's exact test/Chi-square. For comparisons between three groups (Prodromal PD, Manifest PD, and HC), we used one-way ANOVA followed by Fisher's least significant difference test/Chi-square (with Bonferroni correction for multiple comparisons). We used Pearson correlation analysis to evaluate correlations between clinical, demographic and pathological variables of interest. The measure of agreement between categorical assessments of the two staining methods (e.g. IHC vs. PET) was estimated applying the Cohen kappa. Receiver Operator Characteristic (ROC) curves were constructed to evaluate the ability of pathology to predict the clinical status.

3. CHAPTER THREE

ASN IHC DETECTION IN GI BIOPSY TISSUE FROM THE *DISCOVERY* COHORT AS A POTENTIAL BIOMARKER FOR PD

3.1 Aims

1. Examine whether the detection of ASN in the GI tract is pathologic and can be used as a biomarker in PD.
2. Define what type of biomarker GI ASN may be in the context of PD – predictive, diagnostic, prognostic, phenotypic stratification?
3. Compare our results to the existing literature, which presents contrasting results on the interpretation of ASN detection in the GI tract in PD subjects.

3.2 Results

3.2.1. Clinical and demographic characteristics of the sample

GI biopsy samples were collected from 72 subjects (51 PD, 21 HC) **(Table 3.1)**. In the overall sample, the mean age at biopsy was 65.3 ± 9.9 years. 31 PD subjects were classified as Prodromal PD, and in this group the mean time from GI biopsy to PD diagnosis was 5.8 ± 3.8 years. In the 20 Manifest PD subjects, the mean time from PD diagnosis to GI biopsy was 1.5 ± 1.4 years. The Manifest PD group was significantly older at the time of biopsy compared to both the Prodromal PD group (p=0.031) and the Healthy Control (HC) group (p=0.029). The mean age at PD symptom onset was 66.6 ± 8.8 years and mean age at PD diagnosis was 69.1

± 8.2, and these characteristics did not differ between the Prodromal and the Manifest PD groups.

Table 3.1: Clinical and Demographic Characteristics across clinical groups

	Prodromal PD	Clinically manifest PD	Healthy Controls	P-value
N	**31**	**20**	**21**	-
males	16 (52)	13 (65)	(35)	0.164
Age at biopsy	63 (43 – 83)	69 (57 – 85)	62 (39-86)	**0.014**
Age at diagnosis	69 (56 – 87)	67 (55 – 83)	-	0.342
Biopsy – Diagnosis	5 (1 – 17)	-1 (-5 – 0)	-	**<0.001**
UPDRS III	26 (6 – 41)	30 (7 – 68)	1 (0-10)	**<0.001**
MMSE	28 (23 – 30)	28 (20 – 30)	29 (24-30)	0.181
Constipation	17 (55)	4 (19)	7 (35)	**0.045**
RBD	16 (52)	9 (43)	4 (21)	0.078
Hyposmia	21 (68)	13 (62)	3 (16)	**<0.001**
probability PD	90	90	-	0.925

Values are presented as N, with range or % in parenthesis, as appropriate. Groups were compared with one way ANOVA, independent samples T-test, or Chi-Square Test, as appropriate. *Age at biopsy*, *Age at diagnosis* and *Biopsy – Diagnosis* values are presented as years.

The time lag between GI biopsy and PD diagnosis varied. The earliest GI biopsy was performed 17 years prior to the diagnosis of PD, while the longest duration of disease at the time of GI biopsy was 5 years. On average, the GI biopsy was performed 2.8 ± 4.7 years prior to diagnosis of PD.

Clinical motor symptoms as assessed by the UPDRS motor exam score were significantly more severe in the Manifest PD group compared to the Prodromal group ($p=0.003$) and in both PD groups compared to the HC group ($p<0.001$ for both comparisons), while there were no significant differences in cognitive ability amongst the three groups when assessed with MMSE scores. On the other hand, MOCA scores were significantly lower in both Manifest PD ($p=0.017$) and Prodromal PD ($p<0.001$) compared to HC, but did not differ between the two PD

groups. Prevalence of constipation was significantly different among the three groups (p=0.045) being highest in the Prodromal PD group (present in 57%), followed by HC (present in 33%) and finally in the Manifest PD group (present in 22%). Prevalence of hyposmia was also statistically different (p<0.001) and was seen equally in the Manifest PD group (72%) and in the Prodromal PD group (68%), whereas only 15% of the HC group suffered from a loss of smell. There were no differences in prevalence of RBD between the three study groups. Probability of PD score did not differ significantly between the Manifest and the Prodromal PD groups.

3.2.2. GI Tissue Biopsies

We retrieved a total of 113 tissue blocks from 51 PD patients and 50 tissue blocks from 21 HC, from a total of 200 Discovery participants declaring a previous GI biopsy. Recall bias or gastroscopy/colonoscopy being done without any biopsies being taken explained why we could not find biopsies in the remaining candidates. Staining was performed on tissue sections from one or more GI tract regions from 72 subjects (51 PD and 21 HC). A single GI region was examined in 53 cases (38 PD and 15 HC), 2 regions in 13 cases (9 PD and 4 HC) and 3 regions in 6 cases (4 PD and 2 HC). Number of blocks and cases studied for each region are detailed in **Table 3.2.**

Large bowel was studied in 101 blocks (47 cases, 35 PD and 12 HC), small bowel in 34 blocks (27 cases, 18 PD and 9 HC), stomach in 12 blocks (12 cases, 7 PD and 5 HC), and oesophagus in 11 blocks (9 cases, 7 PD and 2 HC).

Table 3.2: Distribution of stained GI regions across clinical groups

	Gastro-Intestinal Region								
	Oesophagus		Stomach		Small Bowel		Large Bowel and Rectum		Total
IHC	Cases	Blocks	Cases	Blocks	Cases	Blocks	Cases	Blocks	C/B
Parkinsons	7	8	5	11	18	23	34	71	51/113
Healthy Control	2	3	4	5	9	11	12	30	21/50

Values are presented as number of cases/blocks. Chi-Square Test showed there were no statistically significant differences in the proportion of stained biopsies in each GI region between the two clinical groups.

3.2.3. IHC

3.2.3.1 Neuronal staining

There were no significant differences between the two groups of PD and HC in the median neuronal score (p=0.167) and in prevalence of submucosal neuronal ganglia, although the total number of ganglia that could be examined was higher in the PD group due to a greater number of available sections in this group (**Table 3.3**). In a small number of cases (7 PD, 4 HC), myenteric plexus was also present due to whole wall resections of large bowel.

Table 3.3: Baseline histologic characteristics

	PD	HC	P-value
Median Calretinin Score (0-3)	2	2	0.167
Submucosa present	47%	63%	0.115
Submucosal Ganglia (Y/N)	28%	36%	0.504
Number of SM Ganglia (Total)	64	43	0.129
Cases with myenteric plexus (Total)	7	4	0.727

3.2.3.2. ASN

We performed ASN staining on 244 sections (68 biopsies) from PD subjects and 98 sections (28 biopsies) from HC. The mean number of sections stained for ASN per case was 4.75 (range 3-18). All cases had at least one tissue section stained with each of the three antibodies reactive for ASN.

Staining positive for ASN was found in GI tissue sections from 44 subjects [31 PD (21 Prodromal and 10 Manifest), 13 HC] **(Table 3.4)**.

Table 3.4A: Prevalence/Mean score of ASN staining patterns

	PD	HC	P-value
N	51	21	-
Neuronal IHC			
Mucosal (Neuritic)	14 (22)	3 (14)	0.326
Submucosal (Ganglionic)	13 (24)	7 (33)	0.378
Any Intraneuronal (neuritic and/or ganglionic)	22 (37)	7 (33)	1.000
Non-Neuronal IHC			
Epithelial	18 (35)	10 (50)	0.289
Cellular	9 (16)	1 (5)	0.429

Values are presented as N (% within clinical group). Comparisons between groups were made with Chi-Square test.

Table 3.4B: Prevalence of staining patterns by PD clinical subgroups

	Prodromal PD	Manifest PD	HC	P-value
N	31	20	21	-
Neuronal				
Neuritic (Mucosal)	8 (26)	6 (30)	3 (14)	0.461
Ganglionic (Submucosal)	8 (26)	5 (25)	7 (33)	0.795
Any Intraneuronal (neuritic or ganglionic)	14 (45)	8 (40)	7 (33)	0.695
Non-Neuronal				
Epithelial	13 (42)	5 (25)	10 (48)	0.299
Cellular	4 (13)	5 (25)	1 (5)	0.169

Values are presented as N (% within clinical subgroup).

Several different staining patterns were observed (**Figure 3.1**). Two of these were suggestive of a neuronal localization of ASN, with a neuritic distribution of staining in one type (Neuritic staining)(**Figure 3.1A**) and a diffuse, intraneuronal pattern with additional, darker granules present in a portion of these (Ganglionic staining)(**Figure 3.1B**). The latter type of staining often co-localized with submucosal ganglia defined by our neuronal marker in adjacent sections (**Figure 3.2**), while the Neuritic pattern was similar to the mucosal distribution of nerve fibres (**Figure 3.3**). Other types of staining observed in a significant proportion of cases were, on the other hand, suggestive of a non-neuronal localization. The most prevalent of this type of staining was found in the mucosa, specifically in the form of round elements compatible with epithelial cells, which we defined 'Epithelial' staining (**Figure 3.1D-E**) or other cellular components of the mucosa, which we defined 'Cellular' staining (**Figure 3.1F**). In a small number of cases, further staining patterns were also observed, some of which have been described in a recent consensus paper on immunohistochemical detection of ASN (100), including "lacy-granular" staining (**Figure 3G**) and vessel wall staining (**Figure 3H**). These were however extremely rare and were judged to be non-specific staining (and were not included in further analysis).

Figure 3.1: ASN IHC Staining Patterns GI biopsy tissue

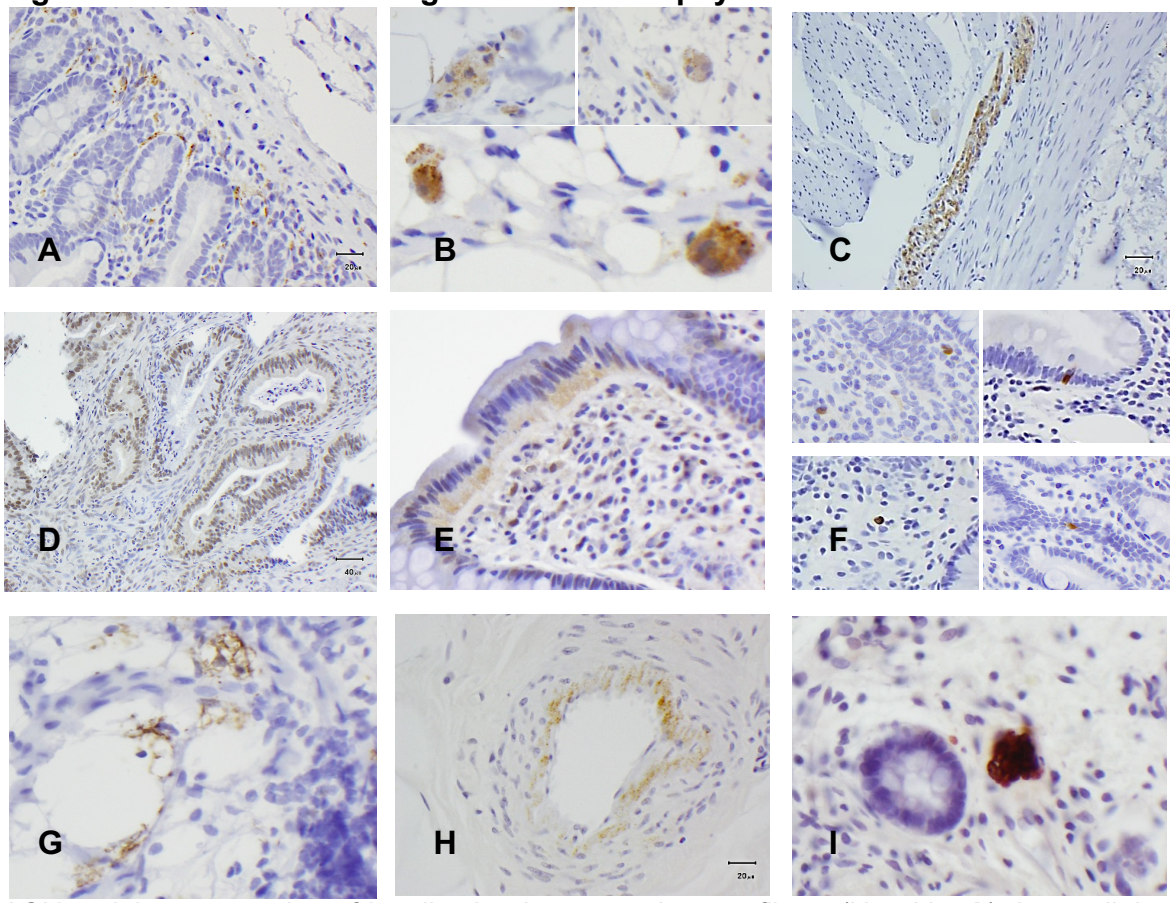

ASN staining suggestive of localization in mucosal nerve fibres (Neuritic, **A**); Intracellular staining with a diffuse distribution occasionally associated with a granular morphology (Ganglionic, **B**); ASN staining in the myenteric plexus (**C**); Non specific staining patterns: Epithelial (**D,E**); Cellular (**F**); Lacy-Granular (**G**); vessel wall staining (**H**); other non specific staining (probable plasma cell, **I**). Antibodies: O2 (**A-C**); pSer129 (**D-I**).

Figure 3.2: Colocalization of ASN staining and neuronal marker

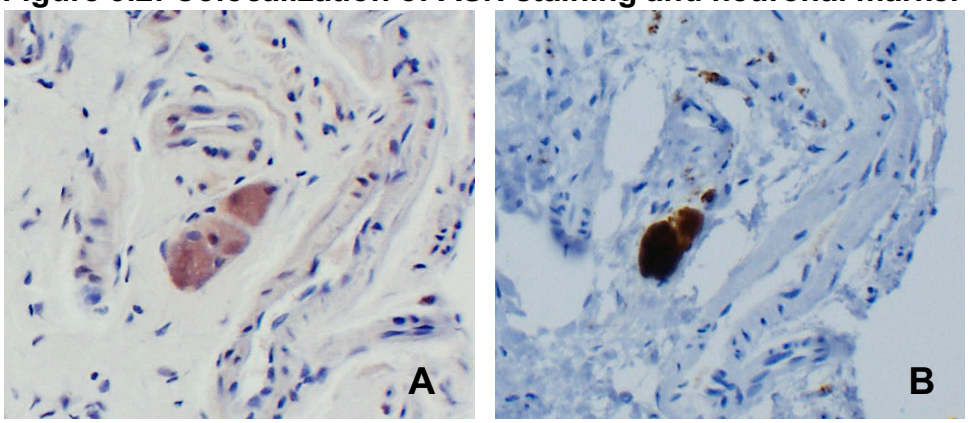

Ganglionic neurons in the colonic submucosa of a prodromal PD case (biopsy taken 1 year before clinical onset) stain positive for ASN-reactive antibody (**A**) and for the colonic neuronal marker Calretinin (**B**). Antibodies: pSer129 (**A**); 5A5 Calretinin (**B**).

Figure 3.3: Neuritic ASN staining in colonic mucosa

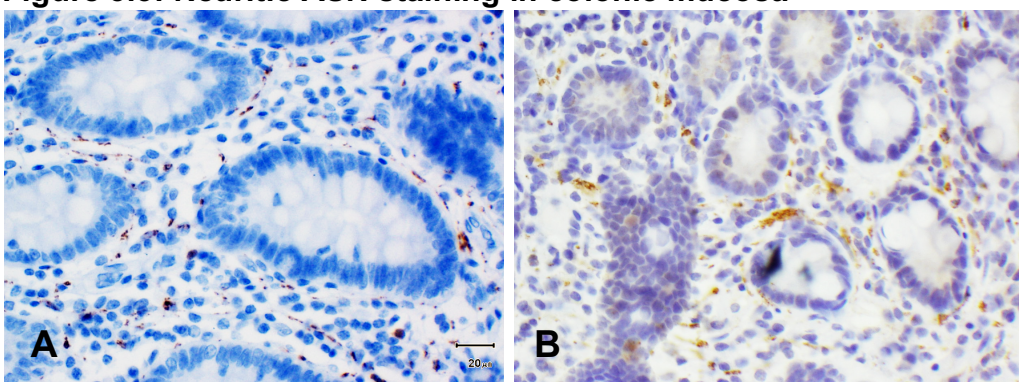

Neuritic staining with ASN-reactive antibodies **(B)** resembles the morphological pattern of staining obtained with the neuronal marker **(A)**, suggesting colocalization. Antibodies: 5A5 calretinin (**A**); O2 (**B**).

Overall, staining for ASN was negative in 263 sections (79% of the whole sample), of which 76 were from HC (82%) and 187 from PD cases (78%).

When we compared the prevalence of the various staining patterns in the two groups of PD and HC and between the three groups of Prodromal PD, Manifest PD, and HC to identify potentially valid markers of disease (**Table 3.4, A-B**), there were no statistically significant differences, although sample size was relatively small. Grouped Intraneuronal (Neuritic or Ganglionic) or non-neuronal (Epithelial or Cellular) staining also did not differ between groups.

Analysis of staining patterns by GI region also revealed a peculiar distribution of specific signals. There was significantly less intraneuronal IHC staining in the large bowel compared to more rostral regions, while the prevalence and intensity of non-neuronal staining of the epithelial type was greater in the distal GI tract (**Table 3.5**).

Table 3.5: Distribution of ASN IHC staining patterns across the GI tract

	Oesophagus	Stomach	Small Bowel	Large Bowel	P-value
IHC Neuronal					
Neuritic (Mucosal)	3 (27)	2 (15)	11 (37)	2 (2)	**<0.001**
Ganglionic (Submucosal)	0	1 (8)	11 (12)	11 (12)	**0.012**
Any Intraneuronal (neuritic or ganglionic)	3 (27)	2 (15)	16 (53)	13 (14)	**<0.001**
IHC Non-Neuronal					
Epithelial	0	0	12 (40)	15 (16)	**0.004**
Cellular	0	0	3 (10)	11 (12)	0.511

Values are presented as N (% within GI region)

Staining patterns were also analysed across the three different ASN antibodies used in this study. Staining with the O-ASN-Ab accounted for 85% of Neuritic staining in the sample, while the T-ASN-Ab showed no Neuritic/Ganglionic staining and the P-ASN-Ab showed Neuritic staining in 2/95 PD sections (15% of all neuritic staining). The latter antibody also revealed the highest prevalence of Epithelial staining (26/131 sections stained with this antibody, 19.8%), but this did not differ significantly between the PD and HC group (20% vs 19.4%, respectively). Interestingly, the T-ASN-Ab showed any kind of staining in only 3 subjects, with an Epithelial pattern in one control and Cellular staining in the mucosa in 2 PD cases (**Table 3.6**). When stained with the O-ASN-Ab, the myenteric plexus consistently showed diffuse staining, both in PD and in HC subjects (**Figure 3.1C**).

Staining for AT8 and for P62 was negative.

Table 3.6: Staining Patterns by Antibody Type across Cases

	WAKO			KM51			O2		
Staining	**Pro**	**Man**	**HC**	**Pro**	**Man**	**HC**	**Pro**	**Man**	**HC**
Neuritic	1	1	0	0	0	0	7	5	3
Ganglionic	3	2	5	0	0	0	7	4	2
Epithelial	10	5	6	0	0	1	2	0	1
Cellular	2	2	0	1	1	0	4	2	1

Values are presented as number of cases. Abbreviations: Pro: Prodromal PD; Man: Manifest PD; HC: Healthy Controls. Comparisons were made with Fisher's Exact Test.

3.3 Discussion

In this study, we aimed to use IHC detection of ASN in the GI tract of a longitudinally followed cohort of clinically well-described PD subjects and HC, to address issues of heterogeneity in interpretation of GI ASN staining which have progressively emerged from previous studies (50).

3.3.1 Sensitivity and Specificity of ASN IHC Staining

PD diagnosis was established clinically, after repeated examinations by neurologists with expertise in movement disorders. According to previous studies, accuracy of diagnosis of PD by neurologists with training in movement disorders is about 85% (35). It would follow that we could expect to find ASN pathology in at least 43 PD subjects in our sample (85% of total sample with a clinical diagnosis of PD), which compares to the actual finding of 11 cases with potentially pathologic ASN staining in the gut (approximately 22% of the PD group), based on the Neuritic ASN staining pattern. Even considering the presence of any kind

of ASN signal, there were 31 PD cases with positive samples, representing about 60% of the PD group. In their recent study, Stokholm and colleagues found a significant difference in the prevalence of pathological staining between PD and control groups, but the absolute prevalence of pathological staining in the PD group was 53%, which similarly to our results represents a lower sensitivity compared to clinical examination (15).

The overall specificity in our study was 67% (i.e. 7 of our 21 HC showed neuronal ASN pathology with at least one of the three types of ASN-reactive antibodies used). The percentage of HC with neuronal ASN pathology in the GI tract has varied a lot between previous studies, with specificity ranging from 90-100% in some studies (7, 8, 10-12), to others reporting 0% specificity with identical neuronal ASN pathology in HC when compared to the PD group (13, 77, 78). Although the prevalence of incidental Lewy body disease (ILBD) (i.e. ASN pathology in the absence of clinical symptoms) is much higher than generally accepted (33, 101), it appears highly unlikely that all healthy subjects included in these studies were affected by ILBD or prodromal PD. Stokholm *et. al.* suggested that using P-ASN-Abs would lead to a lower proportion of healthy controls being positive, based on the hypothesis that phosphorylation is a marker of choice to delineate pathological aggregates from normal, native ASN accumulation (64). However, we found no difference in specificity whether we used O-ASN-Abs or P-ASN-Abs. Furthermore, using P-ASN-Abs, Bottner *et. al.* (77) and Visanji *et. al.* (13) detected neuronal ASN pathology in all of their HC.

Table 3.6: Previous studies on GI ASN pathology

Reference	Antibody	Technique	Tissue Source	Organ – Tissue (region)	PD staining[a]	Non-PD staining[b]
2006 Braak	Syn-1	IHC	Post Mortem	Stomach (fundus, cardia, corpus)	5/5	Healthy Controls 0/5
2006 Bloch	LB509	IHC	Post Mortem	Sacral plexus, vagus, paravertebral ganglia, oesophagus	-	ILBD17/98
2008 Lebouvier	P129Syn	DIF	Ad-Hoc Fresh Biopsy	Colonic submucosa (ascending)	4/5	Healthy Controls 0/5 Chronic Constipation 0/3
2009 Beach	P129Syn	IHC	Post Mortem	Multi-organ (including GI tract)	11/17	Healthy controls 0/23 DLB 5/9; ADLB 1/19; ILBD 1/7
2010 Lebouvier	P129Syn	DIF	Ad-Hoc Fresh Biopsy	Colonic submucosa (ascending and descending)	21/29	Healthy Controls 0/10
2012 Pouclet	P129Syn	DIF	Ad-Hoc Fresh Biopsy	Colonic submucosa (ascending and descending) + rectum	17/26	Healthy Controls 0/9
2012 Shannon	LB509	IHC DIF	Archival Biopsy Material	Colonic submucosa	3/3	Healthy Controls 0/23
2012 Shannon	LB509	IHC	Ad-Hoc Fresh Biopsy + Archival	Colonic submucosa (sigmoid)	9/9	Healthy Controls 2/24 Irritable Bowel 3/24
2012 Bottner	P129Syn	IHC DIF	Ad-Hoc Fresh Biopsy	Colonic submucosa (sigmoid) + rectum	-	Colorectal Carcinoma or Prolapse 11/11
2013 Gold	KM51	IHC	Post Mortem	Colonic submuscosa	10/10	Healthy Controls: 40/77 AD 3/8
2014 Hilton	KM51	IHC DIF	Archival Biopsy Material	Various GI (stomach, duodenum, colon)	7/62	Healthy Controls 0/161
2014 Sanchez-Ferro	KM51	IHC DIF	Ad-Hoc Fresh Biopsy	Stomach (antrum, pylorus)	17/20	Healthy Controls 2/23
2014 Gelpi	KM51	IHC	Post Mortem	Multi-organ (including GI tract)	8/10	5/5 DLB 0/8 AD
2014 Gray	LB509	IHC DIF	Surgical Specimens	Stomach, colon	-	Healthy Controls 20/20
2015 Visanji	LB509 P129Syn	IHC PET blot	Ad-Hoc Fresh Biopsy	Colonic submucosa (descending) + rectum	22/22	Healthy Controls 9/11
2016 Stokholm	MJFR MJF-R13	IHC	Archival Biopsy Material	Various GI (salivary glands, oesophagus, stomach, duodenum, colon, appendix)	30/57	HC 23/90

Abbreviations - AD: Alzheimer's disease; ADLB: Alzheimer's disease with Lewy bodies; DIF: Double immunofluorescence; DLB: Dementia with Lewy bodies; HC: Healthy Controls; IHC: Immunohistochemistry; ILBD: Incidental Lewy body disease; P-ASN-Ab: Antibody reactive for phosphorylated ASN; PET blot: Paraffin-embedded tissue blot; T-ASN-Ab: Antibody reactive for total ASN; [a]: ASN-positive staining in PD cases; [b]: ASN-positive staining in non-PD subjects.

3.3.2 Morphology of ASN IHC Staining

To date, empirical interpretation of morphological features of staining has been the standard approach to judge ASN IHC staining in the GI tract as pathological or non-pathological, and this has been inconsistently effective in differentiating PD cases from controls. In some studies, IHC ASN staining could reliably identify PD cases and was absent or significantly less prevalent in controls (8, 12, 14, 15), while in others (13, 79) and in this study, the same staining patterns were observed in PD cases and controls. In contrast to brain ASN IHC, where morphologically well-defined LBs allow a straightforward identification of pathological ASN staining, it is difficult to define 'pathologic' staining of ASN in the GI tract using IHC. Staining with a density comparable to that of CNS LBs and LNs found in our positive control GI sections was extremely rare and generally lighter, which shed doubts on the actual pathologic nature of the detected protein. In other words, ASN-positive GI tissue staining was often more similar in shade to the background staining often found in the control brain tissue. Furthermore, staining patterns were not always easily traceable to a definite anatomic localization and were at times suggestive of non-specific, non-neuronal and possibly artefactual staining. Indeed, in addition to neurons, ASN is physiologically expressed in hematopoietic (102), endothelial and neuroendocrine cells (103) and in muscle fibers (104). Therefore, the detection of non-neuronal ASN does not necessarily indicate a disease state. Conversely, we cannot currently rule out the potential pathogenic role of non-neuronal ASN either. Neuroendocrine, smooth muscle, and plasma cells, which are highly represented in the GI tract (as opposed to the CNS) and located in close proximity to neuronal elements, could represent possible sources of ASN. ASN may be taken up by neurons from

neighbouring cells or from the extracellular space, and further studies assessing transport of ASN between neuronal and non-neuronal cells would be informative (105-107).

The staining morphology found in this study is broadly similar to previously reported results. In a recent consensus paper, four staining types were identified and defined by morphology and/or localization into *granular lamina propria, perivascular, lacy-granular in submucosa,* and *epithelial-nuclear* (100). In a similar way, we categorised staining into major subgroups based on morphological characteristics and localisation **(Figure 3.1 and Table 3.4)**. For the most part, we agree with the classification adopted by Corbillé et al, although our staining patterns do not entirely overlap with theirs. We did encounter granular staining in the mucosa/lamina propria, which we termed as Neuritic since it is suggestive of localization in peripheral nerve endings as demonstrated by staining with our neuronal marker. We also found several cases with staining of epithelial cells in our colonic biopsies, and we also encountered staining of other, non-epithelial cell-like elements in the mucosa. None of these mucosal patterns segregated into the disease group and were thus judged as non-specific. Similarly, we came across a few instances of lacy-granular and vessel wall staining, which were also suggestive of a non-specific signal. In addition to the staining patterns described by Corbillé et al, we found a group of sections containing submucosa with staining of neuronal ganglia of both a diffuse and granular pattern, which we defined Ganglionic, but this pattern also failed to discriminate cases from controls.

3.3.3. Antibody Type and Staining Results

In this study, three antibodies were chosen to detect ASN: KM51 (T-ASN-Ab); pSer129 (P-ASN-Ab); and O2 (O-ASN-Ab). The KM51 and pSer129 antibodies have previously been applied to GI ASN detection **(Table 3.6)**, making our results comparable, whilst O-ASN-Abs were applied to GI ASN detection for the first time in this study (58, 96).

Hilton and colleagues reported staining with P-ASN-Abs to be more extensive compared to that obtained with T-ASN-Abs such as KM51, although this was not formally quantified (11). Rather surprisingly, other studies found T-ASN-Abs to be more sensitive and specific in detecting PD patients than P-ASN-Abs (12, 13). IHC detection of ASN with P-ASN-Abs was previously demonstrated in HC (13, 77), and western blot analysis failed to detect significant differences in expression levels of phosphorylated ASN between PD and HC groups (108). One study described more intense staining with T-ASN-Abs compared to P-ASN-Abs in neurologically unimpaired subjects but also an age-related increase in the density of the latter, suggesting that P-ASN staining may be age-related (77). Furthermore, case-control studies reporting 100% specificity for enteric ASN detection in PD do describe immunoreactivity with both T- and P-ASN-Abs in control cases but interpret this as “normal” or “non-specific” staining (10, 11).

These results highlight the need for a better understanding of ASN phosphorylation in PD pathogenesis. Although the majority of Lewy pathology is phosphorylated at Ser129 (64), whether phosphorylation actually accelerates the aggregation process, at what conformational stage of ASN fibrillization it occurs, and whether it mediates neurotoxicity at all remain controversial issues.

Overall, in this study the majority of stained sections showed no specific staining using ASN-Abs. Indeed, staining was completely absent with all 3 antibodies in 91 sections, of which 27 were from HC (64% of the HC group) and 64 from PD cases (60% of the PD group). There were however, some trends for particular types of staining patterns using different antibodies. For example, Epithelial type staining was highly prevalent using the P-ASN-Ab, while Neuritic staining was more prevalent with the O-ASN-Ab, suggesting the latter type of antibody might be more sensitive in detecting putatively pathologic staining patterns. Indeed the O2 antibody showed the highest sensitivity for neuronal (Neuritic/Ganglionic) staining, with 23/51 PD patients (42%) showing this pattern compared to 5/21 HC (24%), although this difference was not significant (0.316, chi-square test). Oligomeric forms of ASN are increasingly recognized as a key player in the pathogenic process of misfolding and aggregation of ASN, and importantly they can be expected to be more abundant in the early phases of PD pathogenesis (58).
Interestingly, the T-ASN-Ab showed staining in only 3 subjects, with an Epithelial pattern in one control and Cellular staining in the mucosa in 2 PD cases, thus this antibody was both the most specific and least sensitive.

Inter-laboratory comparisons have shown that different ASN-Abs do not significantly differ in terms of LB counts but vary considerably in their ability to reveal ASN-immunoreactive staining in the neurites and axonal terminals (109-111). This antibody-dependent variability in ASN expression is well known in the CNS but has recently also been demonstrated in the GI tract. Aldecoa and colleagues showed that some Abs detected diffuse, synaptic-type staining reminiscent of physiological immunoreactivity, whereas others preferably labelled

coarse ASN aggregates in the ganglionic soma and neurites that were considered to be pathological (112). Non-neuronal staining was also seen in the epithelial cells of gastric glands and vessel walls, in the smooth muscle cells of the muscularis propria and in the leucocytes of the submucosa, as has been described by others (77).

3.3.4 Insights from Individual cases

Assessment of serial sections of GI tissue in a few cases in this study shed further doubts on the viability of GI ASN detection as a PD biomarker. Our positive control subject, who had a post mortem diagnosis of PD, showed Neuritic staining suggestive of pathologic deposition of ASN in 3 out 20 serial sections of large bowel and appendix, yielding a sensitivity of 15%. In another PD biopsy with abundant fixed tissue following whole wall resections, 10 serial sections of stained with T-ASN-Abs failed to disclose any ASN accumulation, despite the presence of abundant nervous tissue with many submucosal ganglia.

The time interval between GI biopsies and PD diagnosis was such that there were few biopsies taken a significant amount of time after the onset of PD. In other words, the available pathologic material for this study allows only limited speculation on the long-term effects of PD duration on GI pathology. On the other hand, the timing of biopsies was such that most of the tissue available antedated the diagnosis of PD, which was ideal to study potential pre-symptomatic markers of PD. We did not detect any ASN signal specific to the Prodromal PD group, and the prevalence of the neuronal type of staining was comparable to that found in the Manifest PD group, which suggests there is no cumulative effect over time.

4. CHAPTER FOUR

PET-BLOT DETECTION OF ASN IN BRAIN AND GI TISSUE (AS-PET-BLOT)

4.1 Aims

1. Optimize and apply the PET-Blot to detection of ASN in CNS tissue
2. Apply the PET-Blot to detection of GI ASN, and compare results in terms of sensitivity and specifity with IHC.
3. Gain insight into the nature of the pathological species of ASN in (1) the brain and (2) the GI tract, based on results with PET-Blot.

4.2 Background

In this study, approach to PET-Blot detection of ASN pathology in PD subjects proceeded in two steps. The PET-Blot protocol was initially optimized on brain tissue (see Methods chapter for full details on optimization), which was defined ASN PET-Blot (AS-PET-Blot), and this was subsequently applied the optimized method to paraffin-embedded biopsies from the GI tract.

For optimization on brain tissue, the AS-PET-Blot was applied to the striatum of PD cases. This region is typically spared or only minimally involved in PD pathology according to the widely accepted Braak staging scheme (39). On the other hand, the striatum receives nerve fibres from the SN, which is an established region of neurodegeneration in PD, and it could thus represent a critical node in the pathogenic mechanism of PD. While IHC analysis of the

striatum in PD does not usually disclose presence of the typical aggregates of ASN that characterize the PD brain, i.e. LBs, it is possible and indeed likely that pathological involvement of the striatum may escape detection with traditional IHC due to limited sensitivity.

4.3 Results

4.3.1. AS-PET-Blot on brain tissue

While the bulk of the optimization of the AS-PET-Blot was carried out on the striatum of a subject with PD Braak stage 6 disease, additional brain regions, including brainstem and cingulate cortex from several subjects with neuropathologically confirmed PD were also stained with AS-PET-Blot in an exploratory manner. In most cases, with AS-PET-Blot LBs and LNs were detected in the same regions that disclosed pathology with IHC. At the level of the striatum, in addition to Lewy pathology, the AS-PET-blot disclosed dot-like, ASN-positive staining localized in the pallidal and putaminal grey matter, suggestive of synaptic localization, which was not detected with traditional IHC applied to the same regions (**Figure 4.1**). This type of staining was not detected in the other examined regions (brainstem and cingulate cortex).

Figure 4.1: Comparison of IHC and PET-Blot for detection of ASN in the striatum of a PD subject

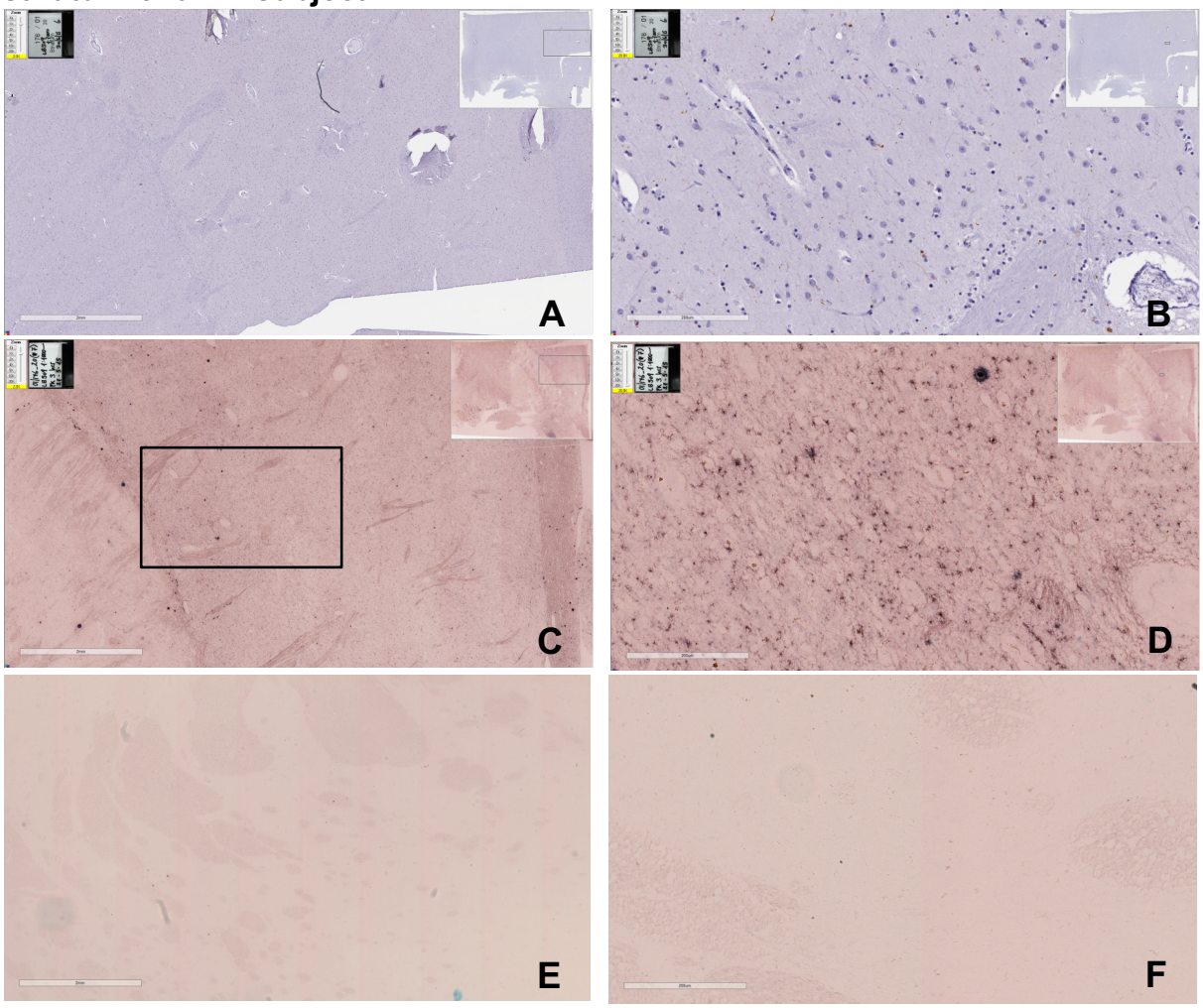

Low (20X, **A**, **C**, **E**) and high (200X, **B**,**D**,**F**) magnification images depicting superior sensitivity of AS-PET-Blot (**C** and **D**) vs traditional IHC (**A** and **B**) in detecting ASN pathology. Note the two discreet patterns of staining highlighted by the AS-PET-Blot, with classical LB-like inclusions alongside finer, dot-like staining throughout the neuropil (**D**). AS-PET-Blot applied to the striatum of a healthy control revealed no staining (**E** and **F**); Antibody: LB509, 1:10000.

4.3.2. AS-PET-Blot on GI biopsy tissue from the *Discovery* cohort

Clinical and demographic characteristics of the sample are summarised in **Table 3.1**.

89 blocks were stained with PET-Blot technique from 51 PD patients and 21 HC, so that at least one tissue block was stained from each case.

Table 3.1: Clinical and Demographic Characteristics across clinical groups

	Prodromal PD	Clinically manifest PD	Healthy Controls	P-value
N	**31**	**20**	**21**	-
males	16 (52)	13 (65)	(35)	0.164
Age at biopsy	63 (43 – 83)	69 (57 – 85)	62 (39-86)	**0.014**
Age at diagnosis	69 (56 – 87)	67 (55 – 83)	-	0.342
Biopsy – Diagnosis	5 (1 – 17)	-1 (-5 – 0)	-	**<0.001**
UPDRS III	26 (6 – 41)	30 (7 – 68)	1 (0-10)	**<0.001**
MMSE	28 (23 – 30)	28 (20 – 30)	29 (24-30)	0.181
Constipation	17 (55)	4 (19)	7 (35)	**0.045**
RBD	16 (52)	9 (43)	4 (21)	0.078
Hyposmia	21 (68)	13 (62)	3 (16)	**<0.001**
probability PD	90	90	-	0.925

Values are presented as N, with range or % in parenthesis, as appropriate. Groups were compared with one way ANOVA, independent samples T-test, or Chi-Square Test, as appropriate. For *Age at biopsy*, *Age at diagnosis* and *Biopsy – Diagnosis,* values represent years.

The most frequently occurring signal we observed with this technique was present in more than half of the examined blocks and consisted of staining along the borders of the mucosal glands or crypts (*peri-crypt* staining) **(Figure 4.2 A-B**).

Another pattern of staining was also seen in 17 (19%) out of 89 examined blocks, which suggested possible ASN deposition (*ASN-localised* staining **(Figure 4.2 D-F)**.

Figure 4.2: GI tract ASN Staining Patterns with AS-PET-Blot

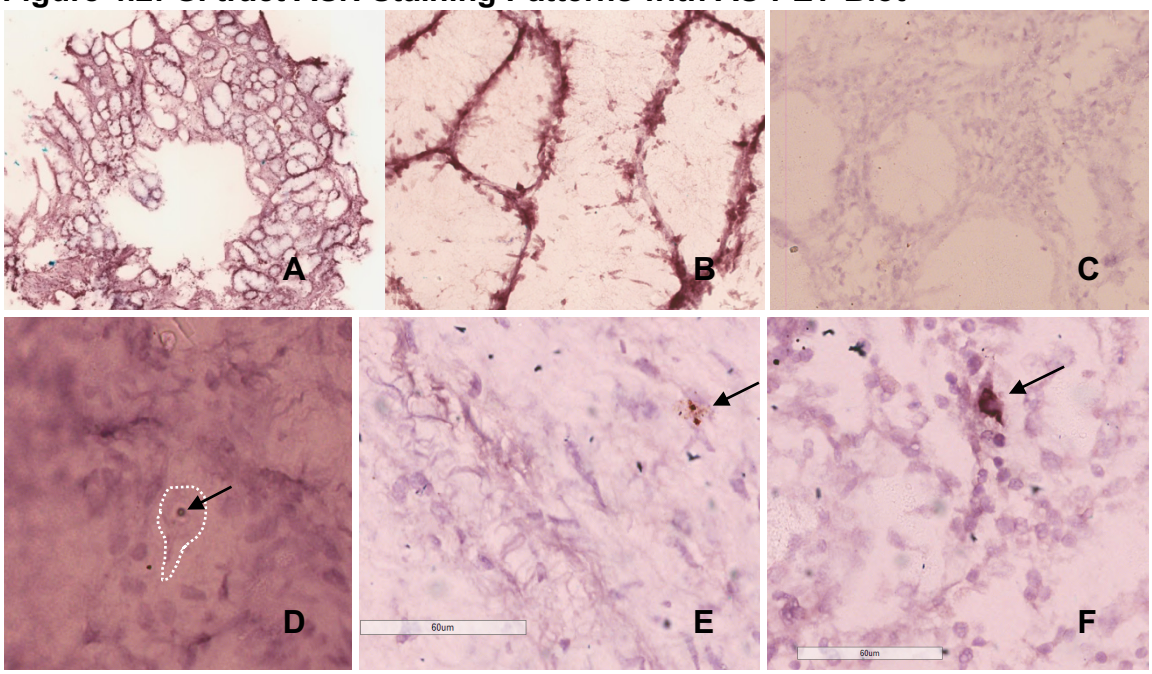

Peri-crypt enhanced AS-PET-Blot signal in colonic tissue of a PD case at low (**A**) and high (**B**) magnification. Absence of a similar signal in colonic tissue of another PD case is seen in **C**. Other staining patterns possibly suggestive of aggregated ASN were also detected occasionally (arrows in **D-F**). Antibody LB509 1:10000.

No statistical differences in either *peri-crypt* or *ASN-localised* staining patterns were found between the study groups (see **Table 4.1**). ROC curve analysis showed that *ASN-localised* PET-blot signal was not a reliable predictor of the clinical status (AUC=0.398).

The prevalence of *ASN-localized* signal was not significantly different in relation to constipation, RBD or hyposmia. The PET-blot *ASN-localised* signal was equally distributed across the GI tract **(Table 4.2)**.

Table 4.1: Prevalence of staining patterns with AS-PET-Blot

	PD	Prodromal PD (N=31)	Manifest PD (N=20)	HC (N=21)	PD vs HC (P-value)	Prodromal PD vs Manifest PD vs HC (p-value)
ASN-localized	9 (18)	5 (16)	4 (20)	8 (38)	0.063	0.170
Peri-crypt	30 (59)	19 (61)	11 (55)	12 (57)	0.217	0.413

Values are presented as N (% within clinical group). Comparison between groups was made with chi-square test.

Table 4.2: Distribution of staining with AS-PET-Blot in the GI tract

	Oesophagus	Stomach	Small Bowel	Large Bowel	P-value
ASN-Localized	0	0	7 (32)	11 (27)	0.392
Peri-crypt	1 (33)	3 (60)	9 (41)	29 (71)	0.100

Values are presented as N (% within GI region). Statistical comparisons were made with Fisher's Exact Test.

4.4 Discussion

4.4.1 AS-PET-blot in PD Brain

4.4.1.1. Characterisation of staining

We have applied the AS-PET-Blot technique to detect possible ASN pathology in the striatal regions of brains affected by PD. Our interest in the PET-Blot approach stemmed from studies reporting increased sensitivity for ASN pathology and of previously undetected morphology of ASN staining, compared to traditional IHC (85, 95).

The first suggestion that PD striatum may indeed be involved in ASN deposition came from Duda et al, who used monoclonal antibodies raised against nitrated/oxidized ASN and revealed abundant pathology in the putamen of subjects with neuropathologically confirmed PD and DLB, with or without

concomitant AD pathology (113). They obtained diverse staining morphology across their sample, with both typical Lewy pathology and unusual patterns consisting of grain-like accumulations of ASN. Using double immunofluorescence, they demonstrated colocalization of the ASN staining with axonal markers (neurofilament) but not with dendritic markers (MAP2) (113).

Using the PET-blot technique, Kramer et al found a novel ASN staining morphology in DLB subjects different to the classical juxtanuclear globose inclusions typically seen in these patients. This staining was characterized by a dot-like, granular signal, which they detected in the neuropil of the cingulate cortex.

(95). They concluded that this staining reflected pre-synaptic ASN aggregates, and that it was this pathology that was driving the clinical manifestations of DLB, rather than perikaryonal LBs, whose relatively low density could hardly account for the symptoms. Using the protein aggregate filtration assay (PAF), these authors demonstrated the presence of small ASN aggregates, in addition to typical Lewy bodies, in brain homogenates from DLB cases. Synaptosomal markers (syntaxin and synaptophisin, taken to be representative of the synapse) migrated to the same sucrose gradient peak as the small ASN aggregates, which was taken as evidence that the dot-like staining on their PET-Blot slides was indeed pre-synaptic ASN staining (95). Unfortunately, the PET-Blot and the PAF assay are by definition conducted on different tissue specimens (i.e. paraffin embedded tissue slides and brain homogenates, respectively), thus it remains to be proven that findings from one of these two techniques, albeit from the same cases, are explanatory of results obtained with the other.

Neumann and colleagues reported high density of ASN-positive PET-blot staining in several brain regions of subjects with PD, DLB, MSA or neurodegeneration with brain iron accumulation (NBIA). In addition to typical LBs, they described 'neuritic' staining, which was more intense with the PET-Blot compared to IHC. While they reported the striatum to be among the brain regions involved by this pathology, they unfortunately did not show relevant images of staining in this region (85).

In this study, neuropil-like staining was detected in the striatum of PD cases, similar to that reported by Kramer et al in the cingulate cortex of DLB cases, and to our knowledge we are the first to present images of this staining (**Figure 4.1, D)**(95). As previously suggested by Neumann and colleagues, neuritic pathology, possibly localized in the nigro-striatal synaptic nerve terminals, could underlie reduced neuronal connectivity and clinical manifestations in PD/DLB (85).

4.4.1.2. Methodolical issues

Previous studies have adopted a wide range of conditions with regards to PK concentration and duration/temperature of PK incubation (82, 84-86, 95)(**Table 4.3**).

PK concentrations have ranged from 20 ug/ml to 250 ug/ml. Looking at PK activity on *in vitro* ASN 16kDa monomers, Neumann and colleagues detected ASN fragments with antibodies reactive for C-terminal epitopes at low PK concentrations, while for PK concentrations above 10ug/ml, ASN fragments were further truncated C-terminally, leaving only the non-amyloid component (NAC) core fragment, and this observation provides some insight into the mechanism of action of PK on ASN fibrils (85), demonstrating that PK sensitivity is highest at the

N terminus of ASN, followed by the C terminus, with the highest resistance in the core NAC fragments (85).

PK incubation times have varied between 8 and 14 hrs. Our initial method was based on published literature, which often applied incubation times of 8 hrs at 55°C (82, 95)**(Table 4.3)**. We found PK incubation time to have a significant impact on tissue damage, with incubation times exceeding 3 hrs associated with significant tissue deterioration **(see Chapter 2, section 2.4.1 and Table 2.1)**.

Antibodies used to detect ASN with PET-blot have also varied, both in epitope reactivity (phosphorylated ASN vs total, or wild-type ASN) and in concentrations used (**Table 4.3**). We attempted PET-Blot with antibodies reactive for oligomeric ASN, but these antibodies were not compatible with PK incubation times above those routinely used in antigen retrieval (i.e. 5-10 minutes).

The most commonly used detection system is based on the alkaline phosphatase reaction, and only one study used biotin-streptavidine complex + Diaminobenzidine (DAB) (84), and this study examined tau and beta-amyloid pathologies in the context of AD, rather than ASN. We found the alkaline phosphatase approach provided a stronger signal, which facilitated interpretation of staining by partially compensating imaging limitations related to the use of NCMs. NCMs cause a degree of reduction in transparency despite use of xylene for membrane clarification.

Table 4.3: Previously applied protocols for PET-Blot with PK digestion

Reference	Schulz-Schaffer 2000	Neumann 2002	Neumann 2004	Kramer 2007	Moh 2010
Sample	CJD (N=42) Other ND (N=24)	PD (4); DLB (5); NBIA (1); MSA (2); AD (2); CT (2)	LBD cases (N=13)		AD
PK concentration (ug/ml)	250	50	50	250	20
PK incubation time (hrs)	8	8 - 14	8 - 14	8	Not specified
Antibody (Ab)	PrP	ASN (15G7)	ASN (15G7)	ASN (LB509)	4G8 PHF-1
Ab dilution	-	1:200	1:50	1:10000	Not specified
Ab incubation time (hrs)	1	8	8	1	1 -12
Visualization method	Dissecting microscope	Dissecting Microscope	Dissecting Microscope		Not specified (light microscope)
Regions examined	Cortex, basal ganglia, brainstem	SN, Striatum, Hippo, Temporal Cortex	Medulla, SN, Cingulate Cortex, ParaHippo, Frontal Cortex		Hippo
Chromogen	Alkaline Phosphatase (NBT/BCIP)	Alkaline Phosphatase (NBT/BCIP)	Alkaline Phosphatase (NBT/BCIP)		Biotin-Streptavidine + DAB
Type of membrane	Nitrocellulose	Nitrocellulose	Nitrocellulose	Nitrocellulose	PVDF

Abbreviations - CJD: Creutzfeldt-Jabob Disease; ND: Neurodegenerative Disease; PD: Parkinson's Disease; NBIA: Neurodegeneration with Brain Iron Accumulation; MSA: Multiple System Atrophy; AD: Alzheimer Disease; CT: Control; LBD; Lewy Body Disease; PrP: Prion Protein; ASN: Alpha-synuclein; SN: Substantia Nigra; ParaHippo: Parahippocampal cortex.

4.4.1.3. Current limitations of the AS-PET-Blot technique

While our results are intriguing and merit further investigation, the PET-Blot technique has methodological issues that may limit its applicability. The main difficulties were poor visualization and tissue damage.

Previous studies have also touched upon limits of visualization with dissecting microscopes, which rarely focus to magnifications required to observe this type of pathology (86). To offset the gross limitations in visualisation that often characterise this technique, the type of staining obtained would ideally need to be significantly less 'equivocal' than that generated with IHC, i.e. more specific.

Initial visualization of PET-Blot treated sections was performed with a dissecting microscope, which allowed for limited morphological detail. We have worked on optimizing visualization, by inducing transparency in the NCM slides allowing observation under a light microsocpe, but this hardly allows for the optimal visualization that one obtains with IHC with additional counterstaining with haematoxylin, which is not possible with the PET-blot. Furthermore, transparency induced by immersion in xylene only lasts a few hours, thus multiple immersions are frequently necessary, with possible alteration of signal.

Scanning of slides with an automated slide scanner (Aperio Scanscope) allowed for improved analysis of staining and obviated the need for multiple immersions in xylene, as sections were saved to a central server and could be retrieved for further analysis.

Tissue preservation is influenced by several factors, including PK concentrations, incubation times and temperature. There is striking variability in these parameters in the literature **(Table 4.3)**, which suggests a particular combination of these, and 'circumstantial' variability of materials such as batch-related PK concentration may play a significant role in the final quality of staining signal.

4.4.2 AS-PET-Blot in GI biopsy tissue from the *Discovery* cohort

Despite optimisation of the PET-Blot on neuropathologically confirmed PD brain tissue, we were unable to obtain a similar, entirely specific signal in GI tissue of subjects with clinically diagnosed PD. This may be due to several reasons. Firstly, GI tissue has a different composition compared to CNS, and this may at least partly explain the higher propensity of GI biopsy tissue to be morphologically damaged by PK incubation at high temperatures. Assessment of different PK concentrations and incubation temperatures resulted in application of lower PK doses and shorter incubation times, which did improve morphological quality of the stained sections, although a part of the GI biopsies still showed significant morphological damage with these milder conditions.

ASN conformations may differ in prevalence between gut and brain, with the former hosting a smaller proportion of fibrillary forms of ASN that are preferentially detected by the AS-PET-Blot. While IHC studies have detected ASN deposition in GI tissue, given the nature of the antibodies used one cannot draw conclusions on the conformational characteristics of the detected ASN (7, 10-12). In other words, most antibodies used in IHC can distinguish between phosphorylated and non-phosphorylated forms of ASN but cannot distinguish between monomeric, oligomeric or fibrillary forms – this must be deduced by observation of staining morphology.

The prevalent type of staining we observed does not suggest localization to specific, anatomically defined structures in the GI tract. The proximity to the glandular structures of dense, rather ill-defined staining could represent

extracellular accumulation of fibrillary ASN **(Figure 4.2)**. However, if this were indeed the case, similar findings in HC would need further explanation **(Table 4.1)**. Interestingly, cross-linking studies in healthy rat and human gut have suggested the native state of ASN in ENS neurons may differ from that found in brain neurons (114). Thus, the prevalence and physiological (or pathological) role of specific ASN conformations may differ between CNS and PNS.

To our knowledge, only one previous study has applied the PET-Blot to detection of ASN in the GI tract in PD cases and HC. Visanji and coworkers could not find distinctive features in ASN staining that could distinguish between the two clinical groups (13). Indeed, in their study all 11 control cases showed some degree of staining with PET-Blot. Their control cases were obtained from cancer screening programs, and it is not clear whether neoplasms were excluded prior to including these samples in their study. CNS tumors of various lineages have been linked to altered expression of 1 or more members of the synuclein family, (115, 116) and γ-synuclein is a well-established marker of breast cancer (117). Thus, mechanisms related to colonic neoplasms could have affected the state of aggregation of ASN in these subjects.

Comparison of our signal to the images presented in their study would suggest a more coarse, less defined signal in our study, which could be due to the different PK digestion conditions that were applied in the two studies, as they used higher PK concentrations and incubation times (250 ug/ml for 8hrs vs 50 ug/ml for 3hrs in our sample)(13).

Overall, in our hands the PET-Blot has proven to be time-consuming (2-3/day procedure) and rather unpredictable, with frequent technical issues including tissue damage and lengthy procedures to obtain optimal visualization. We would

not currently recommend using this technique for routine assessment of pathological tissue, and the inability of PET-Blot staining to differentiate PD cases and controls would enforce this opinion. However, further optimisation of this technique, with particular attention to visualization using scanning software programs could provide the necessary fine tuning for a more reliable interpretation of the PET-blot signal.

5. CHAPTER FIVE

PLA DETECTION OF ASN IN BRAIN AND IN GI BIOPSY TISSUE (AS-PLA)

5.1 Aims

1. Apply the optimized PLA for the detection of ASN in (1) the brain and (2) GI biopsy tissue from the *Discovery* cohort.
2. Assess AS-PLA GI tissue staining results in terms of sensitivity/specificity for diagnosis of PD and possible further applications as a biomarker for PD.
3. Gain insight into the nature of the pathological oligomeric species of ASN in (1) the brain and (2) GI tract based on results with the PLA staining.

5.2 Results

5.2.1. AS-PLA on Brain Tissue

Several brain regions from 10 subjects with CNS Lewy pathology were stained with AS-PLA. Prevalence of AS-PLA and ASN-IHC O2 staining in the various brain regions examined is summarized in **Table 5.1**. The PD Braak staging scheme was used to provide information on the extent and distribution of pathological changes in the different subjects analysed, but it must be clarified that not all analysed subjects would meet the criteria necessary for a definite diagnosis of PD. Specifically, all subjects with PD Braak stages 1 – 3 did not manifest PD clinical symptoms and should thus be considered cases of ILBD.

Table 5.1: AS-PLA and ASN IHC in different brain regions of PD subjects

	Braak	Med	Pons	SN	CA2	Amy	Str	CG	TC	FC
PD1	1			PLA 0 O2 0			PLA 3 O2 1			
PD2	1	PLA 1 O2 1	PLA 1 O2 0	PLA 1 O2 0	PLA 0 O2 0	PLA 0 O2 0	PLA 0 O2 0	PLA 0 O2 0	PLA 0 O2 0	PLA 0 O2 0
PD3	1	PLA 1 O2 1	PLA 0 O2 0	PLA 1 O2 0						
PD4	3			PLA 0 O2 2			PLA 0 O2 0			
PD5	3	PLA 0 O2 2	PLA 0 O2 1	PLA 0 O2 1	PLA 0 O2 0	PLA 0 O2 0	PLA 1 O2 0	PLA 0 O2 0		
PD6	3			PLA 1 O2 3			PLA 0 O2 2			
PD7	5	PLA 1 O2 2	PLA 1 O2 2	PLA 2 O2 2	PLA 1 O2 1		PLA 1 O2 1	PLA 2 O2 2		PLA 0 O2 0
PD8	6	PLA 0 O2 1	PLA 1 O2 1	PLA 2 O2 1		PLA 2 O2 1	PLA 3 O2 1	PLA 2 O2 1		PLA 2 O2 1
PD9	6	PLA 0 O2 2	PLA 0 O2 2	PLA 0 O2 2	PLA 0 O2 na	PLA 0 O2 2	PLA 0 O2 2	PLA 0 O2 2	PLA 0 O2 2	PLA 0 O2 1
PD10	6	PLA 0 O2 2	PLA 0 O2 2	PLA 0 O2 2	PLA 0 O2 2		PLA 0 O2 1	PLA 0 O2 2		PLA 0 O2 1
Total[a]	-	7	7	10	5	4	9	6	2	5
PLA prevalence	-	4/7	3/7	5/10	1/5	1/4	4/9	2/6	0/2	1/5
O2 prevalence	-	7/7	5/7	7/10	2/4	2/4	6/9	4/6	1/2	3/5
Mean PLA	-	0.43	0.43	0.7	0.2	0.5	**0.89**	0.67	0	0.4
Mean O2	-	**1.57**	1.33	1.30	0.75	1.33	0.89	1.17	0.75	0.5

Abbreviations – Amy: Amygdala; Braak: PD Braak Stage (range 1-6); CA2: CA2 region of the Entorhinal Cortex; CG: Cingulate Cortex; FC: Frontal Cortex; Med: Medulla; O2: Antibody for IHC ASN detection; PLA: Proximity Ligation Assay; SN: Substantia Nigra; Str: Striatum; TC: Temporal Cortex; [a]: Total number of cases stained (N).
Range for semiquantitative scoring of PLA and O2 is 0 (no staining) – 3 (high staining signal).

With AS-PLA, we detected diverse staining patterns (**Figure 5.1**).

Figure 5.1: AS-PLA staining of intraneuronal inclusions

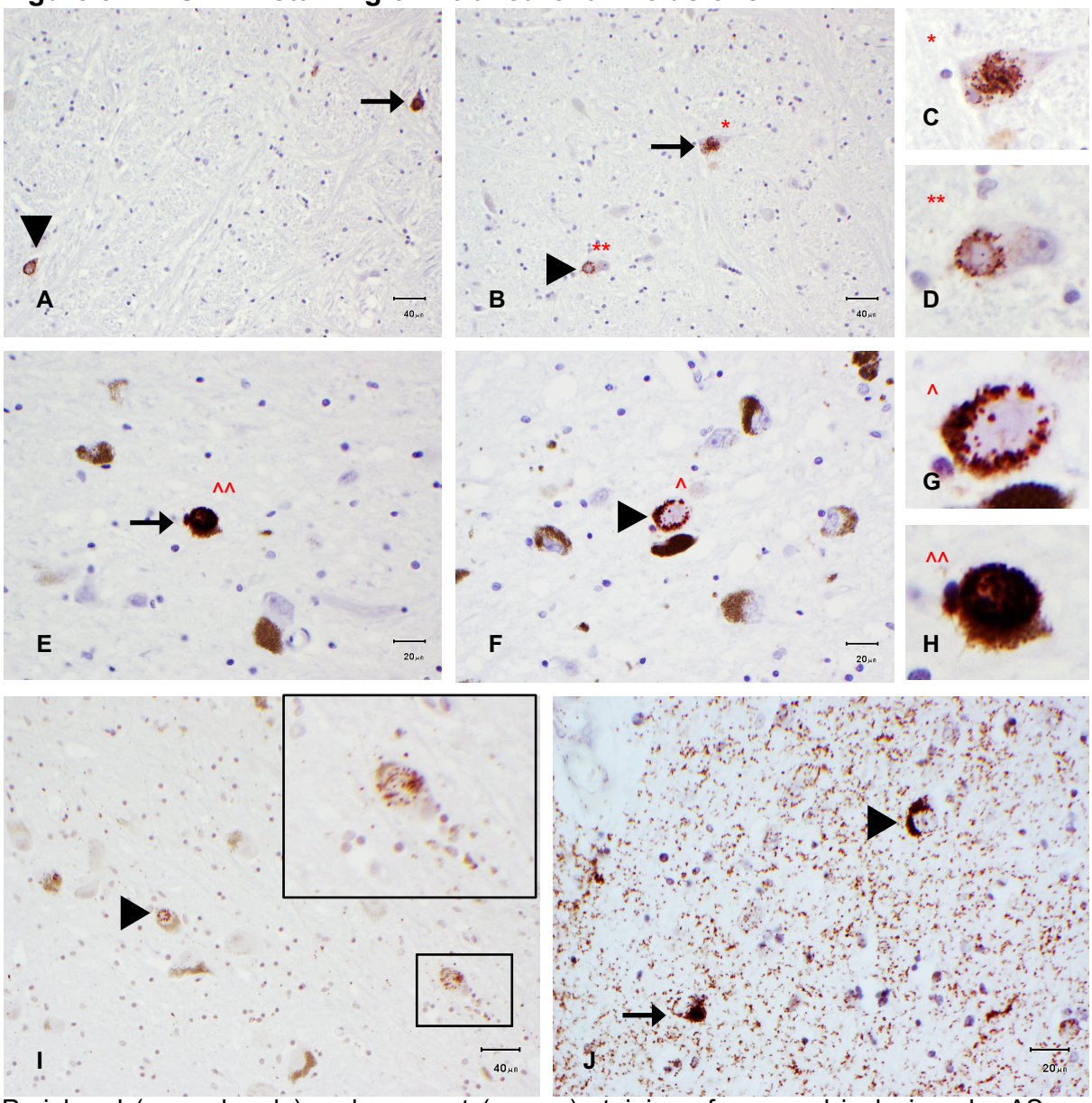

Peripheral (arrow heads) and compact (arrows) staining of neuronal inclusions by AS-PLA in the pons **(A-D),** substantia nigra **(E-I)** and entorhinal cortex **(J)** of the PD brain. Note the rather diffuse, intracytoplasmic staining pattern of a neuron in the substantia nigra in **I** (box and inset), while several surrounding neurons appear healthy.

We categorized staining as *diffuse* when it consisted of dot-like, granular staining which could be found both at the intra- **(figure 5.1,I)** and extracellular **(figure**

5.1,J; 5.2,A-E) level. This staining pattern involved the grey matter and tended to spare the white matter, although we found regions of the brainstem, specifically the pons, where the white matter seemed to be affected as well. We also observed more dense, round staining of compact formations suggestive of inclusions of aggregated ASN, and we defined this as *cellular* staining. This type of staining was at times limited to the peripheral rim of the inclusion-like structures suggestive of LBs **(Figure 5.1)**. The density of cellular staining of inclusions varied, suggesting detection of different stages of development of ASN inclusions **(Figure 5.1,I)**.

We performed semi-quantitative assessment of AS-PLA signal and of IHC staining with the O2 antibody in all stained regions, assigning a score of 0 – 3 (none, mild, moderate, severe staining) **(Figure 5.2)**. For each region, we calculated the mean scores of AS-PLA and O2 staining both in the overall sample **(Table 5.2)** and subdivided by PD Braak stages **(Table 5.3)**.

Figure 5.2: AS-PLA and O2 IHC semiquantitative grading

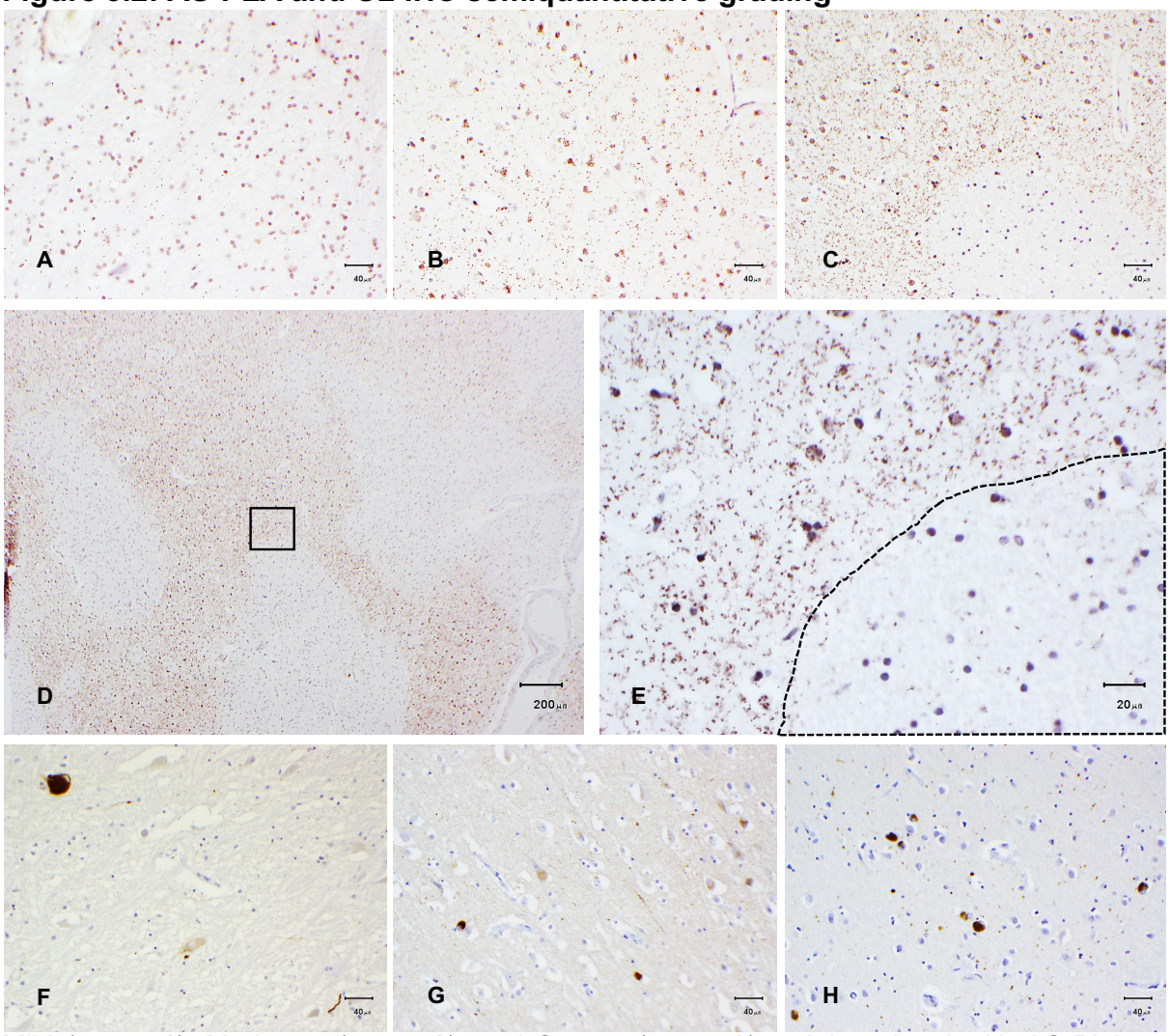

Mild (score=1), Moderate (score=2), and Severe (score=3) staining signal with AS-PLA (**A**,**B**, and **C**, respectively) and O2 ICH (**F**, **G**, and **H**, respectively). AS-PLA signal was almost exclusively present in grey matter regions and tended to spare the white matter (small magnification of the striatum in **D** showing the sparing of the white matter; area enclosed in black box in **D** is magnified in **E**, with dotted line enclosing the white matter, where there is no AS-PLA staining). **(A):** Medulla from PD3; **(B):** SN from PD8; **(C-E):** Striatum from PD1; **(F):** Medulla from PD2; **(G):** Temporal cortex from PD9; **(H):** Amygdala from PD8. See **Table 5.1** for further information on individual cases.

We also semiquantitatively assessed density of alternative staining morphology (*diffuse/cellular*) in each region **(Table 5.4)**.

Table 5.2: AS-PLA and O2 regional staining in the overall sample

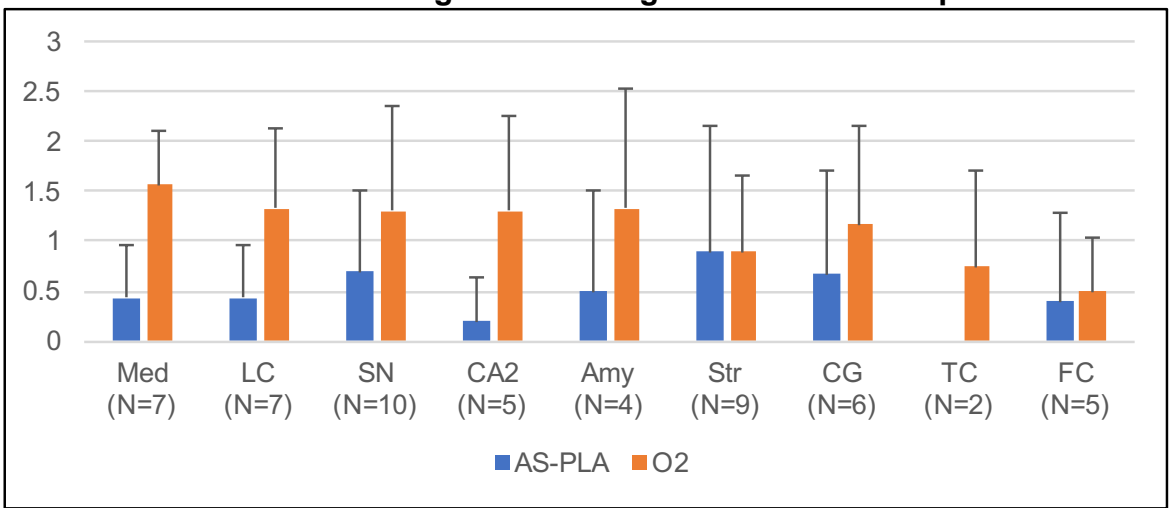

Mean semiquantitative scores for AS-PLA (blue columns) and O2 IHC (orange columns) staining by brain region, in the overall sample. Amy: Amygdala; CA2: CA2 region of the Entorhinal Cortex; CG: Cingulate Cortex; FC: Frontal Cortex; LC: Locus Coeruleus; Med: Medulla; O2: Antibody for IHC ASN detection; PLA: Proximity Ligation Assay; SN: Substantia Nigra; Str: Striatum; TC: Temporal Cortex. Error bars represent standard deviation.

AS-PLA staining in the striatum was consistently found up to and including Braak PD stage 6 cases, and particularly in early PD Braak stages (1-3). No AS-PLA staining was detected in any brain region in two out of three PD Braak stage 6 cases. In the overall sample, ASN IHC staining prevailed in all brain regions except the striatum, where AS-PLA and O2 staining were equally represented **(Table 5.2)**.

Table 5.3: AS-PLA and O2 regional staining by PD Braak stage

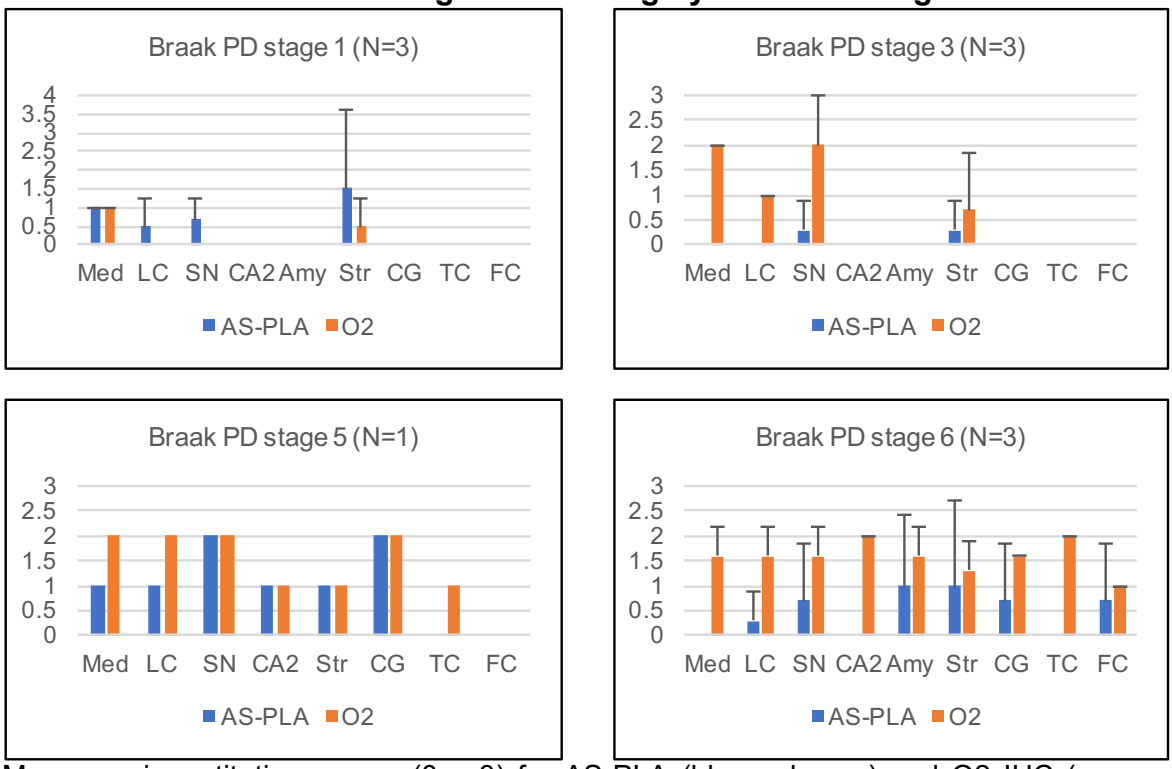

Mean semiquantitative scores (0 – 3) for AS-PLA (blue columns) and O2 IHC (orange columns) staining by brain region, across progressive PD Braak stages. Amy: Amygdala; CA2: CA2 region of the Entorhinal Cortex; CG: Cingulate Cortex; FC: Frontal Cortex; LC: Locus Coeruleus; Med: Medulla; O2: Antibody for IHC ASN detection; PLA: Proximity Ligation Assay; SN: Substantia Nigra; Str: Striatum; TC: Temporal Cortex. Error bars represent standard deviation.

Table 5.4: AS-PLA staining subtypes

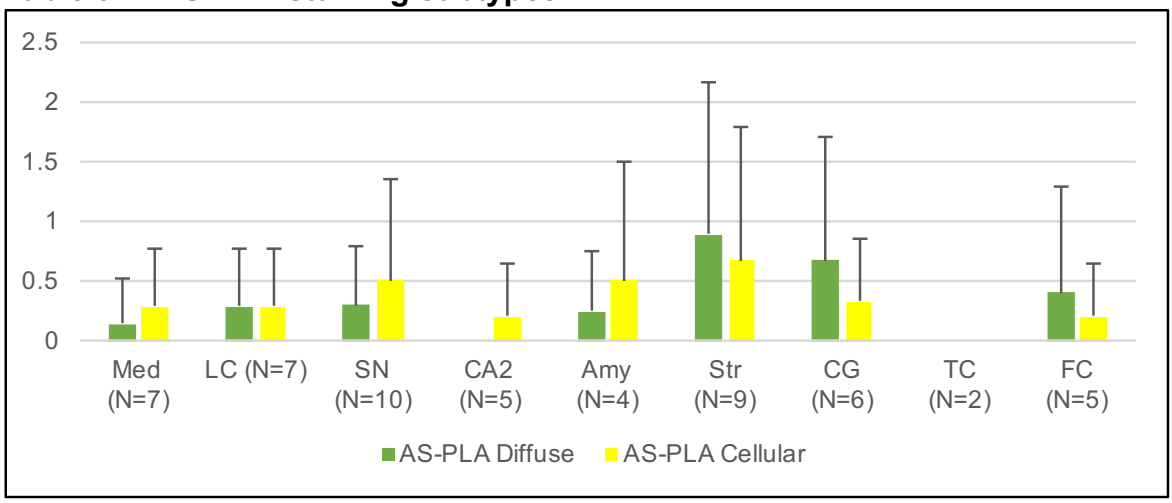

Mean semiquantitative scores for *Diffuse* (green columns) and *Cellular* (yellow columns) AS-PLA staining by brain region, in the overall sample. Amy: Amygdala; CA2: CA2 region of the Entorhinal Cortex; CG: Cingulate Cortex; FC: Frontal Cortex; LC: Locus Coeruleus; Med: Medulla; O2: Antibody for IHC ASN detection; PLA: Proximity Ligation Assay; SN: Substantia Nigra; Str: Striatum; TC: Temporal Cortex. Error bars represent standard deviation.

The sample size was insufficient to assess correlation between AS-PLA and O2 scores. In 20 out of a total of 54 stained sections, there was a concordant semiquantitative grading score between AS-PLA and O2 staining **(Table 5.1)**. Of these 20 sections, no staining was detected with either technique in 13. Of the 7 sections where AS-PLA and O2 detected signals were judged to be of equivalent intensity, there was no clear pattern, although 4/7 were in the brainstem (2 medulla from 2 PD Braak stage 1 subjects, 1 pons from a PD Braak stage 4 subject, and 1 SN from a PD Braak stage 5 case). Also of potential relevance, 4/7 of these sections were from the same case. It must be stated however, that comparison of staining between AS-IHC and AS-PLA is difficult to interpret, due to different staining patterns observed with these two approaches. Indeed, even when semiquantitative scores were equivalent for a given section, staining patterns varied significantly in any given area of the same brain region **(Figure 5.3)**.

Table 5.5: Mean PLA and O2 scores by PD Braak stage (A) and by PD subject (B)

(A)

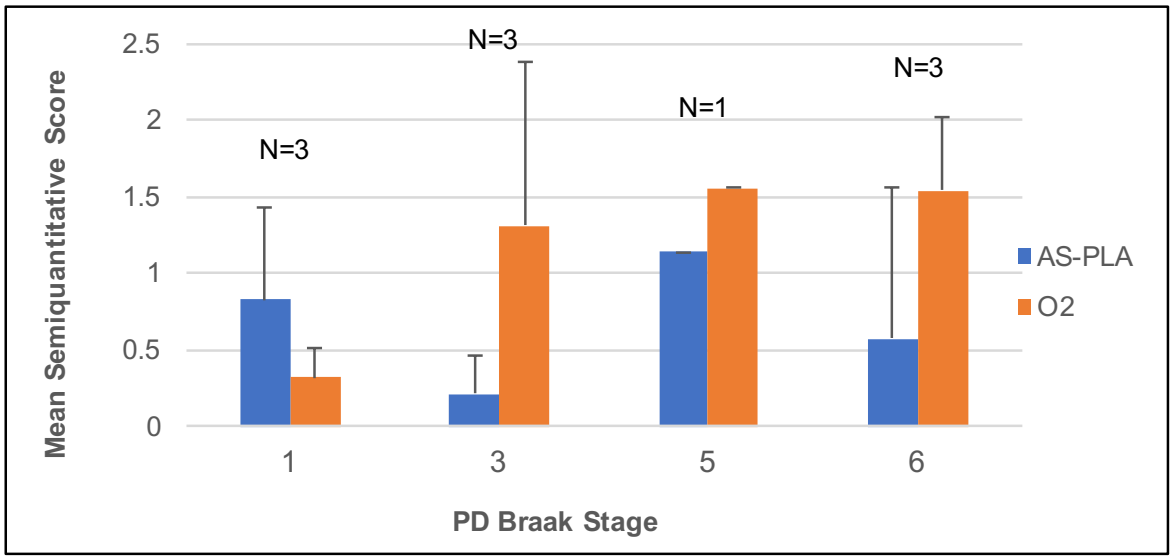

(B)

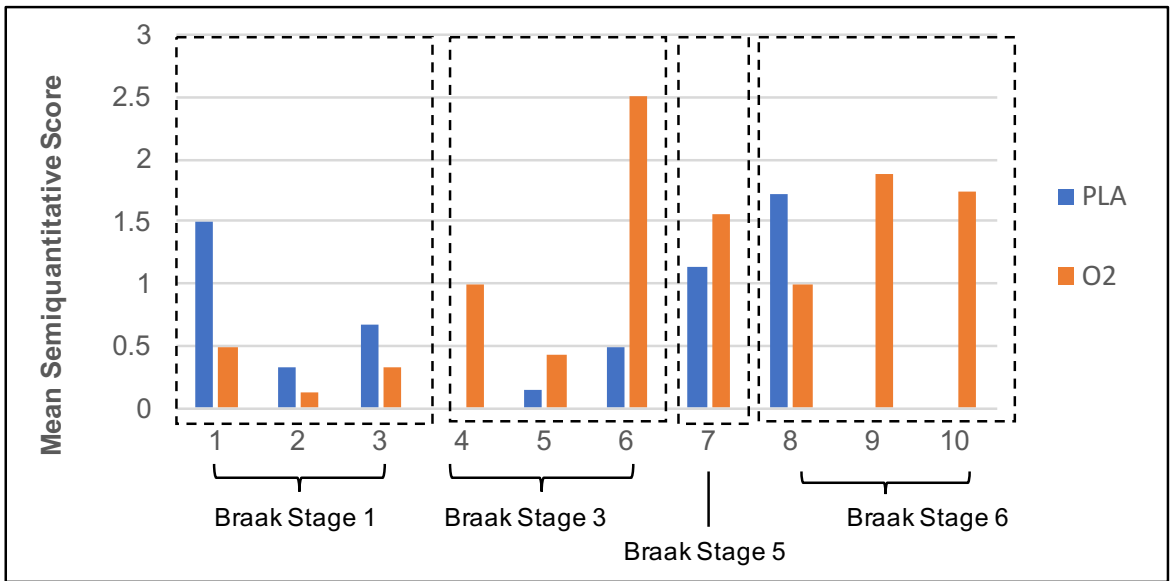

Mean semiquantitative scores for AS-PLA (blue columns) and O2 IHC (orange columns) staining by Braak stage **(A)** and by PD subject **(B)**. AS-PLA signal prevails consistently in PD Braak stage 1 cases, both within the group **(A)** and at the individual level **(B)**. Note the absence of AS-PLA signal in two of three PD Braak stage 6 cases **(B)**, which highlights the significant variability in AS-PLA staining between cases, whilst O2 IHC staining appeared more consistent. Error bars in (A) represent standard deviation.

Figure 5.3: Comparison of O2 (IHC) and AS-PLA staining patterns

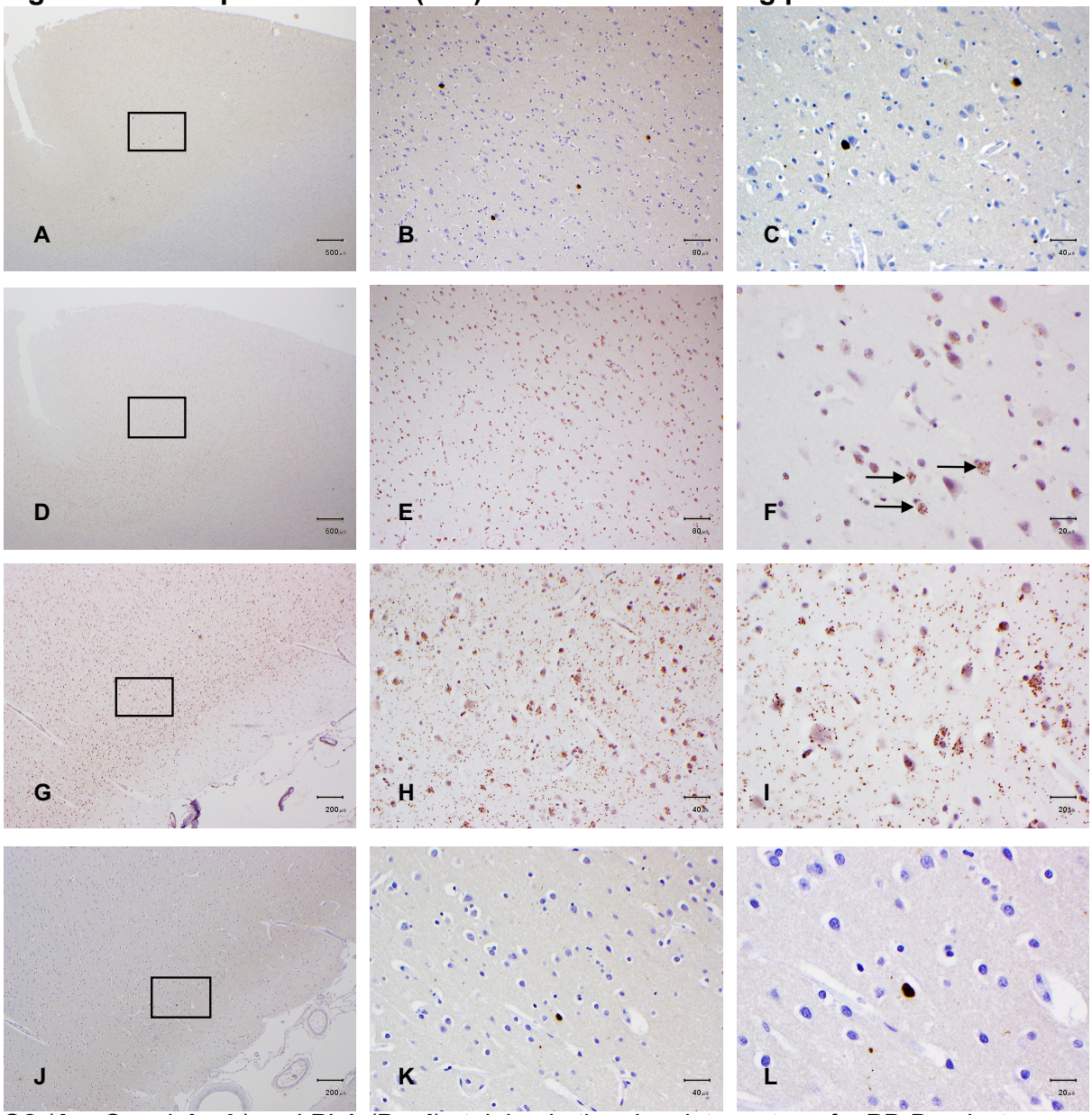

O2 (**A – C** and **J – L**) and PLA (**D – I**) staining in the cingulate cortex of a PD Braak stage 5 subject (PD Case 8 – see also Table 4.1). Note the high density of Lewy bodies detected with O2 IHC (**A-C**) compared to AS-PLA staining in the same region (**D-F**), which does not detect any Lewy bodies, although intraneuronal diffuse AS-PLA staining is detected at higher magnification (arrows in **F**). Conversely, in a different area from the same specimen, high density of diffuse intra- and extra-cellular AS-PLA staining is observed (**G – I**) in a region with low density of O2 staining (i.e. a single Lewy body, **H – J**). Boxed regions are displayed at higher magnification in the adjacent image (e.g. **B** represents boxed area in **A**).

5.2.2. AS-PLA on GI Biopsy tissue from the *Discovery* cohort

104 blocks from 58 individuals (40 PD and 18 HC) were stained for AS-PLA. Immunofluorescent AS-PLA was optimized in order to achieve a comparable signal to brightfield AS-PLA, followed by double immunolabelling with the neuronal marker calretinin (see Methods chapter).

Two types of staining were detected with AS-PLA-calretinin double immunofluorescence: 1) cellular-like formations in the mucosa, which partly co-stained with the neuronal marker calretinin (i.e. *cellular* signal) and 2) a dot-like pattern detected throughout the section, with no specific anatomic localisation (i.e. *diffuse* signal) **(Figure 5.4)**. AS-PLA *cellular* signal was statistically higher in the group with high neuronal score (as assessed with IHC) compared to low ($p=0.008$) and correlated significantly with the number of ganglia/section ($p=0.026$).

In 104 blocks, the mean scores for the *cellular* and *diffuse* AS-PLA signals were 0.02±0.02 and 0.66±0.50, respectively but there were no significant differences for either signal between any of the study groups **(Table 5.6)**. Furthermore, the two different types of AS-PLA staining did not correlate with each other. ROC curve analysis showed that neither signal was a reliable predictor of the clinical status (AUC=0.737 for *cellular* and AUC=0.597 for *diffuse* AS-PLA signal).

Table 5.6: GI AS-PLA staining scores by clinical group

	PD	Prodromal PD	Manifest PD	HC	PD vs HC (P-value)	Prodromal PD vs Manifest PD vs HC (p-value)
Cellular	0.02±0.03	0.02±0.04	0.02±0.02	0.02±0.02	0.737	0.716
Diffuse	0.69±0.49	0.65±0.51	0.74±0.48	0.76±0.50	0.597	0.662

Values are presented as mean score ± SD.

Figure 5.4: AS-PLA staining patterns in GI biopsy tissue

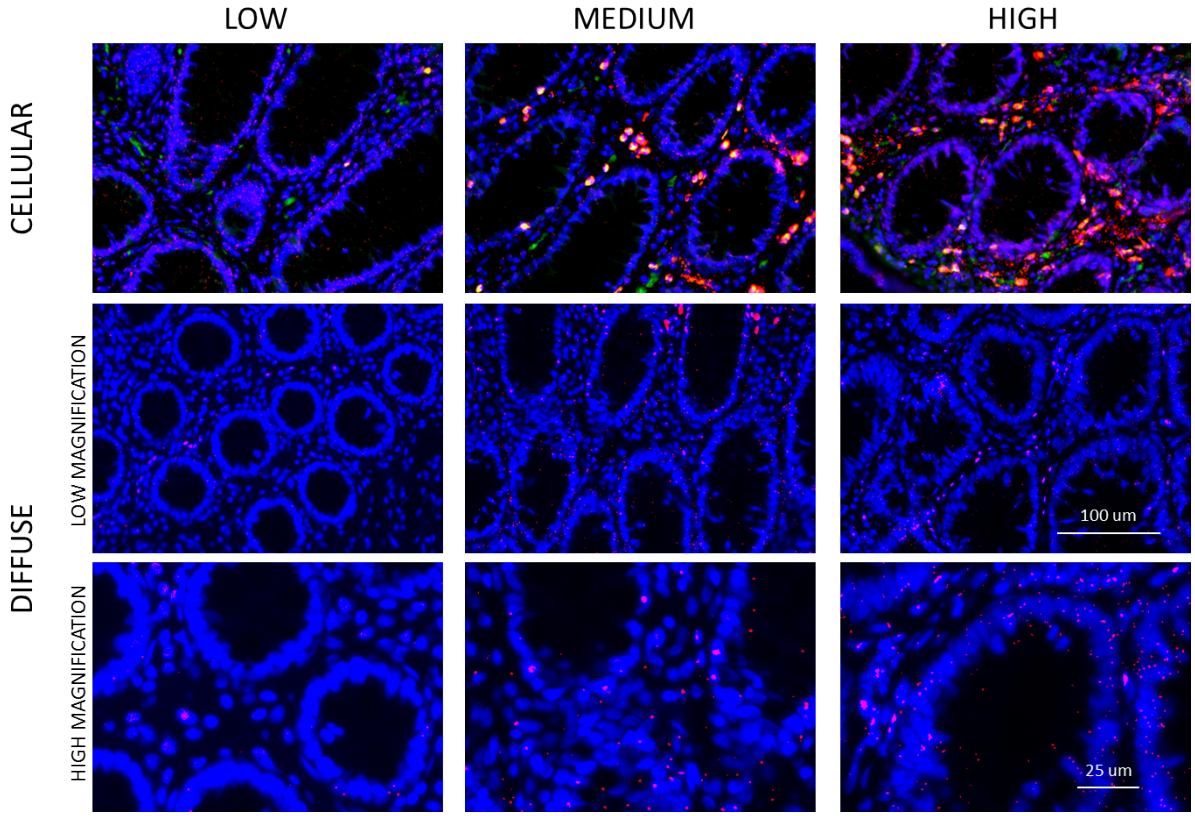

AS-PLA (red) – calretinin (green) double immunofluorescence detected two types of staining: (1) *cellular* signal **(top row)**, i.e. cellular-like formations in the mucosa partly co-stained with the neuronal marker calretinin (B) and (2) *diffuse* signal **(bottom two rows)**, i.e. a dot-like pattern detected throughout the section without any specific anatomic localisation. Magnification ×100 in top two rows, ×200 in in bottom row.

Neither AS-PLA signal correlated with UPDRS motor score or MMSE, but the *cellular* AS-PLA signal correlated positively with MOCA score ($p=0.030$, $r_s=0.288$). AS-PLA *cellular/diffuse* signals were not significantly different in subjects who were constipated or had hyposmia compared to subjects who did not present with

these symptoms. However, the mean *diffuse* AS-PLA signal was found to be statistically higher (p=0.020) in subjects without RBD (0.84 ± 0.51) than with RBD (0.54 ± 0.42).

The *cellular* AS-PLA signal was statistically higher in the large (p=0.038) and small bowel (p=0.012) compared to stomach and in small bowel compared to oesophagus (p=0.024). The *diffuse* AS-PLA signal showed no differences in regard to GI tract regional distribution.

5.3 Discussion

5.3.1. AS-PLA in the brain of PD subjects

5.3.1.1. Regional staining patterns

We used the recently developed AS-PLA technique to gain a better understanding of ASN pathology underlying PD (93). To our knowledge, for the first time AS-PLA was used to investigate striatal pathology in PD in this study. We have previously focused on ASN detection in the striatum of PD subjects (see chapter 3) following detection of novel pathology in this region using the paraffin-embedded tissue blot (PET-blot, see chapter 3). Interestingly, striatal AS-PLA signal was well represented in most cases, particularly in the early neuropathological stages of PD, while it was notable by its absence in two PD Braak stage 6 cases out of three. One possible explanation for the difference in striatal AS-PLA signal between early and late PD is that oligomeric species of ASN prevail in perikaryal aggregates (corresponding to *cellular* staining) and in axonal, possibly pre-synaptic aggregates (corresponding to the *diffuse* staining signal) in the early

stages of PD pathologic progression. Depletion of neurons in the SN and of the corresponding nigro-striatal pathway could account for the absence of staining in end stage PD. O2 IHC staining in the striatum in PD Braak stage 6 subjects possibly reflects conformationally different (i.e. fibrillary) ASN aggregates that are found at the end of the progressive development of ASN pathological changes associated with PD. These conformational variants may co-exist to different degrees in different patients and brain regions.

5.3.1.2. Morphology of Staining

In the recent study by Roberts and colleagues, AS-PLA was shown to specifically label very early perikaryal aggregates (i.e. pale bodies) but often not late stage inclusions such as LBs. Moreover, AS-PLA revealed previously unrecognized pathology in the form of extensive diffuse deposition of ASN which was not detected by IHC or observed in controls (93).

In agreement with Roberts et al's findings, we found that AS-PLA often revealed diffuse cytoplasmic staining in apparently healthy neurons, which might represent early pathologic changes such as oligomerization of ASN **(Figure 5.1,I) (93)**. Interestingly, in our overall sample the brain region with the highest density of *diffuse* AS-PLA staining was the striatum, followed by cingulate and frontal cortex, while brainstem regions displayed lower densities of AS-PLA *diffuse* signal **(Table 5.4)**.

In this study, LBs were inconsistently stained with AS-PLA, which is in agreement with the only previous study applying AS-PLA to brain regions in PD subjects, where LBs detected by AS-PLA were prevalently extra-somal and in the cortical regions (93). Areas with high density of Lewy pathology as detected by the O2

antibody were at times almost entirely devoid of AS-PLA staining, although often higher magnification inspection revealed intracellular diffuse AS-PLA patterns in these regions **(Figure 5.3, F)**. Thus, whilst AS-PLA often did not detect LBs, it did reveal different patterns of ASN reactive staining within the same region. Conversely, areas with high density of AS-PLA staining often did not show equally intense classical Lewy pathology detected with O2 staining **(Figure 5.3, G-L)**.

5.3.1.3. AS-PLA staining and staging of progression of pathology

Based on the hypothesis of progressive spread of PD pathology detected with IHC, one might expect to observe a correlation of AS-PLA staining with progression through PD Braak stages as well in our sample. However, compared to O2 IHC staining, which did show a relatively canonical increase in parallel with increasing Braak PD stages, AS-PLA signal did not follow any clear trend **(Table 5.3)**. The frequent discordance of staining intensity in the same brain region, and the lack of progression of AS-PLA staining with increasing PD Braak stages can potentially be explained by the fundamental structural differences in ASN conformations detected by IHC as opposed to those detected by AS-PLA (93). In other words, there could be differences in the route of progression of pathology explained by the conformational characterisitcs of the ASN species on which the Braak classification is based (i.e. classical fibrillary Lewy pathology detected by IHC vs oligomeric ASN species detected by AS-PLA)(31, 118). Staining results in PD case 1 are a fitting example in this scenario. In this subject, who according to the PD Braak assessment scheme was in stage 1, there was intense AS-PLA staining in the striatum, where O2 staining was also found, albeit less intense. As highlighted by others, this raises the question as to whether we are looking at the

relevant brain regions when assessing progression and staging of PD pathology (119). Also, the use of IHC may not be entirely reliable for staging of PD pathology, due to variable sensitivity for Lewy pathology of different ASN antibodies. Indeed, one of the subjects in this sample was re-staged, from Braak PD stage 4 to Braak PD stage 6 following detection of Lewy pathology in the frontal cortex with the O2 antibody, which had not been detected with the ASN-reactive antibody originally applied for Braak staging at the time of post-mortem examination (PD case 8). AS-PLA staining of extensive brain regions in larger samples of subjects with neuropathologically confirmed PD in variable stages will provide insight into possible alternative staging schemes based on oligomeric ASN species.

5.3.1.4. Insights from individual cases

There was striking inter-individual variability in the mean AS-PLA score in our sample, both between and within different PD Braak stages **(Table 5.5)**. Although difficult to assess in such a small sample, PLA signal seemed to vary more between individuals in the same Braak stage than did the O2 signal. One of the three PD stage six cases (PD case 8) had intense, widespread PLA staining throughout the brain, with the highest mean PLA score of the whole sample (PD case 8=1.71; mean PLA score for whole sample=0.59). On the other hand, the other two PD Braak stage 6 cases examined in this sample demonstrated complete lack of PLA staining. If this inter-individual variabililty were to be confirmed in larger, clinically well characterized samples, it could potentially explain phenotypic variation or even different underlying pathogenic mechanisms. There was slightly less variability between the three PD Braak stage 1 cases,

where AS-PLA was consistently positive, albeit to variable degrees. This would be in keeping with the hypothesis of oligomeric ASN being more abundant in early pathologic stages of PD.

5.3.2. AS-PLA in GI biopsy tissue from the *Discovery* cohort

This is the first study to have applied the PLA technique to the detection of pathological ASN conformations in the GI tract. We hypothesized that we could apply the PLA's specific reactivity for oligomeric species to detect these ASN conformations appearing as early markers in GI biopsies. One could expect to encounter such pathological changes in tissue harvested early in the disease progression, possibly at a stage preceding the onset of clinical manifestations, as in the subgroup of prodromal PD cases, which has been suggested to occur based on IHC ASN staining (14)

Of the two types of AS-PLA signal that were observed in GI biopsies in this study, the *cellular* staining was positively correlated to neuronal score and number of ganglionic neurons as assessed with IHC neuronal markers, which supports the idea that this staining was localized mainly to neuronal elements in the mucosa and submucosa. The *diffuse* staining pattern we observed in the GI tract was reminiscent of what is seen in the neuropil of the cortex of PD and ILBD patients that may represent synaptic distribution, but this needs to be examined further. One limitation to the interpretation of AS-PLA staining morphology is represented by the limited definition of the neuronal network that we were able to obtain in the GI tract, both with IHC and immunofluorescence. Indeed, immunofluorescence

can be preferable over IHC to determine colocalisation of targeted proteins, but it allows limited interpretation of morphology compared to brightfield IHC (7, 50).

While AS-PLA did detect oligomeric ASN in the majority of sections stained, there was no distinctive pattern or quantitative threshold that could distinguish between PD patients (Prodromal or Manifest PD groups) and HC. Furthermore, the *cellular* AS-PLA signal was actually found to be higher in those patients that performed better in their cognitive testing, and *diffuse* AS-PLA signal was lower in the patients with RBD compared to those without. Thus, clearly, the role of oligomeric forms of ASN in the GI tract needs further elucidation, but it could be that these conformations are rather transient and their quantification in a single time point may not be a meaningful approach as a biomarker.

6. CHAPTER SIX

COMPARISON OF RESULTS WITH ASN IHC, AS-PET-BLOT, AND AS-PLA AND OVERALL DISCUSSION

In this study, for the first time ASN in the GI tract was targeted by three different methods, each specific for alternative conformations of ASN, in an attempt to increase specificity and sensitivity of detecting ASN in GI tract biopsies as a potential diagnostic biomarker for PD. The design of this study was supposed to facilitate validation of AS-PLA and AS-PET-blot, by comparing results from these two novel techniques with traditional IHC. This approach was applied to both brain and GI tissue. Although, as expected, we detected specific staining patterns with each method, some of which could be considered potentially pathological, the level of agreement between different techniques (i.e. IHC, PET blot and PLA) was generally rather poor in terms of sensitivity and specificity, and no single technique or staining pattern was able to reliably distinguish PD patients (Prodromal or Manifest PD) from HC.

6.1 AS-PET-Blot

The PET-blot reveals fibrillary, insoluble protein aggregates and has been reported to reveal pathological inclusions which are smaller than LBs and potentially localized to the pre-synaptic region (95). Thus, application of the PET-Blot to GI tract tissue of subjects with PD could reveal this conformational variant of ASN more reliably than IHC. In the brain tissue samples analysed in this study, the PET-Blot did reveal dot-like staining in the neuropil of specific brain regions

(i.e. striatum), in addition to typical Lewy pathology. On the other hand, staining in the GI tract with the PET-Blot failed to identify a specific pattern of staining that could distinguish PD subjects from controls, although in both groups a *peri-crypt* staining morphology was identified which was unique to this technique. Furthermore, PET-blot staining only rarely agreed with IHC staining. This is not entirely unexpected, considering the different ASN conformational target these two techniques would be expected to reveal, with IHC revealing all forms of ASN, ranging from monomeric to fibrillary, and the PET-Blot detecting only those with a beta-sheet fibrillary pattern.

Lower visual resolution and partial tissue damage were further limitations inherent to the PET-Blot technique that made staining less morphologically defined and more difficult to localise anatomically.

6.2 AS-PLA

The AS-PLA is an adaptation of the original PLA method and has been reported to reveal oligomeric forms of ASN (88). To date, the AS-PLA has only ever been applied to the brain, and in the only reported study a small sample was analysed (93). Thus, the AS-PLA remains an extremely promising technique that needs further validation. In this context, the staining observed in the brain samples in this study probably generates more questions than answers. While morphology of staining broadly overlapped with results reported by Roberts et al, inconsistency of staining between different cases in similar PD neuropathological stages and also in comparison to IHC staining in the same region merit further investigation. Why is there significant AS-PLA staining in only one of 3 PD Braak stage 6 cases? Why is there such low overlap between IHC ASN staining with antibodies

specific for oligomeric ASN and AS-PLA detection of ASN oligomers? Answers to these questions probably depend mainly on application of this technique to larger samples and on further optimisation of this technique. For example, while many studies have looked at the effect of post-mortem delay and fixation time on immunohistochemistry (120), this is still an open question with regards to PLA staining, and it may be that the cross-linking action of formalin (and its duration) has an impact on detection of oligomeric ASN pathology with this technique.

6.3 Comparison of ASN IHC, AS-PET-Blot and AS-PLA on Brain tissue

In one case, all three detection techniques were applied to the same sample of brain tissue, specifically the striatum of a subject with neuropathologically confirmed PD in Braak stage 6. Interestingly, this region of the brain demonstrated relatively mild Lewy pathology, with rare LBs and occasional LNs with IHC, whilst AS-PET-Blot staining demonstrated intense staining suggestive of synaptic pathology **(Figure 4.1)**, and finally AS-PLA was entirely negative. It is not possible to extract conclusive information from a single case, however these results would suggest oligomeric ASN pathology might disappear, or possibly be integrated in more fibrillary structures, by the time the pathologic changes reach end stage, whereas the fibrillary, insoluble species of ASN are detected by the PET-blot, interestingly with a pattern suggestive of synaptic localisation rather than perikaryal inclusions. Comparison of these techniques on larger samples, including diverse brain regions and PD Braak stages will provide more conclusive data on conformational variants of ASN and their role in PD pathologic staging.

6.4 Comparison of ASN IHC, AS-PET-Blot and AS-PLA on GI Tissue from the *Discovery* cohort

Compared to brain tissue, much less is known about the prevalence and conformational characteristics of ASN in the GI tract, despite the growing interest in recent years.

For the first time in this study the PLA technique was applied to GI ASN detection, and only one study previously applied the PET-blot in this field (13).

There was a positive correlation between different staining patterns, both within the same technique and across the three applied detection methods **(Table 6.1)**.

Amongst IHC staining patterns, Neuritic staining correlated with Ganglionic (r=0.299) and Epithelial (r=0.287) staining, while Epithelial staining correlated with Cellular (r=0.191) and Intraneuronal (i.e. either Neuritic or Ganglionic staining) (r=0.219) staining. When comparing IHC to AS-PET-Blot and AS-PLA, we found that Intraneuronal IHC staining correlated with the *cellular* AS-PLA signal (r=0.253), while the Cellular IHC signal correlated with the AS-PET-Blot *ASN-specific* signal (r=0.242). Finally, the *peri-crypt* AS-PET-Blot signal correlated with the AS-PET-Blot *ASN-specific* staining (r=0.249). There was also a trend for a significant inverse correlation between the *diffuse* AS-PLA signal and the *peri-crypt* AS-PET-Blot signal (r=-0.267).

Table 6.1: Correlation between ASN IHC, AS-PET-Blot and AS-PLA staining in GI biopsy tissue from the *Discovery* cohort

	Neuritic	Ganglionic	Epithelial	Cellular	Intraneuronal	PLA Diffuse	PLA Cellular	PET-B PeriCrypt	PET-B ASN
Neuritic *r* P-Value	1	.299 **<0.001**	0.287 **<0.001**	0.094 0.252	- -	0.048 0.631	0.139 0.165	-0.119 0.324	0.136 0.257
Ganglionic *r* P-Value		1	0.120 0.145	-.008 0.918	- -	0.072 0.472	0.154 0.123	-0.133 0.268	0.167 0.163
Epithelial *r* P-Value			1	0.191 **0.019**	0.219 **0.007**	-0.146 0.147	0.117 0.248	-0.019 0.877	0.029 0.812
Cellular *r* P-Value				1	-0.008 0.919	-0.053 0.597	0.105 0.297	0.131 0.276	0.242 **0.042**
Intraneuronal *r* P-Value					1	0.053 0.598	0.253 **0.011**	-0.184 0.125	0.073 0.544
PLA Diffuse *r* P-Value						1	-0.013 0.900	-0.267 0.059	-0.080 0.575
PLA Cellular *r* P-Value							1	-0.211 0.137	-0.087 0.546
PET-B Pericrypt *r* P-Value								1	0.249 **0.037**
PET-B ASN *r* P-Value									1

Pearson correlation analysis of the correlation between different staining patterns obtained with each technique. Significant correlations are highlighted in **bold**.

We attempted to increase specificity for pathological staining by analysing those samples with various possible combinations of a positive/intense signal with two or all three of the applied techniques. Only one case, a healthy control, had intense PLA *diffuse* signal, Neuritic IHC staining and AS-PET-Blot *peri-crypt* staining in the same single tissue section (**Figure 6.1**). This was a male, who had had a small bowel biopsy at the age of 59. Interestingly, he screened positive for RBD and had prominent anxiety and depression, and his UPDRS motor score was 9, mainly due to mild bradykinesia in the legs. One cannot exclude that this individual would eventually develop PD.

Figure 6.1: ASN detection in GI biopsy samples comparing IHC, AS-PET-Blot and AS-PLA

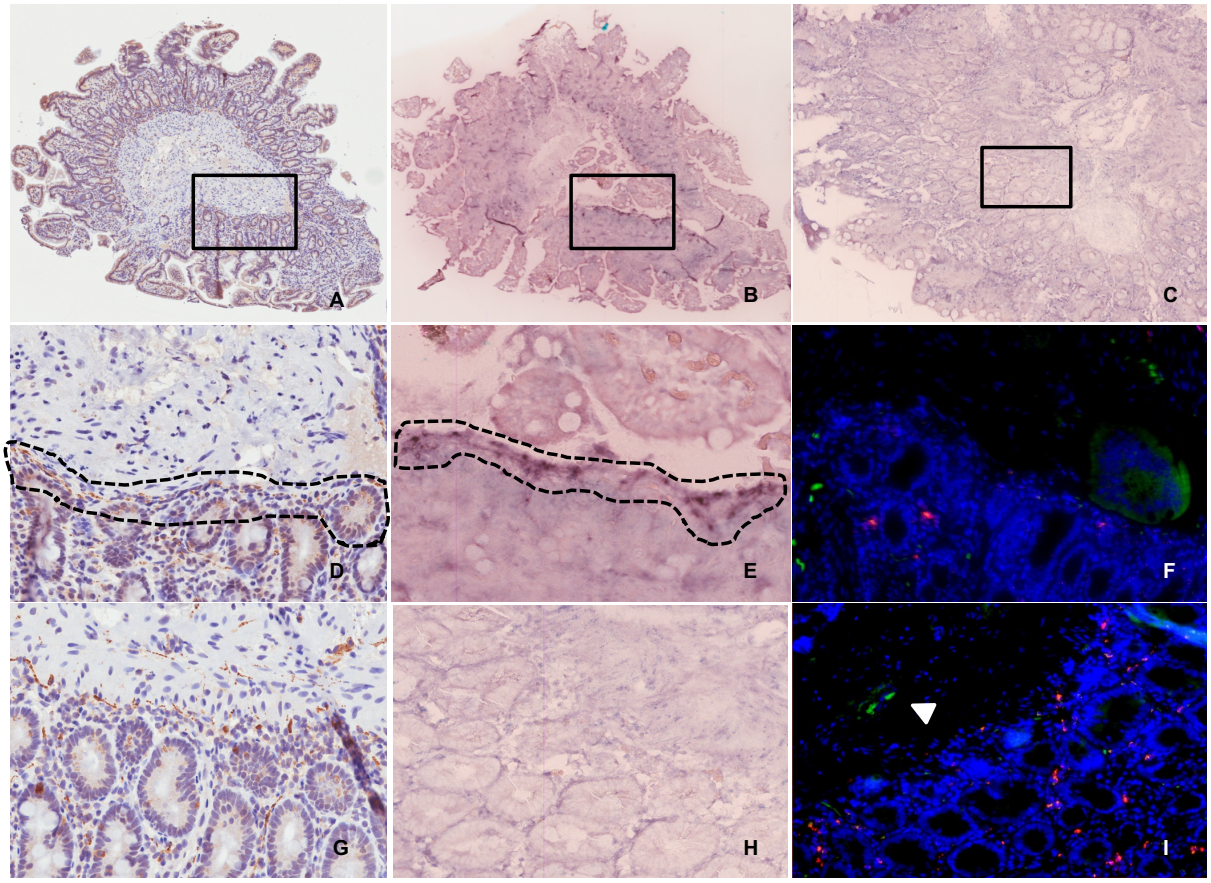

Comparison of staining patterns between IHC, AS-PET-Blot and AS-PLA. ASN-positive, neuritic-like staining is observed with IHC (**A,D,G**), while the PET-Blot on the same region shows variable staining (negative in **H,** positive in **E**). Immunofluorescent AS-PLA also returns a variable signal of (mixed, mild cellular and diffuse staining in **I**, and mostly cellular in **F**); note the green signal in (**I**) representing a submucosal ganglionic neuron (arrowhead). Magnification 40X in **D-I**, 10X in **A-C**; Antibodies: IHC - O2, 1:5000; PET-Blot – LB509, 1:10000.

On the other hand, when results from all available blocks for each case were analysed, 6 subjects met the criteria of positive staining signal with one of the three techniques of IHC, AS-PET-Blot and AS-PLA, in at least one block of tissue (2 Prodromal PD, 1 Manifest PD, and 3 HC). This small subgroup had a significantly higher average number of sections assessed in IHC (8.7 ± 6.3) compared to the rest of the sample (4.4 ± 2.3). From a histopathological point of view, calretinin score was marginally higher in these 6 cases (1.8 ± 1.5) compared

to the remaining cases (1.4 ± 1), although this difference did not reach significance (p=0.08). Clinical and demographic characteristics did not differ between this subgroup and the overall sample.

One of the potential strengths of this study was represented by the detailed clinical information collected from participating subjects with detailed phenotypic characterisation and prospective monitoring. However, none of the pathologic staining patterns were seen to correlate with severity of clinical symptoms; in contrast, some staining patterns were more prevalent in those patients that performed better with their motor and cognitive tests. Thus, detailed detection of pathological ASN in GI tract in a large, clinically and demographically well-characterized cohort would not seem to support any predictive or diagnostic value for using GI tract biopsies.

Biopsies from the upper GI tract were rare in this sample. This includes the oesophagus and the stomach, which are innervated by the vagus nerve rather than the sacral plexus, which innervates most of the small and large bowel. According to anatomical studies by Del Tredici *et. al.* (55), the sacral plexus is not affected by ASN pathology until the later stages of disease and would thus not seem to be linked to early ASN accumulation in the distal GI tract. It could be that some of our novel techniques may increase sensitivity or specificity when examining the more rostral part of the GI tract.

A further limitation of this study was represented by the available GI tissue, which was not from *ad hoc* biopsies performed for the specific goal of detecting ASN as

a potential biomarker but instead represented excess tissue from biopsies taken for unrelated clinical reasons. This probably reduced the quality of tissue specimens and introduced potential confounders such as neoplastic pathologic changes. Furthermore, available information on the primary indication for biopsy in each case was limited and often difficult to obtain. To obviate for this, screening of all obtained GI tissue biopsies was performed by a pathologist, and specimens with clearly abnormal tissue composition were excluded from further analysis.

Virtual microscopy and whole slide imaging could allow a more robust quantitative analysis of enteric ASN aggregates and potentially facilitate definition of reliable cut-off scores to distinguish PD patients from HC. To date, only one study has used computerized scanning of stained sections, but the authors did not attempt any software-based quantification of the density of ASN pathology on single sections (13). Software-based image analysis could also be helpful as it allows adjustment for significant variability between biopsies in regard to surface area, density and morphology (cell body vs fibres) of nervous tissue, and representation of different organ layers (mucosa, submucosa, muscle, etc), all of which may affect the yield of ASN-positive staining.

Currently, results on GI ASN detection in the ENS to diagnose or predict PD are controversial, with some studies reporting high sensitivity and specificity rates, whereas others, including this study, report a failure to identify a reliable PD biomarker based on ASN detection in the ENS. For the first time in this study the PLA technique was applied to GI ASN detection, and only one study previously applied the PET-blot in this field (13). Thus, it is still too early to draw conclusions,

and further fine tuning of these approaches, and possibly development of composite scoring systems might prove to be more reliable and clinically useful.

REFERENCES

1. Dorsey ER, Constantinescu R, Thompson JP, Biglan KM, Holloway RG, Kieburtz K, et al. Projected number of people with Parkinson disease in the most populous nations, 2005 through 2030. Neurology. 2007;68(5):384-6.
2. Reid WG, Hely MA, Morris JG, Loy C, Halliday GM. Dementia in Parkinson's disease: a 20-year neuropsychological study (Sydney Multicentre Study). J Neurol Neurosurg Psychiatry. 2011;82(9):1033-7.
3. George S, Brundin P. Immunotherapy in Parkinson's Disease: Micromanaging Alpha-Synuclein Aggregation. J Parkinsons Dis. 2015;5(3):413-24.
4. Dickson DW, Braak H, Duda JE, Duyckaerts C, Gasser T, Halliday GM, et al. Neuropathological assessment of Parkinson's disease: refining the diagnostic criteria. Lancet Neurol. 2009;8(12):1150-7.
5. Beach TG, Adler CH, Sue LI, Vedders L, Lue L, White Iii CL, et al. Multi-organ distribution of phosphorylated alpha-synuclein histopathology in subjects with Lewy body disorders. Acta Neuropathol. 2010;119(6):689-702.
6. Gelpi E, Navarro-Otano J, Tolosa E, Gaig C, Compta Y, Rey MJ, et al. Multiple organ involvement by alpha-synuclein pathology in Lewy body disorders. Mov Disord. 2014;29(8):1010-8.
7. Lebouvier T, Chaumette T, Damier P, Coron E, Touchefeu Y, Vrignaud S, et al. Pathological lesions in colonic biopsies during Parkinson's disease. Gut. 2008;57(12):1741-3.
8. Lebouvier T, Neunlist M, Bruley des Varannes S, Coron E, Drouard A, N'Guyen JM, et al. Colonic biopsies to assess the neuropathology of Parkinson's disease and its relationship with symptoms. PLoS One. 2010;5(9):e12728.
9. Pouclet H, Lebouvier T, Coron E, des Varannes SB, Rouaud T, Roy M, et al. A comparison between rectal and colonic biopsies to detect Lewy pathology in Parkinson's disease. Neurobiology of disease. 2012;45(1):305-9.
10. Shannon KM, Keshavarzian A, Mutlu E, Dodiya HB, Daian D, Jaglin JA, et al. Alpha-synuclein in colonic submucosa in early untreated Parkinson's disease. Movement disorders : official journal of the Movement Disorder Society. 2012;27(6):709-15.
11. Hilton D, Stephens M, Kirk L, Edwards P, Potter R, Zajicek J, et al. Accumulation of alpha-synuclein in the bowel of patients in the pre-clinical phase of Parkinson's disease. Acta Neuropathol. 2014;127(2):235-41.
12. Sanchez-Ferro A, Rabano A, Catalan MJ, Rodriguez-Valcarcel FC, Fernandez Diez S, Herreros-Rodriguez J, et al. In vivo gastric detection of alpha-synuclein inclusions in Parkinson's disease. Mov Disord. 2015;30(4):517-24.
13. Visanji NP, Marras C, Kern DS, Al Dakheel A, Gao A, Liu LW, et al. Colonic mucosal a-synuclein lacks specificity as a biomarker for Parkinson disease. Neurology. 2015;84(6):609-16.
14. Shannon KM, Keshavarzian A, Dodiya HB, Jakate S, Kordower JH. Is alpha-synuclein in the colon a biomarker for premotor Parkinson's disease? Evidence from 3 cases. Movement disorders : official journal of the Movement Disorder Society. 2012;27(6):716-9.
15. Stokholm MG, Danielsen EH, Hamilton-Dutoit SJ, Borghammer P. Pathological alpha-synuclein in gastrointestinal tissues from prodromal Parkinson disease patients. Annals of neurology. 2016;79(6):940-9.
16. Marek K, Jennings D. Can we image premotor Parkinson disease? Neurology. 2009;72(7 Suppl):S21-6.
17. Lees A. An essay on the shaking palsy. Brain. 2017;140(3):843-8.
18. Baig F, Lawton M, Rolinski M, Ruffmann C, Nithi K, Evetts SG, et al. Delineating nonmotor symptoms in early Parkinson's disease and first-degree relatives. Mov Disord. 2015.

19. Visanji N, Marras C. The relevance of pre-motor symptoms in Parkinson's disease. Expert Rev Neurother. 2015;15(10):1205-17.
20. Kempster PA, Hurwitz B, Lees AJ. A new look at James Parkinson's Essay on the Shaking Palsy. Neurology. 2007;69(5):482-5.
21. Bower JH, Maraganore DM, McDonnell SK, Rocca WA. Incidence and distribution of parkinsonism in Olmsted County, Minnesota, 1976-1990. Neurology. 1999;52(6):1214-20.
22. de Rijk MC, Breteler MM, Graveland GA, Ott A, Grobbee DE, van der Meche FG, et al. Prevalence of Parkinson's disease in the elderly: the Rotterdam Study. Neurology. 1995;45(12):2143-6.
23. Pringsheim T, Jette N, Frolkis A, Steeves TD. The prevalence of Parkinson's disease: a systematic review and meta-analysis. Mov Disord. 2014;29(13):1583-90.
24. Kalia LV, Lang AE. Parkinson's disease. Lancet. 2015;386(9996):896-912.
25. Jankovic J, McDermott M, Carter J, Gauthier S, Goetz C, Golbe L, et al. Variable expression of Parkinson's disease: a base-line analysis of the DATATOP cohort. The Parkinson Study Group. Neurology. 1990;40(10):1529-34.
26. van Rooden SM, Heiser WJ, Kok JN, Verbaan D, van Hilten JJ, Marinus J. The identification of Parkinson's disease subtypes using cluster analysis: a systematic review. Mov Disord. 2010;25(8):969-78.
27. Martinez-Martin P, Rodriguez-Blazquez C, Kurtis MM, Chaudhuri KR. The impact of non-motor symptoms on health-related quality of life of patients with Parkinson's disease. Mov Disord. 2011;26(3):399-406.
28. Khoo TK, Yarnall AJ, Duncan GW, Coleman S, O'Brien JT, Brooks DJ, et al. The spectrum of nonmotor symptoms in early Parkinson disease. Neurology. 2013;80(3):276-81.
29. Trinh J, Farrer M. Advances in the genetics of Parkinson disease. Nat Rev Neurol. 2013;9(8):445-54.
30. Perrett RM, Alexopoulou Z, Tofaris GK. The endosomal pathway in Parkinson's disease. Mol Cell Neurosci. 2015;66(Pt A):21-8.
31. Braak H, Rub U, Gai WP, Del Tredici K. Idiopathic Parkinson's disease: possible routes by which vulnerable neuronal types may be subject to neuroinvasion by an unknown pathogen. J Neural Transm. 2003;110(5):517-36.
32. Bolam JP, Pissadaki EK. Living on the edge with too many mouths to feed: why dopamine neurons die. Mov Disord. 2012;27(12):1478-83.
33. Parkkinen L, Kauppinen T, Pirttila T, Autere JM, Alafuzoff I. Alpha-synuclein pathology does not predict extrapyramidal symptoms or dementia. Ann Neurol. 2005;57(1):82-91.
34. Gibb WR, Lees AJ. The relevance of the Lewy body to the pathogenesis of idiopathic Parkinson's disease. J Neurol Neurosurg Psychiatry. 1988;51(6):745-52.
35. Hughes AJ, Daniel SE, Kilford L, Lees AJ. Accuracy of clinical diagnosis of idiopathic Parkinson's disease: a clinico-pathological study of 100 cases. J Neurol Neurosurg Psychiatry. 1992;55(3):181-4.
36. Fearnley JM, Lees AJ. Ageing and Parkinson's disease: substantia nigra regional selectivity. Brain : a journal of neurology. 1991;114 (Pt 5):2283-301.
37. Kordower JH, Olanow CW, Dodiya HB, Chu Y, Beach TG, Adler CH, et al. Disease duration and the integrity of the nigrostriatal system in Parkinson's disease. Brain : a journal of neurology. 2013;136(Pt 8):2419-31.
38. Berg D, Postuma RB, Bloem B, Chan P, Dubois B, Gasser T, et al. Time to redefine PD? Introductory statement of the MDS Task Force on the definition of Parkinson's disease. Movement disorders : official journal of the Movement Disorder Society. 2014;29(4):454-62.
39. Braak H, Del Tredici K, Rub U, de Vos RA, Jansen Steur EN, Braak E. Staging of brain pathology related to sporadic Parkinson's disease. Neurobiology of aging. 2003;24(2):197-211.
40. Goedert M, Spillantini MG, Del Tredici K, Braak H. 100 years of Lewy pathology. Nat Rev Neurol. 2013;9(1):13-24.

41. Hardy J. Expression of normal sequence pathogenic proteins for neurodegenerative disease contributes to disease risk: 'permissive templating' as a general mechanism underlying neurodegeneration. Biochem Soc Trans. 2005;33(Pt 4):578-81.
42. Sigurdsson EM, Wisniewski T, Frangione B. Infectivity of amyloid diseases. Trends Mol Med. 2002;8(9):411-3.
43. Kordower JH, Brundin P. Lewy body pathology in long-term fetal nigral transplants: is Parkinson's disease transmitted from one neural system to another? Neuropsychopharmacology. 2009;34(1):254.
44. Hawkes CH, Del Tredici K, Braak H. Parkinson's disease: a dual-hit hypothesis. Neuropathol Appl Neurobiol. 2007;33(6):599-614.
45. Sacino AN, Brooks M, Thomas MA, McKinney AB, Lee S, Regenhardt RW, et al. Intramuscular injection of alpha-synuclein induces CNS alpha-synuclein pathology and a rapid-onset motor phenotype in transgenic mice. Proceedings of the National Academy of Sciences of the United States of America. 2014;111(29):10732-7.
46. Holmqvist S, Chutna O, Bousset L, Aldrin-Kirk P, Li W, Bjorklund T, et al. Direct evidence of Parkinson pathology spread from the gastrointestinal tract to the brain in rats. Acta neuropathologica. 2014;128(6):805-20.
47. Svensson E, Horvath-Puho E, Thomsen RW, Djurhuus JC, Pedersen L, Borghammer P, et al. Vagotomy and subsequent risk of Parkinson's disease. Annals of neurology. 2015;78(4):522-9.
48. Furness JB. The enteric nervous system. Malden, Mass.: Blackwell Pub.; 2006.
49. Furness JB. The enteric nervous system and neurogastroenterology. Nat Rev Gastroenterol Hepatol. 2012;9(5):286-94.
50. Ruffmann C, Parkkinen L. Gut Feelings About alpha-Synuclein in Gastrointestinal Biopsies: Biomarker in the Making? Mov Disord. 2016;31(2):193-202.
51. Sprenger FS, Stefanova N, Gelpi E, Seppi K, Navarro-Otano J, Offner F, et al. Enteric nervous system alpha-synuclein immunoreactivity in idiopathic REM sleep behavior disorder. Neurology. 2015;85(20):1761-8.
52. Berthoud HR, Jedrzejewska A, Powley TL. Simultaneous labeling of vagal innervation of the gut and afferent projections from the visceral forebrain with dil injected into the dorsal vagal complex in the rat. J Comp Neurol. 1990;301(1):65-79.
53. Chang HY, Mashimo H, Goyal RK. Musings on the wanderer: what's new in our understanding of vago-vagal reflex? IV. Current concepts of vagal efferent projections to the gut. Am J Physiol Gastrointest Liver Physiol. 2003;284(3):G357-66.
54. Koeppen BM SB, Berne RM. . Berne & levy physiology. 6th ed, updated ed Philadelphia, Mosby/Elsevier 2010.
55. Del Tredici K, Braak H. Spinal cord lesions in sporadic Parkinson's disease. Acta neuropathologica. 2012;124(5):643-64.
56. Ueda K, Fukushima H, Masliah E, Xia Y, Iwai A, Yoshimoto M, et al. Molecular cloning of cDNA encoding an unrecognized component of amyloid in Alzheimer disease. Proc Natl Acad Sci U S A. 1993;90(23):11282-6.
57. Jakes R, Spillantini MG, Goedert M. Identification of two distinct synucleins from human brain. FEBS letters. 1994;345(1):27-32.
58. Kalia LV, Kalia SK, McLean PJ, Lozano AM, Lang AE. alpha-Synuclein oligomers and clinical implications for Parkinson disease. Ann Neurol. 2013;73(2):155-69.
59. Bartels T, Choi JG, Selkoe DJ. alpha-Synuclein occurs physiologically as a helically folded tetramer that resists aggregation. Nature. 2011;477(7362):107-10.
60. Chandra S, Gallardo G, Fernandez-Chacon R, Schluter OM, Sudhof TC. Alpha-synuclein cooperates with CSPalpha in preventing neurodegeneration. Cell. 2005;123(3):383-96.
61. Spillantini MG, Schmidt ML, Lee VM, Trojanowski JQ, Jakes R, Goedert M. Alpha-synuclein in Lewy bodies. Nature. 1997;388(6645):839-40.

62. Kruger R, Kuhn W, Muller T, Woitalla D, Graeber M, Kosel S, et al. Ala30Pro mutation in the gene encoding alpha-synuclein in Parkinson's disease. Nat Genet. 1998;18(2):106-8.
63. Polymeropoulos MH, Lavedan C, Leroy E, Ide SE, Dehejia A, Dutra A, et al. Mutation in the alpha-synuclein gene identified in families with Parkinson's disease. Science. 1997;276(5321):2045-7.
64. Fujiwara H, Hasegawa M, Dohmae N, Kawashima A, Masliah E, Goldberg MS, et al. alpha-Synuclein is phosphorylated in synucleinopathy lesions. Nat Cell Biol. 2002;4(2):160-4.
65. Schildknecht S, Gerding HR, Karreman C, Drescher M, Lashuel HA, Outeiro TF, et al. Oxidative and nitrative alpha-synuclein modifications and proteostatic stress: implications for disease mechanisms and interventions in synucleinopathies. J Neurochem. 2013;125(4):491-511.
66. Hartl FU, Bracher A, Hayer-Hartl M. Molecular chaperones in protein folding and proteostasis. Nature. 2011;475(7356):324-32.
67. Tyedmers J, Mogk A, Bukau B. Cellular strategies for controlling protein aggregation. Nat Rev Mol Cell Biol. 2010;11(11):777-88.
68. Tofaris GK, Goedert M, Spillantini MG. The Transcellular Propagation and Intracellular Trafficking of alpha-Synuclein. Cold Spring Harb Perspect Med. 2017;7(9).
69. Walsh DM, Lomakin A, Benedek GB, Condron MM, Teplow DB. Amyloid beta-protein fibrillogenesis. Detection of a protofibrillar intermediate. J Biol Chem. 1997;272(35):22364-72.
70. Hinault MP, Cuendet AF, Mattoo RU, Mensi M, Dietler G, Lashuel HA, et al. Stable alpha-synuclein oligomers strongly inhibit chaperone activity of the Hsp70 system by weak interactions with J-domain co-chaperones. J Biol Chem. 2010;285(49):38173-82.
71. Lindersson E, Beedholm R, Højrup P, Moos T, Gai W, Hendil KB, et al. Proteasomal inhibition by alpha-synuclein filaments and oligomers. J Biol Chem. 2004;279(13):12924-34.
72. Colla E, Coune P, Liu Y, Pletnikova O, Troncoso JC, Iwatsubo T, et al. Endoplasmic reticulum stress is important for the manifestations of α-synucleinopathy in vivo. J Neurosci. 2012;32(10):3306-20.
73. Dehay B, Bourdenx M, Gorry P, Przedborski S, Vila M, Hunot S, et al. Targeting alpha-synuclein for treatment of Parkinson's disease: mechanistic and therapeutic considerations. Lancet Neurol. 2015;14(8):855-66.
74. Wakabayashi K, Takahashi H, Takeda S, Ohama E, Ikuta F. Parkinson's disease: the presence of Lewy bodies in Auerbach's and Meissner's plexuses. Acta Neuropathol. 1988;76(3):217-21.
75. Qualman SJ, Haupt HM, Yang P, Hamilton SR. Esophageal Lewy bodies associated with ganglion cell loss in achalasia. Similarity to Parkinson's disease. Gastroenterology. 1984;87(4):848-56.
76. Braak H, de Vos RA, Bohl J, Del Tredici K. Gastric alpha-synuclein immunoreactive inclusions in Meissner's and Auerbach's plexuses in cases staged for Parkinson's disease-related brain pathology. Neuroscience letters. 2006;396(1):67-72.
77. Bottner M, Zorenkov D, Hellwig I, Barrenschee M, Harde J, Fricke T, et al. Expression pattern and localization of alpha-synuclein in the human enteric nervous system. Neurobiology of disease. 2012;48(3):474-80.
78. Gray MT, Munoz DG, Gray DA, Schlossmacher MG, Woulfe JM. Alpha-synuclein in the appendiceal mucosa of neurologically intact subjects. Movement disorders : official journal of the Movement Disorder Society. 2014;29(8):991-8.
79. Gold A, Turkalp ZT, Munoz DG. Enteric alpha-synuclein expression is increased in Parkinson's disease but not Alzheimer's disease. Mov Disord. 2013;28(2):237-40.
80. Beach TG, Corbille AG, Letournel F, Kordower JH, Kremer T, Munoz DG, et al. Multicenter Assessment of Immunohistochemical Methods for Pathological Alpha-Synuclein in Sigmoid Colon of Autopsied Parkinson's Disease and Control Subjects. J Parkinsons Dis. 2016.
81. Rawlings ND, Salvesen G. Handbook of proteolytic enzymes. Third edition ed. Amsterdam London: Elsevier Academic; 2013.

82. Schulz-Schaeffer WJ, Tschoke S, Kranefuss N, Drose W, Hause-Reitner D, Giese A, et al. The paraffin-embedded tissue blot detects PrP(Sc) early in the incubation time in prion diseases. Am J Pathol. 2000;156(1):51-6.
83. Taraboulos A, Jendroska K, Serban D, Yang SL, DeArmond SJ, Prusiner SB. Regional mapping of prion proteins in brain. Proceedings of the National Academy of Sciences of the United States of America. 1992;89(16):7620-4.
84. Moh CF, Siedlak SL, Tabaton M, Perry G, Castellani RJ, Smith MA. Paraffin-embedded tissue (PET) blot method: application to Alzheimer disease. Journal of neuroscience methods. 2010;190(2):244-7.
85. Neumann M, Kahle PJ, Giasson BI, Ozmen L, Borroni E, Spooren W, et al. Misfolded proteinase K-resistant hyperphosphorylated alpha-synuclein in aged transgenic mice with locomotor deterioration and in human alpha-synucleinopathies. J Clin Invest. 2002;110(10):1429-39.
86. Neumann M, Muller V, Kretzschmar HA, Haass C, Kahle PJ. Regional distribution of proteinase K-resistant alpha-synuclein correlates with Lewy body disease stage. J Neuropathol Exp Neurol. 2004;63(12):1225-35.
87. Steinacker P, Berner C, Thal DR, Attems J, Ludolph AC, Otto M. Protease-resistant SOD1 aggregates in amyotrophic lateral sclerosis demonstrated by paraffin-embedded tissue (PET) blot. Acta neuropathologica communications. 2014;2:130.
88. Soderberg O, Gullberg M, Jarvius M, Ridderstrale K, Leuchowius KJ, Jarvius J, et al. Direct observation of individual endogenous protein complexes in situ by proximity ligation. Nat Methods. 2006;3(12):995-1000.
89. Weibrecht I, Leuchowius KJ, Clausson CM, Conze T, Jarvius M, Howell WM, et al. Proximity ligation assays: a recent addition to the proteomics toolbox. Expert Rev Proteomics. 2010;7(3):401-9.
90. Greenwood C, Ruff D, Kirvell S, Johnson G, Dhillon HS, Bustin SA. Proximity assays for sensitive quantification of proteins. Biomol Detect Quantif. 2015;4:10-6.
91. Fredriksson S, Gullberg M, Jarvius J, Olsson C, Pietras K, Gustafsdottir SM, et al. Protein detection using proximity-dependent DNA ligation assays. Nature biotechnology. 2002;20(5):473-7.
92. Gullberg M, Gustafsdottir SM, Schallmeiner E, Jarvius J, Bjarnegard M, Betsholtz C, et al. Cytokine detection by antibody-based proximity ligation. Proceedings of the National Academy of Sciences of the United States of America. 2004;101(22):8420-4.
93. Roberts RF, Wade-Martins R, Alegre-Abarrategui J. Direct visualization of alpha-synuclein oligomers reveals previously undetected pathology in Parkinson's disease brain. Brain. 2015;138(Pt 6):1642-57.
94. Szewczyk-Krolikowski K, Tomlinson P, Nithi K, Wade-Martins R, Talbot K, Ben-Shlomo Y, et al. The influence of age and gender on motor and non-motor features of early Parkinson's disease: initial findings from the Oxford Parkinson Disease Center (OPDC) discovery cohort. Parkinsonism Relat Disord. 2014;20(1):99-105.
95. Kramer ML, Schulz-Schaeffer WJ. Presynaptic alpha-synuclein aggregates, not Lewy bodies, cause neurodegeneration in dementia with Lewy bodies. J Neurosci. 2007;27(6):1405-10.
96. Vaikath NN, Majbour NK, Paleologou KE, Ardah MT, van Dam E, van de Berg WD, et al. Generation and characterization of novel conformation-specific monoclonal antibodies for alpha-synuclein pathology. Neurobiol Dis. 2015;79:81-99.
97. Hughes AJ, Daniel SE, Kilford L, Lees AJ. ACCURACY OF CLINICAL-DIAGNOSIS OF IDIOPATHIC PARKINSONS-DISEASE - A CLINICOPATHOLOGICAL STUDY OF 100 CASES. Journal of Neurology Neurosurgery and Psychiatry. 1992;55(3):181-4.
98. Rolinski M, Szewczyk-Krolikowski K, Tomlinson PR, Nithi K, Talbot K, Ben-Shlomo Y, et al. REM sleep behaviour disorder is associated with worse quality of life and other non-motor

features in early Parkinson's disease. Journal of neurology, neurosurgery, and psychiatry. 2014;85(5):560-6.
99. Esiri M, Chance S, Joachim C, Warden D, Smallwood A, Sloan C, et al. Cerebral amyloid angiopathy, subcortical white matter disease and dementia: literature review and study in OPTIMA. Brain Pathol. 2015;25(1):51-62.
100. Corbille AG, Letournel F, Kordower JH, Lee J, Shanes E, Neunlist M, et al. Evaluation of alpha-synuclein immunohistochemical methods for the detection of Lewy-type synucleinopathy in gastrointestinal biopsies. Acta neuropathologica communications. 2016;4:35.
101. Markesbery WR, Jicha GA, Liu H, Schmitt FA. Lewy body pathology in normal elderly subjects. Journal of neuropathology and experimental neurology. 2009;68(7):816-22.
102. Nakai M, Fujita M, Waragai M, Sugama S, Wei J, Akatsu H, et al. Expression of alpha-synuclein, a presynaptic protein implicated in Parkinson's disease, in erythropoietic lineage. Biochem Biophys Res Commun. 2007;358(1):104-10.
103. Tamo W, Imaizumi T, Tanji K, Yoshida H, Mori F, Yoshimoto M, et al. Expression of alpha-synuclein, the precursor of non-amyloid beta component of Alzheimer's disease amyloid, in human cerebral blood vessels. Neurosci Lett. 2002;326(1):5-8.
104. Askanas V, Engel WK, Alvarez RB, McFerrin J, Broccolini A. Novel immunolocalization of alpha-synuclein in human muscle of inclusion-body myositis, regenerating and necrotic muscle fibers, and at neuromuscular junctions. J Neuropathol Exp Neurol. 2000;59(7):592-8.
105. Luk KC, Song C, O'Brien P, Stieber A, Branch JR, Brunden KR, et al. Exogenous alpha-synuclein fibrils seed the formation of Lewy body-like intracellular inclusions in cultured cells. Proc Natl Acad Sci U S A. 2009;106(47):20051-6.
106. Desplats P, Lee HJ, Bae EJ, Patrick C, Rockenstein E, Crews L, et al. Inclusion formation and neuronal cell death through neuron-to-neuron transmission of alpha-synuclein. Proc Natl Acad Sci U S A. 2009;106(31):13010-5.
107. Volpicelli-Daley LA, Luk KC, Patel TP, Tanik SA, Riddle DM, Stieber A, et al. Exogenous alpha-synuclein fibrils induce Lewy body pathology leading to synaptic dysfunction and neuron death. Neuron. 2011;72(1):57-71.
108. Corbille AG, Preterre C, Rolli-Derkinderen M, Coron E, Neunlist M, Lebouvier T, et al. Biochemical analysis of alpha-synuclein extracted from control and Parkinson's disease colonic biopsies. Neuroscience letters. 2017;641:81-6.
109. Croisier E, DE MR, Deprez M, Goldring K, Dexter DT, Pearce RK, et al. Comparative study of commercially available anti-alpha-synuclein antibodies. Neuropathol Appl Neurobiol. 2006;32(3):351-6.
110. Beach TG, White CL, Hamilton RL, Duda JE, Iwatsubo T, Dickson DW, et al. Evaluation of alpha-synuclein immunohistochemical methods used by invited experts. Acta Neuropathol. 2008;116(3):277-88.
111. Alafuzoff I, Parkkinen L, Al-Sarraj S, Arzberger T, Bell J, Bodi I, et al. Assessment of alpha-synuclein pathology: a study of the BrainNet Europe Consortium. J Neuropathol Exp Neurol. 2008;67(2):125-43.
112. Aldecoa I, Navarro-Otano J, Stefanova N, Sprenger FS, Seppi K, Poewe W, et al. Alpha-synuclein immunoreactivity patterns in the enteric nervous system. Neurosci Lett. 2015;602:145-9.
113. Duda JE, Giasson BI, Mabon ME, Lee VM, Trojanowski JQ. Novel antibodies to synuclein show abundant striatal pathology in Lewy body diseases. Annals of neurology. 2002;52(2):205-10.
114. Corbille AG, Neunlist M, Derkinderen P. Cross-linking for the analysis of alpha-synuclein in the enteric nervous system. Journal of neurochemistry. 2016.
115. Fung KM, Rorke LB, Giasson B, Lee VM, Trojanowski JQ. Expression of alpha-, beta-, and gamma-synuclein in glial tumors and medulloblastomas. Acta Neuropathol. 2003;106(2):167-75.
116. Kawashima M, Suzuki SO, Doh-ura K, Iwaki T. alpha-Synuclein is expressed in a variety of brain tumors showing neuronal differentiation. Acta Neuropathol. 2000;99(2):154-60.

117. Wu K, Quan Z, Weng Z, Li F, Zhang Y, Yao X, et al. Expression of neuronal protein synuclein gamma gene as a novel marker for breast cancer prognosis. Breast Cancer Res Treat. 2007;101(3):259-67.
118. Alafuzoff I, Ince PG, Arzberger T, Al-Sarraj S, Bell J, Bodi I, et al. Staging/typing of Lewy body related alpha-synuclein pathology: a study of the BrainNet Europe Consortium. Acta Neuropathol. 2009;117(6):635-52.
119. Kalaitzakis ME, Graeber MB, Gentleman SM, Pearce RK. Evidence against a reliable staging system of alpha-synuclein pathology in Parkinson's disease. Neuropathol Appl Neurobiol. 2009;35(1):125-6.
120. Howat WJ, Wilson BA. Tissue fixation and the effect of molecular fixatives on downstream staining procedures. Methods. 2014;70(1):12-9.